Nuclear Science and Technology

1987
Programme Progress Report
Radioactive Waste Management

Commission of the European Communities
Directorate-General for Science Research and Development
Joint Research Centre, Ispra Establishment

EUR 11914

1988

Nuclear Science and Technology

1987
Programme Progress Report
Radioactive Waste Management

Commission of the European Communities
Directorate-General for Science Research and Development
Joint Research Centre, Ispra Establishment

EUR 11914

1988

Published by the
COMMISSION OF THE EUROPEAN COMMUNITIES
Directorate-General
Telecommunications, Information Industries and Innovation
Batiment Jean Monnet
LUXEMBOURG

LEGAL NOTICE

Cataloguing data can be found at the end of this publication.

Luxembourg: Office for Official Publications of the European Communities, 1988

Printed in Italy

CONTENTS

EXECUTIVE SUMMARY

The safe and cost-effective management of the radioactive waste produced in the exploitation of nuclear energy requires an important research and development effort in order to be fully implemented at an industrial level.

The Joint Research Centre initiated its activities in the field of radioactive waste management in 1973. Four multiannual plans have been completed (1973-76, 1977-79, 1980-83 and 1984-87).

The activities of the JRC are carried out under the Plan of Action on Fission, which also includes programmes on Nuclear Materials Management and Control, Reactor Safety, Decommissioning of Nuclear Plants and Nuclear Fuels and Actinide Research. These programmes are carried out by the JRC and by shared-cost actions.

Coordination and Management Committees assure coordination among the various actions and with similar activities carried out in national laboratories.

In addition to the research action programmes, the Council approved in February 1980 a Community Plan of Action in the field of Radioactive Waste (1980-1982) which assures the continuity of the R&D effort throughout the period and entrusts the Commission with a wider role in the implementation of waste management practices.

The activities of the radioactive waste management programme of the JRC are largely executed by the Ispra Estbalishment, with a participation of the Karlsruhe Establishment. Strict relationships are maintained with the corresponding shared-cost action programme on radioactive waste management. Important Community projects such as PAGIS (Performance Assessment of Geological isolation Systems) and MIRAGE (Migration of Radioisotopes in the Geosphere) are jointly coordinated.

The JRC programme is structured in three research areas :

1. ***Waste Management and the Fuel Cycle** aims at characterizing waste streams of the nuclear fuel cycle and minimizing them, particularly for what concerns the radionuclides which are responsible of long-term risks.*
2. ***Safety of Waste Disposal in Continental Geological Formations** aims at evaluating the long-term risks of waste disposal. It includes both theoretical evaluation activities and experimental activities in view of providing the necessary models and data base for the evaluation.*
3. ***Feasibility and Safety of Waste Disposal in Deep Oceanic Sediments** aims at evaluating feasibility and long-term risks of this advanced disposal option. These activities are carried out in the framework of a NEA-coordinated programme and the JRC contributes both in experimental and theoretical activities and in the programme coordination.*

Research Area 1
Waste Management and the Fuel Cycle

Setting-Up of PETRA

All orders for standard components were completed in 1986. The installation of components and their connection has proceeded, with some delay as compared with the original planning. Upon request of the Italian licensing authority, a programme of seismic upgrading of the building has been initiated. As a result, the latest planning indicates mechanical and electrical connections completed by September 1988. Hot commissioning is scheduled to start in March 1989.

The denitration process has been studied with a special care in view of the possible safety implications. A cold unit has been constructed and operated for 16 months, leading to improved operational procedures.

The PETRA users' group has met twice in 1987. Several proposals for activities to be implemented in the facility have been put forward and they are being ranked in priority order.

Analytical Support Activities

The pneumatic transfer system, connecting the PETRA cells to the analytical laboratories, located in another building about 200 metres away from the cells, has been completed and tested. Departure and arrival stations in alpha-tight boxes will be assembled in 1988.

The analytical handbook of 1984 has been revised and updated. General analytical support for the programme has been provided upon request, particularly on clay samples and seabed sediments. The techniques of inductively-coupled plasma - mass spectrometry (ICP-MS) has been evaluated for analytical capability and sensitivity in routine use, taking advantage of an instrument temporarily available for demonstration purposes. The technique appears particularly suited to our analytical requirements, and the acquisition of an ICP-MS has been planned for 1988.

Radioisotope production by cyclotron irradiation was limited in 1987 to the production of $2x10^7$ Bq of ^{95}Tc.

The OXAL-MAW Process

Tests on about 20 liters of "real" MAW, obtained from the WAK plant, have been carried out using procedures previously set up on simulated solutions, which lead to decontamination factors higher than 5000 for Am using Ca as a carrier, while lower DF, around 50-80, were obtained for Pu.

The verification of the process with real waste solutions gave decontamination factors similar to those obtained using simulate solutions. It appears that by a careful control of the precipitation conditions an alpha-free final product could be obtained, when the resulting filtrate is solidified, e.g. in a cement matrix.

Characterization of High Activity Glass

An exploratory activity on the feasibility of characterising fully active vitrified waste has been carried out, using glasses prepared in the ESTER facility of ENEA at Ispra. This activity was carried out in collaboration with ENEA COMB-SVITE/JRC-Ispra, in view of an increased engagement of the Transuranium Institute in this area.

Tests included the determination of the exial distribution of fission products by gamma scanning and radiography techniques, and microstructure determination on three polished sections of the glass by quantitative microscopy, scanning electron microscopy, backscatter imaging and EDAX analysis.

Actinide Monitoring

Techniques of passive neutron assay by time correlation analysis are being developed at JRC-Ispra for Pu monitoring in waste drums prepared for ultimate storage in geological formation. The laboratory version of the instrument is continuously upgraded to an industrial version, characterized by heavy hardware components and on-line data elaboration. Several correlation analysis methods have been evaluated for optimizing data elaboration.

A contract has been signed with ENEA-Casaccia to apply that technique to in-field tests on 200 liters waste drums stored at the Casaccia centre.

A gamma scanner is also being set up for measuring Pu in 200 liters waste drums. The determination is based on measurement of the emitted gamma rats by high resolution gamma ray spectroscopy, and correlation for gamma attenuation by gamma transmission measurements using a ^{75}Se gamma source.

The collaboration with DNPDE at Dounreay is continuing, particularly on correction methods for neutron multiplication and absorption, corrections due to presence of Cm isotopes, and modification of the neutron interrogation model to allow the use of a californium shuffler.

JRC-Ispra has participated and assured the secretariat of a European intercomparison exercise for the monitoring of Pu in Pu-contaminated waste. The final report of the exercise is in preparation.

Research Area 2
Safety Assessment

Risk Assessment

Contribution to the PAGIS action (Performance Assessment of Geological formation Systems) has continued in view of terminating the project in 1988. The activity of the JRC was mainly to support the various institutes on the methodological issues, particularly on sensitivity and uncertainty analysis.

A contribution to the NEA activities in the area of probabilistic safety assessment was given by participation to the NEA-PSAC group and help in organizing intercomparison exercises, which are of major importance for quality assurance of the codes used in safety assessment.

A 3rd release of the probabilistic risk assessment code LISA was issued in 1987; this version, which includes pre- and post-processors (PREP and SPOP) will be delivered by the NEA data bank. A 4th release, including a commercial geosphere model (THOUGH) has been prepared for customers.

A cooperation agreement has been signed with ENRESA (Spain) for the preparation of a new version of LISA, specifically designed for probabilistic risk assessment of waste disposal in hard rock geological formations.

Preparatory work was made to held in May 1988 an advanced seminar on risk analysis in nuclear waste management.

Near Field Evolution

The study of glass leaching in clay and seabed sediments at constant temperature has continued and is approaching termination. Experiments carried out on a ^{95}Tc spiked glass have confirmed a lower mobility of Tc for clays and sediments with a low Eh.

An equipment has been constructed to study corrosion and leaching phenomena under a thermal gradient, with upper temperatures of about 90°C and thermal gradients of about 1°C/cm. The equipment was used to study corrosion of mild steel in seabed sediments. Provisional results indicate that a crust mainly composed of calcium carbonate and iron silicate is formed, acting as an additional barrier against diffusion.

The study of surface phenomena by the ESCA technique has continued, particularly on the role of $-HCO_3$ ions, building up on previous experience on the role of pH and Eh in leaching.

The on-going study on waste glasses doped with ^{244}Cm in order to realistically simulate radiation damage in an acceptable short time nave continued. Damage levels corresponding to storage times of real waste glasses in excess of ten thousand years have been produced. The results obtained confirm previous findings, indicating little effect of radiation damage on glasses, while waste ceramics show significant increase in swelling and leaching. Explortory work on possible temperature effects during damage production has been carried out by implanting 50-200 keV Kr ions to produce temperatures between 100 and 250°C during implantation. Fracture toughness, radiation-enhanced Na diffusion and leaching seem to be affected enough to justify inclusion of temperature during damage as a relevant parameter in future works.

Activities on alkali diffusion within the glass block under the temperature profiles existing in the blocks in disposal conditions have been terminated and discussed in an international workshop on radiation effects in waste matrices. It is now possible to affirm that these effects will have no practical impact on the long term behaviour of the glass block at disposal.

The effect of various stable elements possibly present in alpha-contaminated waste (Cr and Ni in particular) on the durability of concrete-based matrices has been studied by preparing concrete with variable quantities of Cr and Ni compounds and measuring the physical properties and leaching characteristics of the product. It appears that concrete is a good host material for Ni and Cr, provided this last is in the reduced Cr_3^+ state.

Far Field Studies

Activities on the migration of radionuclides in geological media have continued in order to provide models and input data for risk assessment codes.

The leaching behaviour of borosilicate glass dopes with Np, Tc, Pu, Am using bicarbonate water, saturated brine and saline aquifers typical of experimental disposal sites has been studied in oxic and anoxic conditions. Np and Tc release rates are similar to those measured for Na in oxic conditions, while considerably lower release rates were found in anoxic conditions. This behaviour is consistent with the release models previouly established. The behaviour of Am, reduced Np and Pu suggests an interaction with the surface gel layer, which deserves further investigations.

The interaction of the released radionuclides and porous geological media has been studied by columns experiments, with special attention to the behaviour of Pu and Np under reducing conditions. The results obtained are indicative for a complex situation which cannot easily be interpreted by the existing models, and additional experimental and modelling activities are underway.

Adsorption on natural colloids, which can be a dominant factor in determining the radionuclide behaviour in natural groundwaters, is being studied in collaboration with the University of Milano. The adsorption behaviour seems strongly dependent on the pH and Eh conditions, although the results are still preliminary.

Techniques of laser spectroscopy, namely thermal lensing and time resolved fluorescence spectroscopy, are being developed to study the behaviour of very dilute chemical species of actinides and fission products. The results obtained up to now on uranium complexation by carbonate ions suggest a greater involvement in the development of the technique as a major tool for the study of actinide chemistry in natural groundwaters.

The hydro-geochemical characterization of a test site near the Radiochemsitry building is under way, in view of its possible use for the in-situ verification of transport models for both radioactive and chemical toxic compounds. Four boreholes have been equipped for hydrological experiments, and sensors connected to an automatic data acquisition system. Experiments are still under way for a full understanding of the hydrodynamic behaviour of the aquifer, which is rather complex. Eh measurements on two boreholes show a strong variations of redox potential from top to bottom, while more constant parameters have been found for the other boreholes.

A review of the literature published on the natural nuclear reactor discovered in 1971 at Oklo (Gabon) is under way in order to assess the potential use of this case as a natural analog of a real waste disposal situation.

The JRC is contributing to two international projects on radionuclide migration, namely the CEC working group in colloids and complexes, and the NEA thermodynamic data base project. A joint project with ENRESA (Spain) is being prepared on investigation of radionuclide migration in crystalline rokcs.

Research Area 3
Feasibility and Safety of Waste Disposal in Deep Oceanic Sediments

Feasibility and Safety Assessment

The probabilistic risk assessment of the sub-seabed option, carried out for the NEA seabed working group, has been completed and forwarded to the relevant task group for inclusion in the final report. The main conclusions are :

- For the base case scenario the peak of the dose rate over time for the maximally exposed group of individuals is over 100,000 times smaller that the ICRP recommended limit of 1 mSv/a.
- The uncertainty rage falls between $3x10^{-15}$ and $4x10^{-8}$ Sv/a and does not affect the conclusions of the deterministic assessment.
- The radionuclides contributing most to the dose are the long-lived poorly adsorbed fission products, principally ^{95}Tc.
- The major pathway is consumption of fish, molluscs and seaweeds.
- No significant different was found between the two sites considered (GME and SNAP), although the quality of their sediments is slightly different.

Instrumentation for In-Situ Experiments

The instrumentation for in-situ experiments developed by the JRC throughout the programme aimed essentially to develop the expertise for long-term experiments utilizing automatic acoustic transmission of data from sensors in the implaced penetrators to a floating buoy or platform and radio transmission through a satellite to the land based laboratory.

The instrumentation has been completed in 1987 with the development of a "soft lander", a vehicle which can

- deploy a reasonable load of specialized instrumentation within the first few meters of the sea floor,
- carry sufficient power for the emplaced sensors for up to one year lifetime,
- transmit data to the platform throughout the experiment,
- be recovered at the end for redeployment.

At present the unit has been constructed and the acoustic link tested. A geochemical commercial package has been tested. Tests will be continued in 1988 on lake Maggiore, in view of successive application in the field of environmental protection.

Participation to Joint In-Situ Experiments and Laboratory Simulation Experiments

No cruise has been done in 1987. The analysis of samples taken fron two cores collected at the Madeira and Nares abyssal plains during the ESOPE cruise in 1985 has been completed. The study oif the two cores has highlighted the significance of the different mineralogies of the sediments found at the two study sites.

The collected sediments were utilized for laboratory studies on radionuclide migration, with techniques similar to those utilized for the study of continental options. The results obtained in 1987 mainly refer to the behaviour of ^{241}Am, which was found largely associated with the carbonate fraction, and to ^{95}Tc, both in oxic and anoxic conditions. An experiment using simulated vitrified waste doped with a mixture of radioisotopes (^{113}Sn, ^{137}Cs, ^{237}Np and ^{241}Am) was started.

Tests have been conducted to study the influence of pressure and temperature on the diffusion of important radionuclides (Pu, Np, Tc) in deep ocean sediments, to check whether measurements of diffusion made under atmospheric pressure can truly represent the behaviour of those radionuclides in the deep sea environment. The results obtained up to now confirm the validity of low pressure simulation experiments.

RESEARCH AREAS

1. Waste Management and the Fuel Cycle

This project aims at studying the present fuel cycle processes with a special reference to the waste produced (considering types, quantities and qualities) and eventually proposing process modifications which could be implemented in future fuel cycle installations, in order to minimize waste arisings and improve the waste quality in relation to the final objective of disposing of radioactive waste in geological formations.

The characterization of conditioned waste products presently produced by fuel reprocessing and fabrication is an important aspect of this project, which will be further expanded in the future, in view of the importance that quality control of waste products is gaining for the practical implementation of radioactive waste management.

Characterization activities range from detailed analysis of vitrified high activity waste to non-destructive determination of actinides in conditioned alpha-contaminated waste. The first subject is studied at the Karlsruhe Establishment of the JRC, which will have in the future an increased involvement in this area, including characterization of spent fuel and other types of high activity waste which may result from fuel process modification proposals.

Such process modifications, which may come from JRC studies (such as the OXAL process) or from national laboratories of EC member states or industries, can be verified at a fully active pre-industrial scale in the PETRA hot cell facility currently under construction at Ispra.

PETRA (Project of Evaluating Treatments for Radwaste Alternatives) is indeed designed to produce various types of fully active conditioned waste resulting from the operation of a Purex type reprocessing plant in either standard or modified modes. The facility is proposed for :

- *studies of optimization of waste management and*
- *the production of typical and off-standard conditioned products for the study of quality control methods or other purposes.*

Contents

1.1 Setting up of PETRA (B. Hunt)

The PETRA plant is an experimental facility which will operate at a pre-industrial, fully active scale, where the treatment of LWR fuel material at high burn-up (33000 MWd/t) will be undertaken for the extraction of uranium and plutonium and the successive treatment of high active waste (HAW) and other waste streams generated during this operation.

The HAW, or indeed fractions of it, will be made available for conditioning in glass or ceramic matrices. The fundamental basic aim of the experimental facility is to implement treatment and conditioning processes on the various waste streams generated during Purex type operations.

The objectives of the PETRA facility are directed towards verification, demonstration and optimisation of concepts under study and already established at the laboratory scale level, rather than on new concepts /1,2/. Their implementation will be achieved by both a "soft" and "hardware" approach, i.e. by evaluation and assessment studies and also by experimental verifications pursuing the following general objectives :

- *characterize, chemically and physically the waste streams from reference and non-standard fuel material,*
- *prepare conditioned waste with the anticipated specific activity levels for characterisation and for testing of source terms in disposal routes,*
- *explore the feasibility of reduction of waste generation and optimisation of waste categories,*
- *study the performance of different waste treatment conditioning procedures and processes and of the corresponding final waste forms.*

On the basis of the invitation to tender in late 1983 for the PETRA project, a consortium composed of Kraftanlagen (Heidelberg), TEAM (Rome) and ZANON (Genoa) were selected. Both Kraftanlagen and TEAM combined in a joint venture for the design, followed by the surveillance during construction and commissioning of the facility. ZANON are the main contractor for component manufacture and installation.

The hardware for the hot experimental verification of this project is to be installed in three hot cells (4305, 4306, 4307) of the ADECO Laboratory on a surface area of 43 m^2. In Fig. 1.1, a cross-section of the ADECO hot cells is given. In particular, the three PETRA hot cells are devoted to the following operations :

- cell 4305, high temperature cell, vitrification, calcination
- cell 4306, treatment of fuel and waste, e.g. dissolution concentration, denitration, etc.
- cell 4307, solvent extraction using mixer settlers.

Another shielded area (cell 4303) is available for the installation of the hot analytical support. Pneumatic systems are used to transfer the samples from process cells and, after appropriate dilution or extraction, to the Radiochemistry building for radiometric assay.

Already two hot cells (4304, 4411) are available for performing mechanical operations on either irradiated fuel material or conditioned waste specimens. The layout of the process equipment in PETRA is referred to a batch-wise treatment capacity of 6 kg U through the following single unit operations :

- dissolution and feed clarification (by filtration)
- co-decontamination cycle and solvent regeneration
- U/Pu concentration
- U/Pu calcination
- HAW concentration
- MAW concentration
- denitration and eventually oxalate precipitation
- vitrification
- actinides purification.

Most of these unit operations will be performed on a day-shift schedule and in anyway in a sequential operating mode. PETRA will also be able to accept waste solutions transported by a "cendrillon' type system, from wherever they may be available, thus enhancing the flexibility of the facility.

The in-cell equipment is composed of :

- 18 vessels of cylindrical and slab shapes respectively with volumes in the range from 10 to 120 litres. Three of them

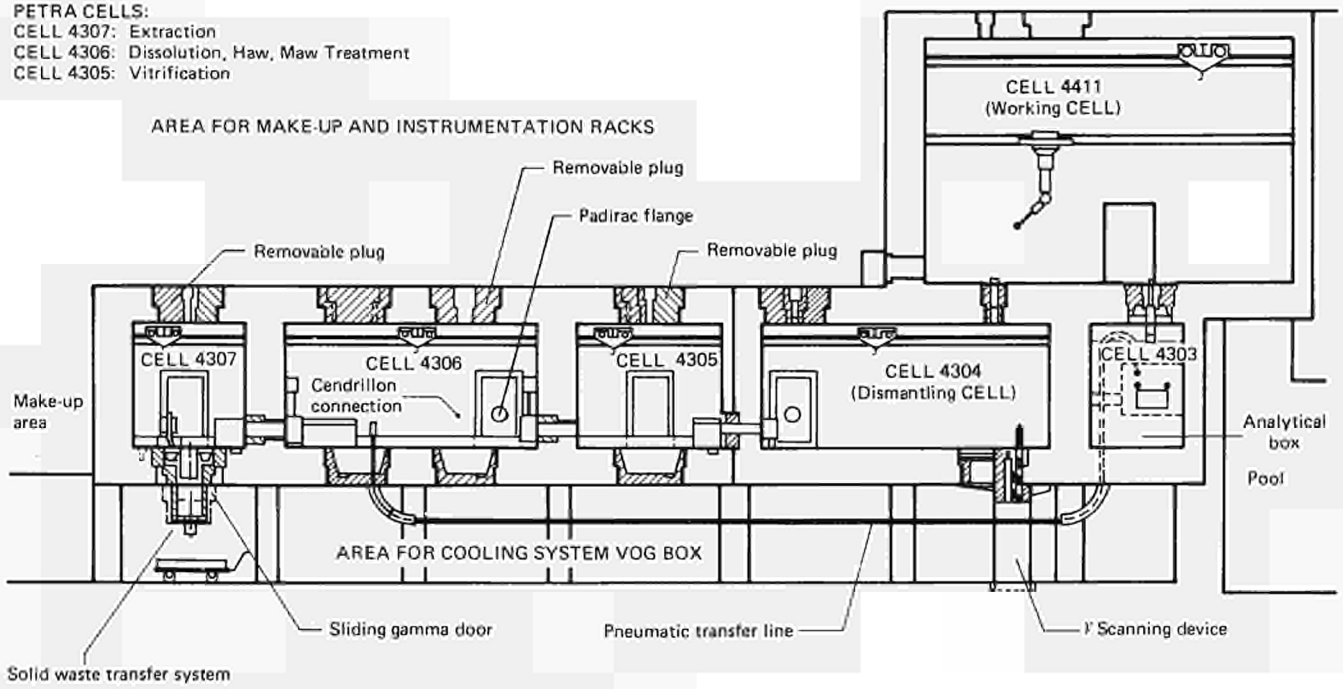

Fig. 1.1 — Vertical cross-section of the ADECO hot cells

can be evacuated and two are equipped with mechanical stirrers;
- 4 heatable units with their condensors, to serve as reactors and evaporators (nominal evaporation rate 10 dm^3/h);
- 2 furnaces for high temperature processes (up to 1600°C);
- 6 mixer-settler banks for counter-current extraction operations;
- 2 off-gas scrubbing columns in series;
- 2 filters for liquids and 2 off-gas filters;
- 8 dosimetric pumps and one peristaltic pump;
- 27 vacuum pots to support liquid transfer by air lifts;
- sampling system for all vessel and heatable units.

An overview on the types and amounts of process streams is shown in Fig. 1.2.

The single units of the in-cell equipment are interconnected with metal to metal couplings, which can be handled remotely. Accordingly to an order of priority established on operation requirements (e.g. filters and crucibles), on forecasted maintenance frequencies (e.g. dosimetric pumps) and eventually on process scheme variations, the units have been placed in positions accessible for remote handling, in order to assure a high degree of flexibility whilst at the same time minimising exposure to operators.

For this purpose, a 1:5 scale model was prepared for layout optimisation purposes. The concept of remote handling has also been extensively applied to all in-cell instrumentation. The construction material is basically AISI 316L SS except the reactors which are built in Incaloy 825.

The PETRA plant process control and information system has been designed in order to satisfy in one logical and physical structure the different needs of its potential users, assuring at the same time flexibility and safety. From the hardware point of view, the system is based on a three-level hierarchical architecture, the low level of which is devoted to data acquisition and process control, whilst the other two levels are devoted to graphical supervision and management (see Fig. 1.3).

The decision to install the PETRA facility in the existing spare hot cells of ADECO which forms a part of the licensed nuclear installations in the ESSOR complex, was motivated by economical reasons and by expected time sharing in the licensing procedure by the Italian safety authorities. Indeed, the facility takes advantage from the extended support possibilities provided by the already operating cells and the connected storage pool, the intervention area, the decontamination facilities, the hot workshop, the ventilation system, the radiation protection surveillance and monitoring of all utilities including highly reliable power supply systems, etc.

The demand for the operational license was therefore presented as a modification of the existing ESSOR license; and after analysis of the "Preliminary Safety Report", ENEA-DISP (the Italian Authority) has decided to initiate control only at the beginning of hot commissioning.

The utilisation of a hot cell facility designed more than 20 years ago implies, of course, the acceptance of some drawbacks and shortcomings with respect to current recommended concepts and standards. Nevertheless, a concept has been developed to achieve minimal radiation exposure during maintenance, modification and eventually decommissioning of most of the PETRA components by remote operation. Equipment and cell walls can be washed by jets and the liquid collected in drip trays, from where it is transferred to sump vessels and evaporators. The integrity of the cells is supported by a high efficient dynamic containment barrier on a very reliable ventilation system.

Modification of the Hot Cell Complex ADECO

In the setting-up of PETRA, a pre-requisite was the need for modification of the ADECO hot cells for housing PETRA. The modification and preparation of ADECO concerned principally :
- decontamination of cell 4305
- various civil work involving penetrations between cells and

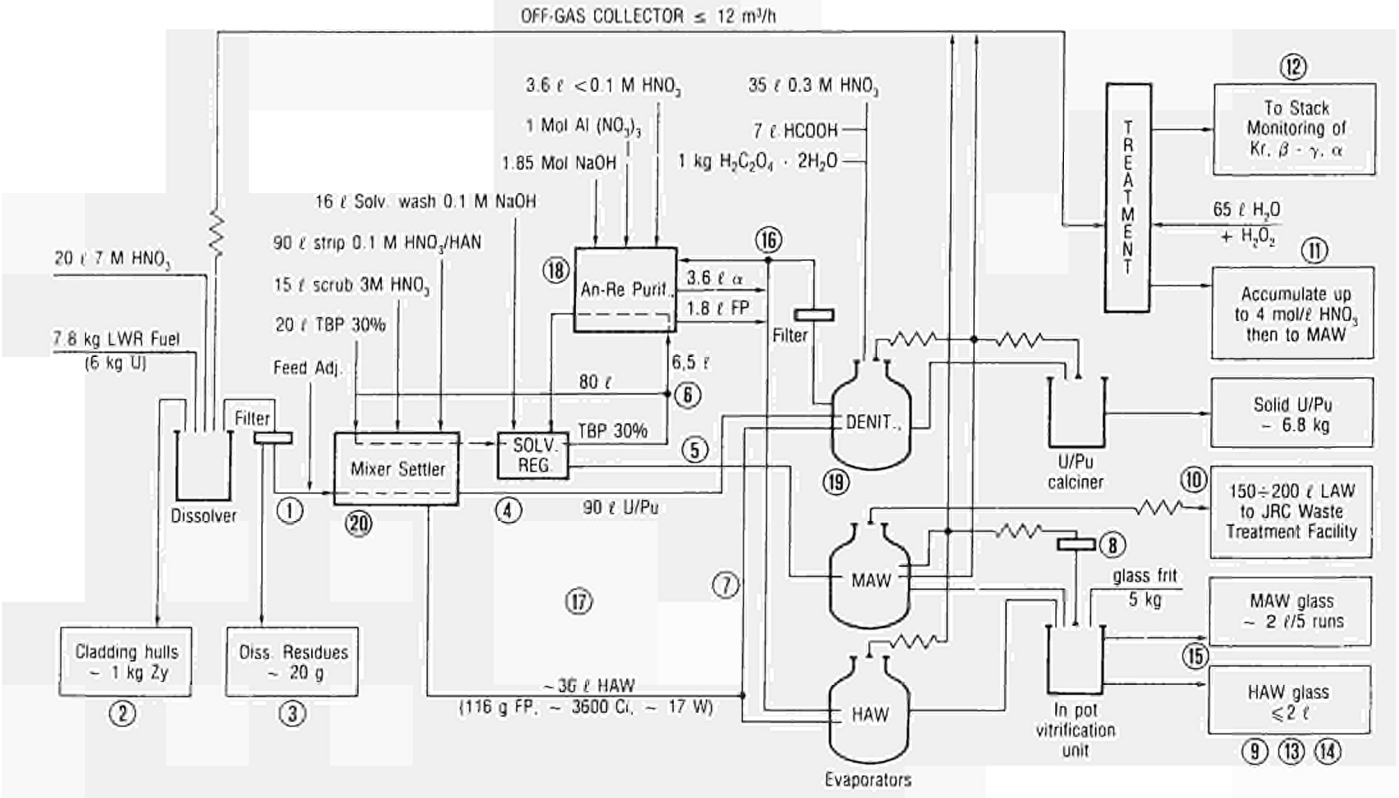

Fig. 1.2 — Process units, input streams and output products of PETRA

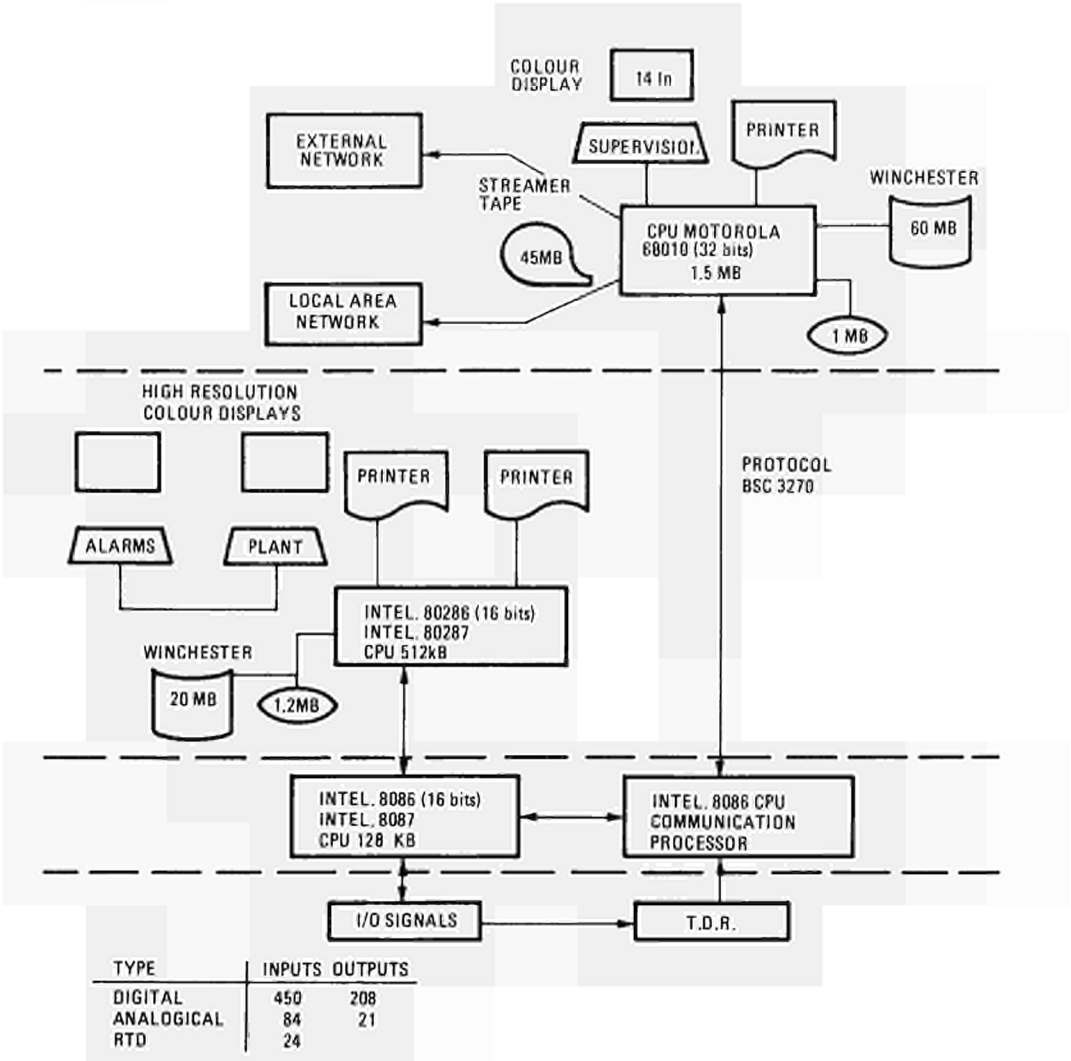

Fig. 1.3 — Hardware set-up for process control system

adjacent rooms for various services, new rooms for make-up and analytical subsystems, etc.
- modifications and replacement of the cells exhaust ventilation duct systems and installation of new instrumentation services to the ADECO ventilation system to accommodate the needs of PETRA;
- installation of a pneumatic system to transfer samples from ADECO to the Radiochemistry building for subsequent radiometric assay.

In 1986, a request by the safety authorities to examine the structure of the walls housing the facilities in the ESSOR complex, resulted in the need to reinforce certain supporting walls. The effect of this civil engineering work is estimated to delay the project by about six months. As a result the latest planning indicates that all the mechanical and electrical installation will be completed by September 1988 and ready for the cold-testing phase. Hot commissioning and testing is foreseen for September 1989.

Construction and Installation of the PETRA Plant

The PETRA plant construction activity has been carried out by the NFCD and NED divisions of the JRC, in close co-operation with the Consortium, in particular on :

- the completion of the detailed designs of piping and layout of the out-of-cell components,
- the completion of detailed designs of constructional drawings of all engineered items,
- the verification of single components telemanipulability.

All orders for standard components were completed in 1986. The construction, delivery, installation and testing of the waste transportation system to be coupled with the PETRA plant in cell 4307 was carried out in 1986 with the first series of functional tests successfully completed. Special mechanical and electrical components with a high engineering content, e.g. mixer settlers, vessels, reactors, plug penetrations, etc., were tested at the manufacturer's workshops prior to site delivery. Figs. 1.4 and 1.5 show views of plant equipment during installation in the hot cells.

Concerning the operational performance of key components and processes a number of cold tests have been performed on a 1:1 scale, in particular on :

- air-lift transfer systems
- drum-dryer heating requirements
- simulated U/Pu calcination process utilising aluminium nitrate solution
- denitration process.

Tests currently undergoing investigation concern :

- the resin absorption capacity for aqueous streams containing organic extractant
- the filtration system adapted for clean-up of the dissolver liquor.

The denitration process is worthy of special mention since this has been adopted for use in the PETRA facility in order to reduce the nitric acid concentration in waste solutions. This process is of particular significance from a safety point of view; a cold pilot plant was constructed on a similar scale to that in PETRA, to establish the design and operating conditions. The pilot plant

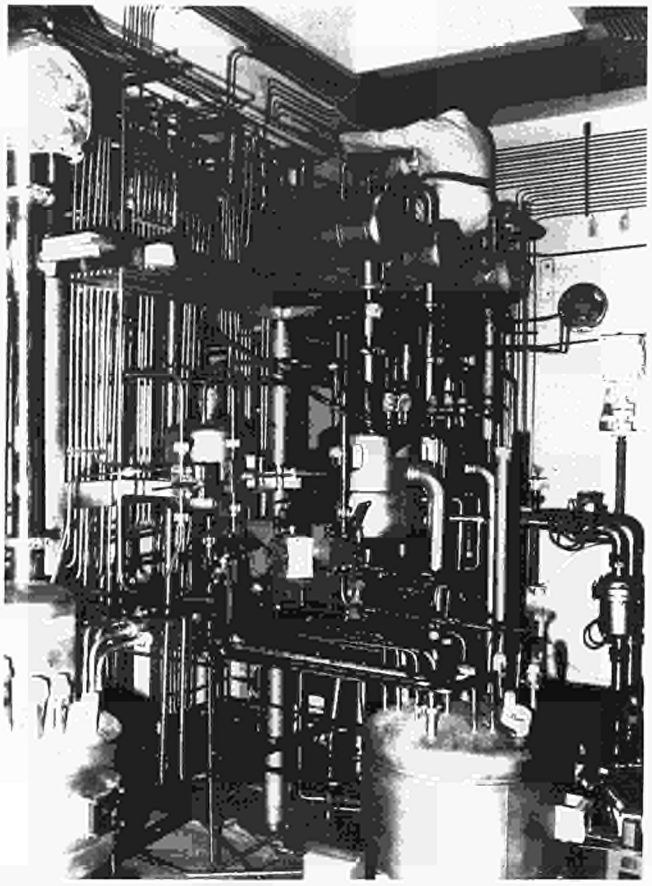

Fig. 1.4 — View of denitrator vessel, evaporator and associated condensers and pipework in cell 4306 (photo taken by ADECO-ESSOR staff)

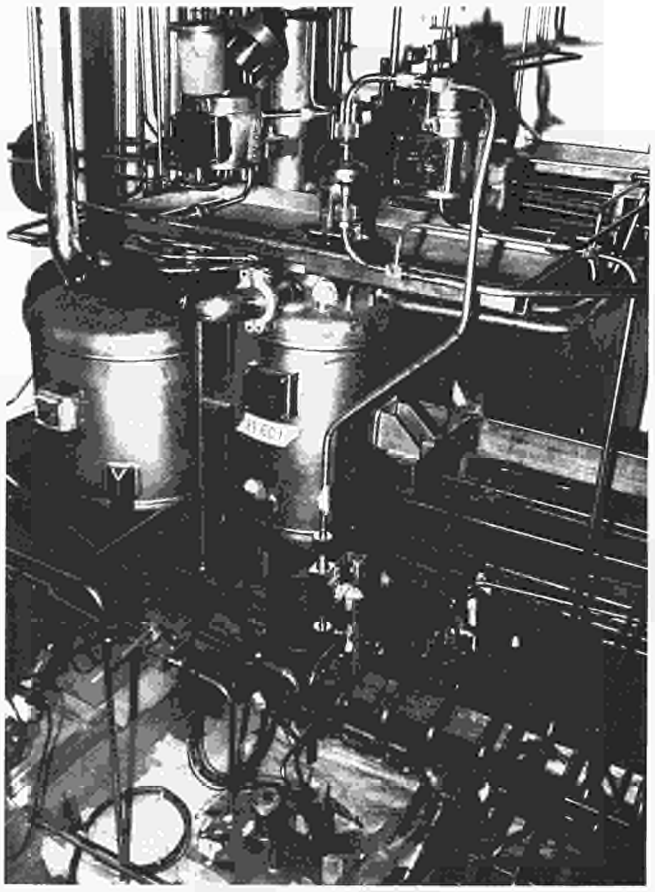

Fig. 1.5 — View of dissolver showing filters and drip tray (photo taken by ADECO-ESSOR staff)

was operated over a period of 16 months. The information acquired led to the adoption of operational safety procedures and process control parameters. The results of this work were also presented at a seminar devoted specifically to the denitration of radioactive liquid waste /3/.

The PETRA facility is open to international co-operation so that management schemes developed in the laboratories of the European Community and other interested countries may be jointly tested. Already a collaboration contract with ENEA has been established, and their personnel are working in close liaison with members of the NFCD and NED divisions of the JRC in pursuing the objective of setting-up of PETRA. This collaboration agreement is foreseen to be renewed for a further four year period from 1988-1991.

Research Activity Planning

The research activity planning of PETRA has been supported by previous waste management assessment studies of alternative management modes and by the creation of a PETRA Users Group comprising experts from the member countries with nuclear programmes. Up to the end of 1987 four meetings of the Users Group had been held.

Already a preliminary screening of proposals has placed in evidence a number of objectives for PETRA, such as :

- generation of reference wastes as source terms arising from standard reprocessing operations
- characterisation of dissolver residues and conditioned waste
- merging of waste streams
- recovery of valuable products
- conditioning of wastes in high quality matrices.

A summary of the proposals is given in Table 1.I. These proposals have been identified as follows :

- processes which could be implemented in PETRA immediately,

Table 1.I - Ranking of the PETRA's User Group Suggestions with an Indication of the Modifications and R&D Requirements

Proposals	Modifications	R & D
Reference Waste	0	0
Dissolver Residues Characterisation	00	0
Separation of actinides PPTN (OXAL)	0	0
Vitrif. of high Na+ glasses	0	00
Merging of wastes	0	00
Sol. Extract. for Act. Sep.	0	00
Separations liq. mem., ultrafilt., etc.	000	00
Volatiles from Vitrification	00	0
Conditioning of MTR	0	00
Selective Sep. (Vitrokele)	000	000
IX for waste treat./cond.	000	00
Waste Manag. Spent Solvent	00	00
Recovery of Cs/Sr from waste	00/000	00
Suspension fines separation	000	000
Iodine balance	00	0
Conditioning in ceramics	00/000	00
Analytical Waste	0	00
Recovery of Valuable Materials	00/000	000
Act. Sep. from Vitrified Waste	0000	00
High Density Fuels C/N	0	00
Rare Gases Separation	0000	00

0 = no effort; 00 = limited effort; 000 = large effort
0000 = intensive effort

- processes where modifications in the cells would be required,
- proposals which can be carried out in parallel with other activities.

Several proposals can indeed be implemented during the hot commissioning phase.

The commissioning of PETRA will, in fact, follow the lines of verifying the conditions taken as a reference case in the safety report already submitted to the Italian Safety Authorities. The reference conditions will treat LWR high burn-up fuel (33,000 MWD/MTHM) in the PETRA facility through the following unit operations.

Dissolution

- off-gas analysis

Filtration

- fines collection and characterisation
- hulls collection and characterisation

Solvent extraction

- HLLW characterisation
- aqueous solvent wash waste (MLLW) characterisation

HLLW concentration

- HLLW concentrate characterisation

Vitrification

- glass product characterisation
- off-gas analysis

Denitration/precipitation

- OXAL process.

In addition to the modifications which may be necessary for PETRA to accommodate new proposals, it is assumed that any R & D work and subsequent hot testing will have been performed before attempting to carry out a proposed activity at the scale and radioactivity level of PETRA. Table 1.I summarises also in a qualitative way the need for modifications or R & D for each proposal. Prior to going hot, studies are underway in greater detail to evaluate and eventually implement any modifications deemed necessary by the future research requirements.

References

/1/ B.A. HUNT, H. DWORSCHAK — A Reference Reprocessing Facility for Waste Management Assessment Studies — Technical Note No. I.06.03.81.30

/2/ B.A. HUNT, H. DWORSCHAK — Alternative Treatment Modes for Medium Level Liquid Waste. Radioactive Waste Management and the Nuclear Fuel Cycle, 5 June 1984, pp. 1-37

/3/ G. VASSALLO et al. — Application of Denitration/Oxalate Precipitation in the PETRA Hot-Cell Facility. Seminar on the Denitration of Radioactive Liquid Waste, Jülich 1988, L. Cecille and S. Halaszovich (Eds.)

1.2 Analytical Support Activities (F. Mousty)

Aim of this activity is mainly to provide the general analytical support (methods and equipment) for the whole programme. It is split into 5 tasks :

1. *to set up analytical methods and to provide the support for PETRA control,*
2. *to provide an analytical support to various experimental activities of the programme,*
3. *to produce special radioisotopes by using the JRC-Ispra cyclotron facility,*
4. *to complete the LMA cells for fully active miniscale tests,*
5. *to develop chemical flowsheets for PETRA.*

The organization of the various facilities and the flow of radioactive samples between the various facilities are shown in Fig. 1.6.

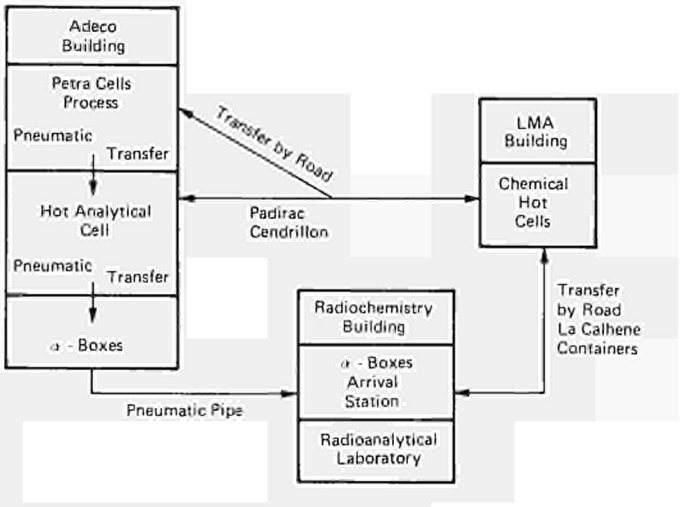

Fig. 1.6 - Organization of the activities

Analytical Support to PETRA

The pneumatic transfer system of low active samples from ADECO to the Radiochemistry building has been completed and several cold tests successfully performed. The system consists of an inner tube (internal diameter 59 mm) and an outer protection tube located about one metre under ground level. The distance between the two buildings is about 200 metres and 8 wells have been built for inspection and maintenance. The transfer containers are commercially available (AIRFIX trade-mark) and can contain 4 penicillin vials (capacity 10 cm^3). Departure and arrival stations will be installed in alpha-tight boxes.

The assembling of the arrival box is under way, while the departure box will be assembled in parallel with the setting up of the hot analytical cell. While the definitive set-up of the PETRA laboratory is being completed, the analytical handbook of May 1984 has been revised and updated. As in the previous version, the PUREX process has been considered as the basic one which gives rise to all the effluents successively treated. Table 1.II shows the main streams of the process together with the elements to be determined, the expected concentration range, the priority of the analysis, the activity level and the selected methods.

All the methods listed in Table 1.II, except polarography and inductively coupled plasma-mass spectrometry (ICP-MS) are or have been used in the frame of the current programmes

Table 1.II - PETRA Analytical Sheet

Effluent	No.	Tank	Analyte	Concentrat.	Priority (1)	Activity (2)	Method
	3		HNO_3	5-7 M/l	r	+	Titrimetry-oxalates
DP 6/8 aqueous safeguards		B01	HNO_3	2-4 M/l	r	+	Titrimetry-oxalates
			U	200-300 g/l	r.s	+.—	Chemical separation dilution, potentiometry, Coulometry-Spectrophotometry
			Pu	2-3 g/l	r.s	+.—	Chemical separation. dilution. α-spectrometry. spectrophotometry
			FP	100-300 Ci/l	r.s	—	Chemical separation. dilution. γ-spectrometry. ETAAS
			Np	0.1 g/l	s	—	Chemical separation. α-spectrometry. polarography
			Am-Cm	0.05 g/l	s	—	Chemical separation. dilution. α- and γ-spectrometry
			Density	1.1	s	+	
HAF 10/3 aqueous		B01	HNO_3	3 M/l	r	+	Titrimetry-oxalates
			U	200 g/l	r	+.—	Chemical separation. dilution. potentiometry, Coulometry - Spectrophotometry
HAW 12/30 aqueous		B12	HNO_3	2.5-3 M/l	r	+	Titrimetry-oxalates
			U	0.1-1 g/l	r.ro	—	Dilution. chemical separation. spectrophotometry.
			Pu	10 mg/l	r	—	Chemical separation. α-spectrometry
			Np	<0.1 g/l	s	—	Chemical separation. α-spectrometry. polarography
			Am-Cm	0.05 g/l	s	—	Chemical separation. dilution. α- and γ-spectrometry
			RE	2 g/l	s	—	Dilution. γ-spectrometry
HAS 15 aqueous		Mu	HNO_3	3-4 M/l	r	*	Titrimetry-oxalates
CP 16 aqueous		B04	U	60-70 g/l	r	+.—	Chemical separation. dilution. potentiometry. Coulometry-Spectrophotometry.
			Pu	0.5 g/l	r	—	Chemical separation. dilution. α-spectrometry. Spectrophotometry
			FP	0.1-1 Ci/l	r	—	Dilution. γ-spectrometry. ETAAS
			Np	<30 mg/l	s	—	Chemical separation. α-spectrometry. polarography
CW 17			U	<1 g/l	ro	—	Chemical separation. spectrophotometry.
CX 18		Mu	HNO_3	0.01 M/l	r	*	pH-dilution
			HAN	0.05 M/l	r	—	Potentiometry Ce^{IV}
31		Mu	HCOOH	pure	r	*	Volume adjustment
32		Mu	$H_2C_2O_4$	solid	r	*	Balance
HAW 35 aqueous		B08	HNO_3	<0.8 M/l	r	+	Titrimetry-oxalates. pH
			U	0.1-1 g/l	s	—	Chemical separation. spectrophotometry.
			Pu	<0.1 mg/l	s	—	Chemical separation. α-spectrometry
			Ce.Eu	traces	s	—	γ-spectrometry. chemical separation
			FP	50-100 Ci/l	s	—	Dilution. γ-spectrometry.
			HCOOH	traces	s	—	Titrimetry. TBAH
			Am-Cm	\0.01 mg/l	s	—	Chemical separation. α-spectrometry
			Np	traces	s	—	α-spectrometry. polarography
34		Mu	HNO_3	0.8 M/l	r	*	Titrimetry-oxalates. pH
36		Mu	HNO_3	8 M/l	r	*	Titrimetry-oxalates
OX 39 aqueous		B03	HNO_3	4 M/l	r	+	Titrimetry-oxalates
			U	0.01-0.1 g/l	s	—	Chemical separation spectrophometry.
			Pu	0.1-0.5 g/l	s	—	Chemical separation. α-spectrometry. spectrophotometry.
			Ba.Sr.Zr		s	—	Dilution. ETAAS.
			Am-Cm	1 g/l	s	—	chemical separation. α-spectrometry
			Np	0.1-0.2 g/l	s	—	Chemical separation. α-spectrometry. polarography
			HCOOH	traces	s	—	Titrimetry. TBAH

Table 1.II - Continued

Effluent	No.	Tank	Analyte	Concentrat.	Priority (1)	Activity (2)	Method
	40	Mu	HNO_3	1 M/l	r	*	Titrimetry-oxalates
aquous	41	BO4	HNO_3	0.5-0.8 M/l	r	+	Titrimetry-oxalates
			U	0.01-0.1 g/l	s	—	Chemical separation, spectrophotometry,
			Pu	0.1-0.5 g/l	s	—	Chemical separation, α-spectrometry, spectrophotometry,
			Np	0.1-0.2 g/l	s	—	Chemical separation, α-spectrometry, polarography
			Am-Cm	traces	s	—	Chemical separation, α- and γ-spectrometry
	42	Mu	HNO_3	0.01 M/l	r	*	pH
			HAN	0.05 M/l	r	*	Ce^{IV} potentiometry
aqueous	44	B10	HNO_3	3.4 M/l	r	+	Titrimetry-oxalates
			U	traces	s	—	ETAAS, spectrophotometry,
			Pu	traces	s	—	Chemical separation, α-spectrometry
			Np	traces	s	—	Polarography
	46	Mu	$Al(NO_3)_xN$		r	*	Titrimetry
aqueous	47	B10	HNO_3	0.2 M/l	r	+	Titrimetry
			Al^{3+}	0.5-0.6 M/l	r	+	Titrimetry (EDTA)
			Na^+	1 M/l	r	+	Titrimetry
aqueous	48	B04	HNO_3	0.1 M/l	r	+	Titrimetry-oxalates
			Am-Cm	0.2-0.4 g/l	s	—	Dilution, α-spectrometry
			RE	20-30 g/l	s	—	Dilution, γspectrometry
			FP	traces	s	—	Dilution, γ-spectrometry,
			Ba-Sr	traces	s	—	ETAAS, ICP
	49	Mu	HNO_3	0.03 M/l	r	*	pH
aqueous	51	B08	Am-Cm	<0.1 mg/l	r,s	—	α- and γ-spectrometry
aqueous	28	B09	HNO_3	1.3 M/l	r	+	Titrimetry-oxalates
			density			+	
			PF		r	—	γ-spectrometry,
	24	B12	HNO_3	11 M/l	r	+	Titrimetry-oxalates
			density	1.4			
	26		HNO_3	2 M/l	r	+	Titrimetry-oxalates
organic	22	B07	TBP	30%	s	—	Titrimetry-ICP-AES
aqueous	21	B06	NaOH-Na_2CO_3	0.1 M/l	r	—	Titrimetry
			DBP-MBP		s	—	Titrimetry,
			FP	mCi	s	—	γ-spectrometry
			Alpha	mCi	s	—	α-spectrometry
	19	Mu	Na_2CO_3	0.1 M/l	r	*	Weight
			$H_2C_2O_4$	0.5 M/l	r	*	Weight
	20	Mu	NaOH	0.1 M/l	r	*	pH
	53	A10/11	HNO_3	4 M	r	—	Titrimetry-oxalates
			FP	mCi	s	—	γ-spectrometry

(1) PRIORITY: r = routine; s = special analysis; ro = routine on-line.
(2) ACTIVITY: + = measurement in the cell; — = sample activity lowered in the cell before sending to building 46;
* = non active sample.
ICP-AES = Inductively Coupled Plasma Atomic Emission Spectrometry
ETAAS = Electrothermal Atomic Absorption Spectrometry.
TBAH = Tributyl Ammonium Hydroxide.
EDTA = Ethylene Diamine Tetra Acetic Acid.

(Radioactive Waste Management and Safeguards and Fissile Materials Management), and need only be adapted to the specific requirements of PETRA. The availability of only one shielded analytical cell imposes to use it mainly as an intermediate station for lowering the radioactivity level of the samples either by dilution or by simple chemical separations. For that reason, only very simple analytical determinations are foreseen in the cell, such as electrochemical or light absorbance measurements Table 1.III shows where the main operations will take place as a consequence of the available facilities and of the analytical needs.

General Analytical Support

This activity provides an analytical support to the different tasks of the programme and is usually done on a routine basis. More than 650 samples of various forms and origins were analysed every year. Among them:

- ground water used in experiments on radionuclide migration,
- saturated sodium chloride solutions simulating brines from salt mines,
- pore water from sea-bed sediments,
- humic acids used for an intercomparison exercise among different European laboratories and from various sites,
- liquid samples produced during denitration tests,
- sediments collected during the 1985 international long core cruise (ESOPE),
- simulated sea-bed sediments used in column tests tc investigate concentration profiles,
- clays.

The principal determined elements are : silicon, calcium, magnesium, iron, sodium, potassium, chromium, etc. The analytical techniques are mostly inductively coupled plasma-emission spectrometry (ICP-AES) and electrothermal atomic absorption spectrometry (ET-AAS) after the suitable preparation of the samples. Often, the standard addition method has to be used to compensate for the matrix effects. In the case of the sediments, the fusion in a platinum crucible followed by digestion in dilute nitric acid is required to keep silicon completely soluble. However, other analytical techniques are used; Fig. 1.7 shows a general layout of the laboratory.

Since mid-1986, two new devices are available in the analytical laboratory, a Polarecord E506 Metrohm polarograph, and a VG ICP-MS.

Polarography can be advantageously used for the determination of many elements and is very attractive for neptunium analysis at the low concentrations existing in the solutions from migration experiments. For that specific application, an alpha glove box has been constructed. Concerning the ICP-MS, a number of tests have been done in order to ascertain its analytical capabilities and sensitivity in routine use.

In Table I.IV, the detection limits for different elements with ICP-MS are compared with those of ET-AAS. It appears from the table that the detection limit is in general lower for ICP-MS than for ET-AAS; furthermore, ICP-MS permits the simultaneous determination of many elements, and gives also information on their isotopic composition. However, the volume needed for the analysis is large, in comparison with that required for ET-AAS. This is an important feature for radioactive samples, in order to limit the operator exposure. Furthermore, the graphite furnace and its accessories can be easily installed into a glove box, which is not the case for the plasma torch.

The adaptation of ICP-MS system for the analysis of radioactive samples, mainly alpha-emitting nuclides, is being studied.

Interesting results have been obtained in the analysis of several sea-bed samples, collected during the 1985 international long core cruise (ESOPE). The purpose of the analysis was to get concentration profiles of different elements either in solid sediments or in pore water, and to correlate them to the stratification profile. Figs. 1.8 and 1.9 show typical profiles of several elements of interest in sediments and pore water.

Several clay samples, drawn at different distances from faults in a clay layer, have been analysed in order to investigate

Table 1.III - Operation Site

	Adeco building	Radiochemistry building	Radiochemistry building
	Hot analytical cell	Alpha-boxes	No radioactivity protection
U	Chemical separation, potentiometry, spectrophotometry	Coulometry, spectrophotometry, potentiometry,	
Pu	Chemical separation	α-targets, Coulometry, spectrophotometry,	
Am-Cm	Chemical separation, dilution	α- and γ-counting	
FP	Chemical separation, dilution	Spectrophotometry, ETAAS, γ-counting	
Np	Chemical separation	α-target, polarography	
HNO_3	Titrimetry, pH		Titrimetry, pH
Al^{3+}	EDTA, titrimetry	EDTA, titrimetry	
HAN			Potentiometry
Na^+	U^{VI}-method		U^{VI}-method, ICP
TBP DBP MBP	Chemical separation	Titrimetry	ICP-AES titrimetry

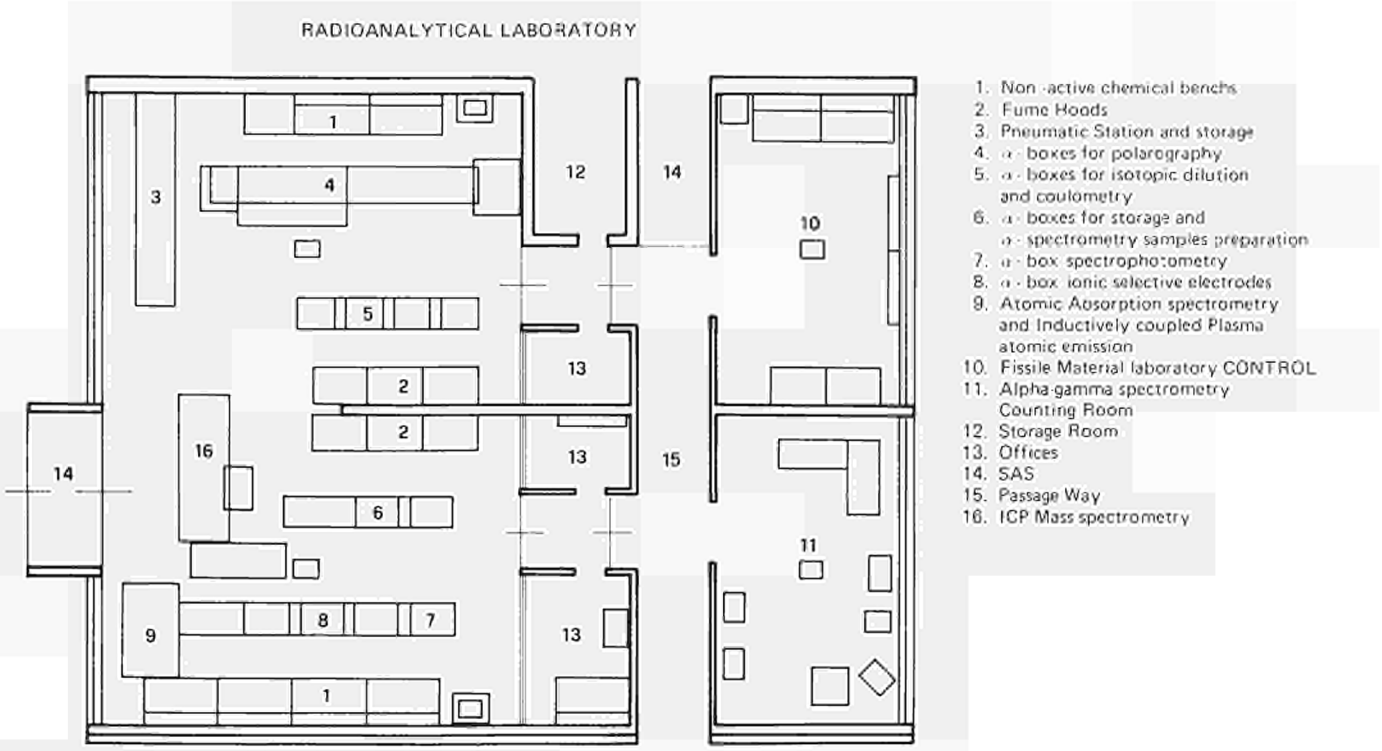

Fig. 1.7 - Radioanalytical laboratory. Layout

Table 1.IV - Typical Detection Limits (ppb)

Element	GF-AAS	ICP-MS
Sr	0.02	0.01
Zr	—	0.01
Mo	0.02	0.07
Rh	1	0.01
Pd	1	0.03
Sn	0.2	0.09
Te	0.1	0.2
Cs	2	0.02
Ba	0.04	0.02
Eu	1	0.01
Al	0.01	0.04
Fe	0.02	0.1
U	1000	0.002
P	40	2

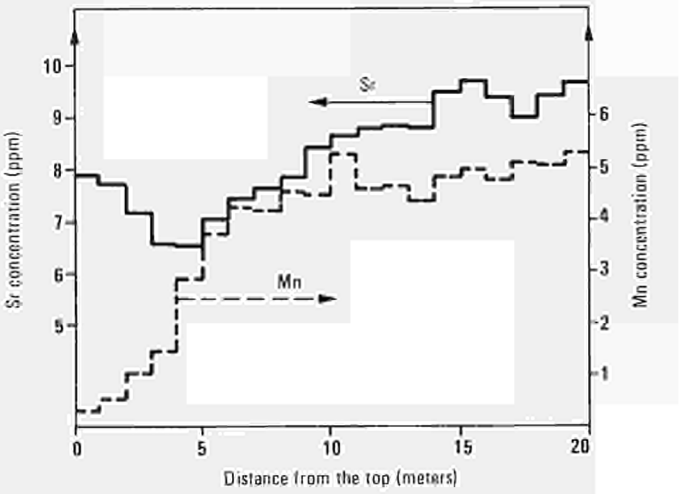

Fig. 1.9 - Concentration profile core 48 - pore water

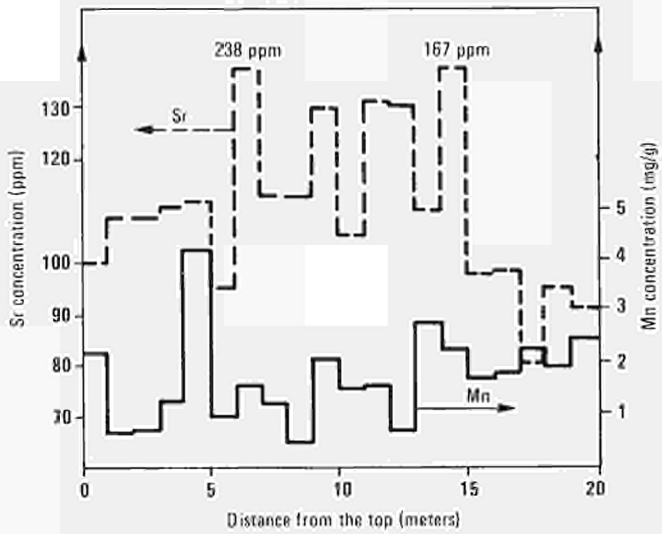

Fig. 1.8 - Concentration profile core 48 - sediments

possible inhomogeneities in the distribution of some trace elements due to water percolation along the fractures. The profiles obtained should give information on the period during which the fault occurred, on the migration velocities, etc.

Some samples have been irradiated at the TRIGA reactor of the Pavia University and measured by gamma spectrometry. Fig. 1.10 shows the distribution obtained for a sample in which the oxidized zone (visually estimated) ends about 3 cm from the fault while in the sample of Fig. 1.11, the oxidation zone could not be clearly identified. In the case of tellurium and caesium (Fig. 1.10), two interpretations can be given concerning the profile : one continuously decreasing from the fault, the other presenting a discontinuity at the interface. Interesting results have been obtained during the analysis of the sample shown in Fig. 1.12. Sampling was made as indicated in Fig. 1.13 following three parallel directions (about 4 cm between each one) until 35 cm from the fault. The clay presents three visually distinct zones :

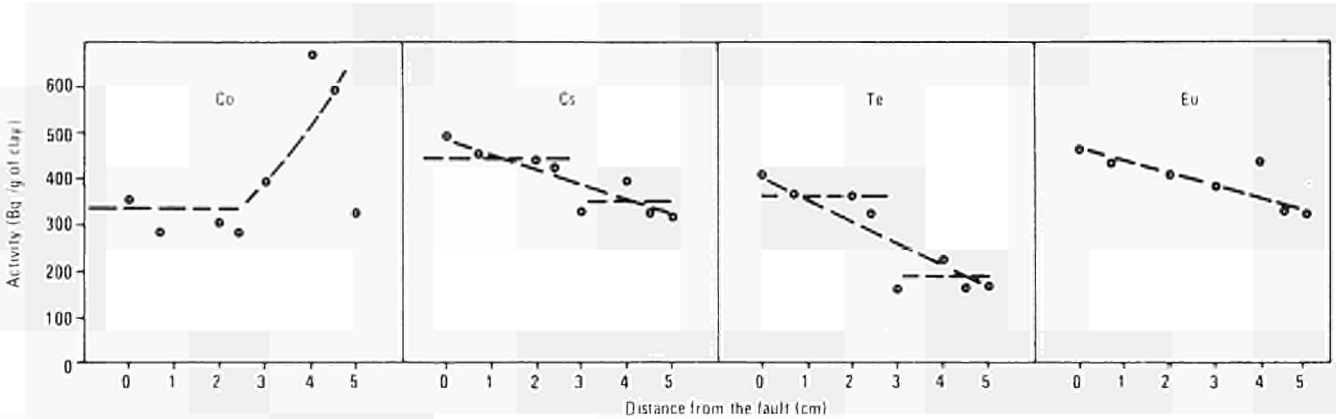

Fig. 1.10 - Co, Cs, Te, Eu distribution

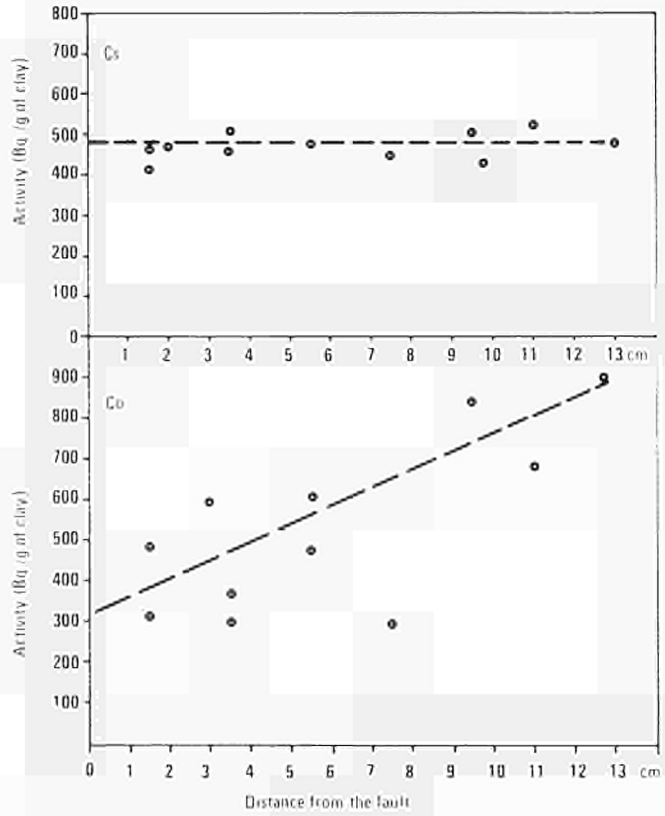

Fig. 1.11 - Cs and Co distribution

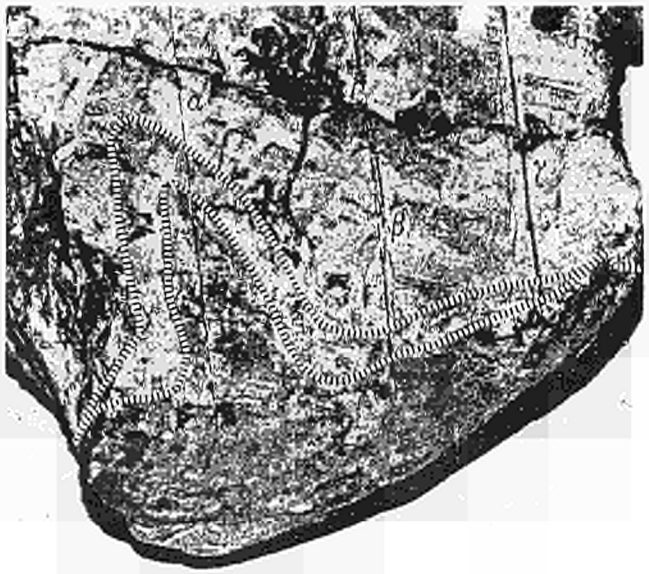

Fig. 1.12 - Clay sample analysed;
α, β and γ are lines along which sampling was performed.

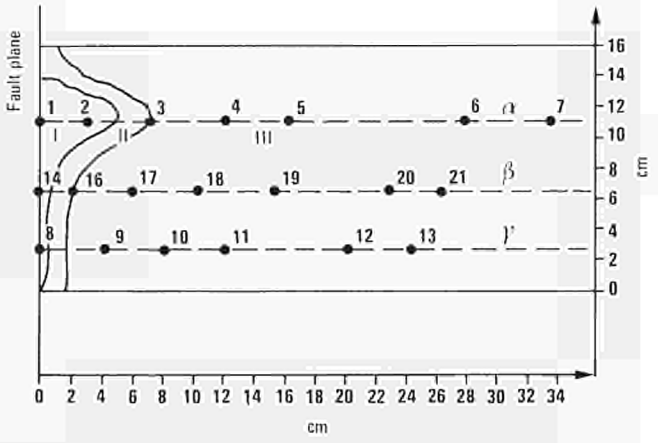

Fig. 1.13 - Schematic sampling map. Numbers indicate the sampling points, along α, β and γ lines; roman numbers show the three visually distinct zones.

- zone I : dark brown,
- zone II : brown,
- zone III : blue-grey,

zones I and II, near the fault being the oxidized zones.

The following elements have been determined :

- U by non-destructive neutron activation analysis;
- Mn, Sr, V, Zn, Fe and Co after dissolution of the clay were measured either by ICP-AES or by ET-AAS.

Uranium samples (0.1 to 0.2 g) from profiles alpha and gamma have been irradiated together with U standards at the TRIGA reactor of the Pavia University, and measured by gamma spectrometry.

For destructive analysis, the dissolution was made by mixing about 0.5 to 0.8 g of sample with 2.5 g anhydrous sodium tetraborate and heating the mixture in a platinum crucible at 1100°C for 1 hour. After cooling, the melt was dissolved in 0.1 N HCl.

Figure 1.14, 1.15 and 1.16 show typical profiles of U, Mn, Fe and Co. The three figures clearly show that the concentrations of the various elements near the fault and in the clay are different, probably due to the action of the percolating water.

Apart from this evident conclusion, a modelling study has been done in order to gain more information from the analytical results.

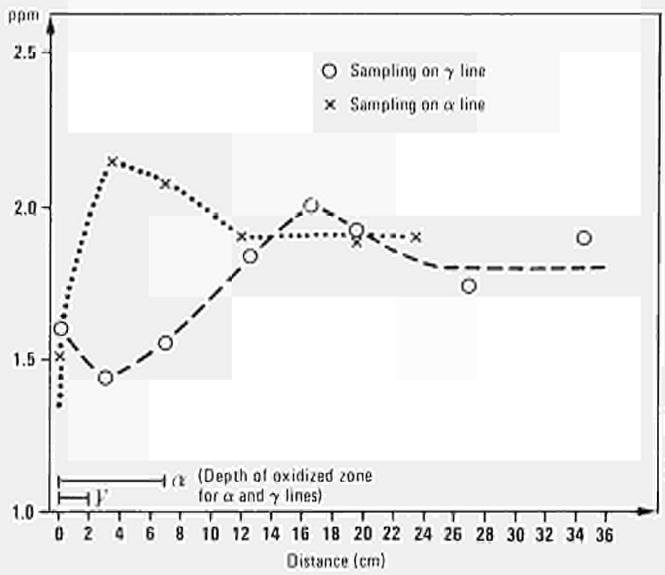

Fig. 1.14 - Uranium concentration profiles (ppm) along the α and γ sampling lines

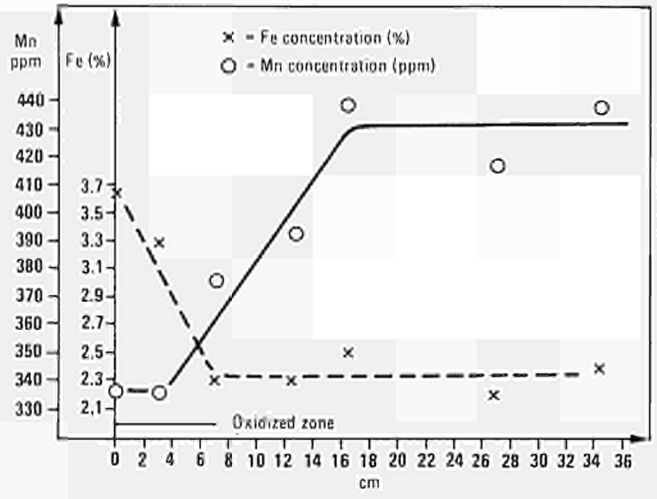

Fig. 1.15 - Mn and Fe concentration profiles along the α line

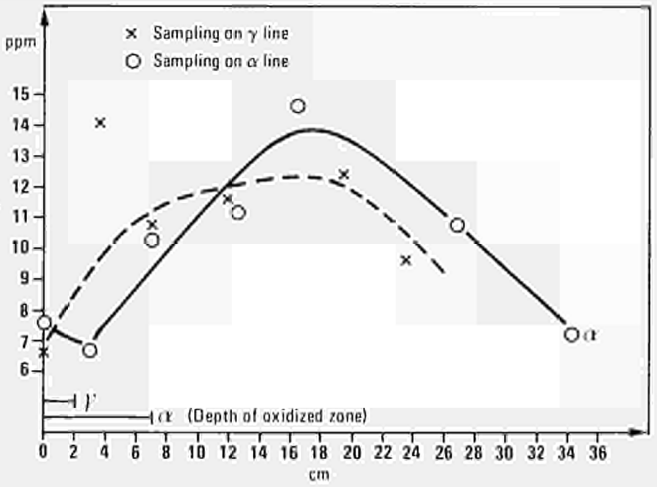

Fig. 1.16 - Co concentration profiles (ppm) along the α and γ sampling lines

Radioisotope Production

^{95m}Tc production : Simulated vitrified waste samples spiked with ^{95m}Tc are employed to study the behaviour of technetium in geological disposal conditions in the JRC programme, and by shared-cost action contractants. A target of high purity molybdenum, thickness 1.5 mm, diameter 10 mm, weight about 1 g, has been irradiated for 5 hours at the JRC-Ispra cyclotron at an incident proton energy of 35 MeV. The target was dissolved in a small volume of hot 7N HNO_3 and slowly evaporated so that a large fraction of molybdenum precipitated.

After cooling, the mixture was filtered on a Whatman filter (No. 41) and washed with water, the final volume being about 40 ml. Not more than a few percent of technetium was retained on the precipitate. A further purification of technetium was obtained by contacting the aqueous solution with an equal volume of 0.25 M HDEHP in mesytilene in order to remove the small quantity of molybdenum still present. The check, by gamma spectrometry, of the nuclear purity of the final product showed gamma activity only from technetium isotopes formed during the irradiation (see Table 1.V).

From the gamma activity measurements we were able to calculate that about 9 mCi ^{96}Tc and 400 μCi ^{95m}Tc have been produced. The product was divided into three fractions, one for use in our own laboratory, while the others were sent to the Imperial College of Science and Technology, London, and to ENEA, Centro PAS, S. Teresa, Italy.

^{235}Np Production : Twenty targets of uranium enriched equal to or greater than 93% ^{235}U are now available for the determination of the excitation function of the reaction $^{235}U(p,n)^{235}Np$.

Table 1.V - Technetium Isotopes Formed by Mo(p,n) Reactions

Tc isotope	Half-life	E gamma (MeV)
95	20.0 hr	0.768 - 0.84 - 1.06
95 m	61 d	0.204, 0.564, 0.78, 0.823, 0.838, 1.042 ...
96	4.3 d	0.32, 0.778, 0.810, 0.851, 1.12, ...
99 m	6.0 hr	0.140

Completion of LMA Cells

At the medium active laboratory (LMA) a set of chemical hot cells is already available for chemical operations on fully active waste samples (~100 ml per run). These facilities will be used in preparatory activities for PETRA runs. In order to complete the sequence of possible operations, an oven for waste vitrification has been installed, by which a few ml samples of fully active vitrified waste may be obtained and may be fully characterized. Fig. 1.17 shows the oven after its installation in the cell.

Flow-Sheets for PETRA

The OXAL process, developed at JRC-Ispra some years ago to separate actinides from high active waste (HAW), will be tested in the PETRA facility. As the first step of the process, rare earths and actinides are precipitated with oxalic acid, the suitable acidity being reached by a formic denitration. The behaviour of technetium during this operation was not known. As now the

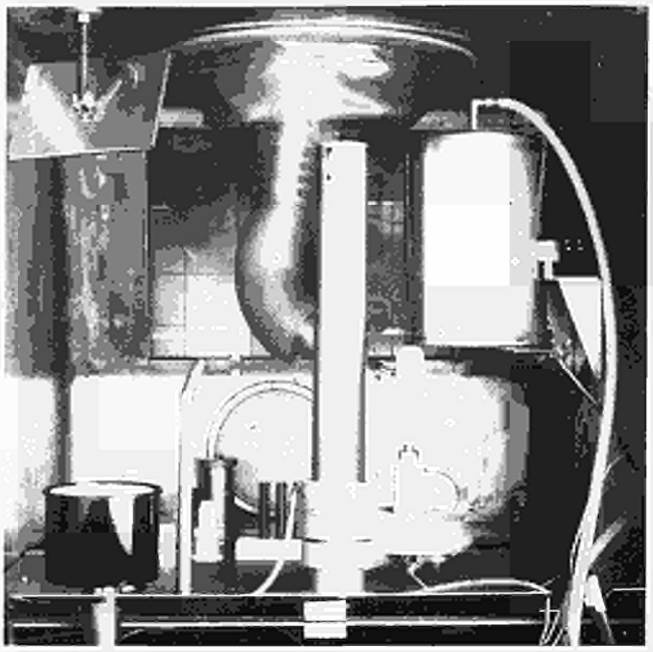

Fig. 1.17 - LMA glass preparation

gamma emitter ^{95m}Tc is available at Ispra, some tests were made by using the simulated HAW solution with composition shown in Table 1.VI. To this solution, apart from radioactive ^{95m}Tc, we added rhenium, which is chemically similar to technetium. In fact, for the reaction :

$$MeO_4^- + 4H^+ + 3e \rightleftarrows MeO_2 + 2H_2O \quad (Me \text{ for Re or Tc})$$

expected to occur during denitration, E° is 0.51 V for rhenium and 0.74 V for technetium /1/. The experimental tests were conducted following the procedure described in /2/.

In each run, more than 99% of technetium was found in the supernatant with the fission products. This result means that the expected reduction of technetium-rhenium and the successive precipitation as TcO_2- ReO_2 does not occur during the denitration and also that technetium-rhenium are not lost by volatilization. This last fact can be probably ascribed to the highly reducing conditions in the vapour phase where Tc^{VII}, if present, is easily transformed to Tc^{IV} which is much less volatile. In the aqueous phase, after condensation, the nitric acid brings back technetium to the VII valency.

Table 1.VI - Simulated HWA Composition

Element	mg/l	Element	mg/l
Sr	178	Nd	869
Zr	770	Sm	244
Mo	733	Fe	221
Cs	533	Rh	80
Ba	326	Pd	280
La	266	Te	110
Ce	772	U	2000
Re	100	HNO_3	3M/1

The OXAL schemes include the vitrification of the fission product effluent, operation requiring the evaporation to dryness of the liquor. As a consequence of the presence of technetium, special precautions should be taken to avoid its loss or to recover it from the vapour phase.

References

/1/ G. CHARLOT — Les méthodes de la Chimie Analytique. Analyse Quantitative Minérale. Masson Cie (1961)

/2/ F. MANNONE and H. DWORSCHAK (Eds.) — Chemical Séparation of Actinides from High Activity Liquid Wastes. Final report. Special Activity Publication No. I.07.03.84.02

1.3 The OXAL-MAW Process (H. Bokelund)

The objective of this activity is to verify the OXAL process with waste solutions of intermediate activity level. The capabilities of this process, previously developed at JRC-Ispra on simulated highly active solutions, to produce an "alpha-free" waste should be investigated on fully active scale with samples of volume of a few litre; the characterization of the resulting solidified product is included in the study.

In the current programme period the activities have been centered around the following items :

a) the development of a new denitration process based on photochemical destruction of the nitrates in the waste solution,
b) the optimization of the carrier used in the oxalic acid precipitation based on a parametric study involving 4 different carriers, 4 carrier-to-actinide ratios, 3 pH-values, 2 temperatures, and 3 different digestion times, and
c) the setting up of a gamma spectrometric measurement system in the low energy range for the simultaneous determination of plutonium and americium in waste solutions.

The experiments were carried out on simulated solutions of intermediate activity level (MAW) to which Pu and Am had been added as tracers, as well as on real active MAW solutions in a hot cell.

Results on OXAL have been given in the current reports, but for convenience the most important results are summarized here. On a) the feasibility of photochemical denitration of MAW solutions has been demonstrated. In alkaline solutions the residual nitrate concentration was a few ppm, the reaction products were only N_2 and O_2. Experiments on b) indicated Ca or Ba to be the better choice as carrier for the actinides; the influence of pH on the yield in the precipitation is pronounced; the decontamination factors for Pu and Am were high, hence an alpha-free waste can be realized. The application of the low energy spectra of Pu and Am, as introduced under c) provided a useful tool for the determination of these elements. Such simultaneous, direct measurements showed adequate sensitivity and precision. They also allowed a considerable saving in man-power to be achieved, as the long counting times needed for low activities do not present an intense load of labour.

Tests on the OXAL Process

The tests on simulated MAW (see PPR 1986, p. 15) were supplemented by a series of precipitations using ^{238}Pu as a tracer isotope. The aim was to check the previous results on decontamination factors for Pu found with ^{239}Pu (including higher isotopes). The gamma ray intensities from the isotope ^{238}Pu are more favourable than those from ^{239}Pu in the low energy range considered, the latter nuclide requiring counting times as long as 4 hours for its determination under our particular circumstances. It is, however, quite feasible to carry out the simultaneous determination of Am and Pu by direct gamma spectroscopy in these samples, which have a very high salt

content (sodium nitrate) and Pu and Am concentrations in the order of 10 mg/l and 3 mg/l, respectively. The experiments with the simulated MAW solutions were verified by hot cell tests on real solutions of intermediate activity level (see below).

Tests on OXAL using active MAW have been completed. About 20 litres of a waste solution of intermediate activity level, MAW, were transferred into a hot cell from a 200 litre drum provided with a special lead shielding. Fig. 1.18 shows a view of the bottle containing the MAW solution inside the newly commissioned hot cell. The MAW solution was taken in the WAK plant during a reprocessing campaign on fuel with a burn-up of 44,000 MWd/t and had been concentrated about 10 times in the HDB, KfK, prior to the transfer to TU. The main part of the solution originated from the reprocessing process itself (process waste).

The as received solution was filtered, brought to a pH of about 2.0 and was subdivided in batches of 2 litres for oxalate precipitation.

The results of the radiochemical analyses of the feed solution are given in Table 1.VII. The main activities were ^{137}Cs and ^{90}Sr, as expected. The precipitate present in the feed was found to contain Ru and Zr.

Based on the results from the experiment on the simulated solutions various conditions were chosen for the oxalate precipitation, parameters such as pH, type of carrier (Ba, Ca, Ce) were varied. The use of mixed carriers (Ba and Ce) was also investigated. The pH was adjusted to the chosen value by NaOH, the solution was thus not nitrated. A saturated oxalic acid solution was used as precipitation agent.

After the precipitation the solutions were filtered, samples of the filtrate as well as of the redissolved precipitate were taken for analyses. The Pu and Am were analysed by direct gamma spectroscopy in the low energy range; the concentration of fission products in the filtrate will also be measured, allowing the calculation of decontamination factors, e.g. for the lanthanides.

Table 1.VII - Analysis of the MAW Feed Solution Employed for the Active Verification of the OXAL Process in a Hot Cell

Nuclide	Activity concentration (Bq/l)
^{137}Cs	6.5 E8
^{90}Sr	5.5 E8
^{60}Co	1.0 E7
^{106}Ru	3.4 E8
^{134}Cs	2.1 E8
^{144}Ce	1.8 E8
^{125}Sb	1.5 E8
^{95}Zr	4.1 E4
Total alpha	1.0 E8
^{239}Pu	2.0 mg/l
^{240}Pu	1.2 mg/l
^{241}Am	0.16 mg/l

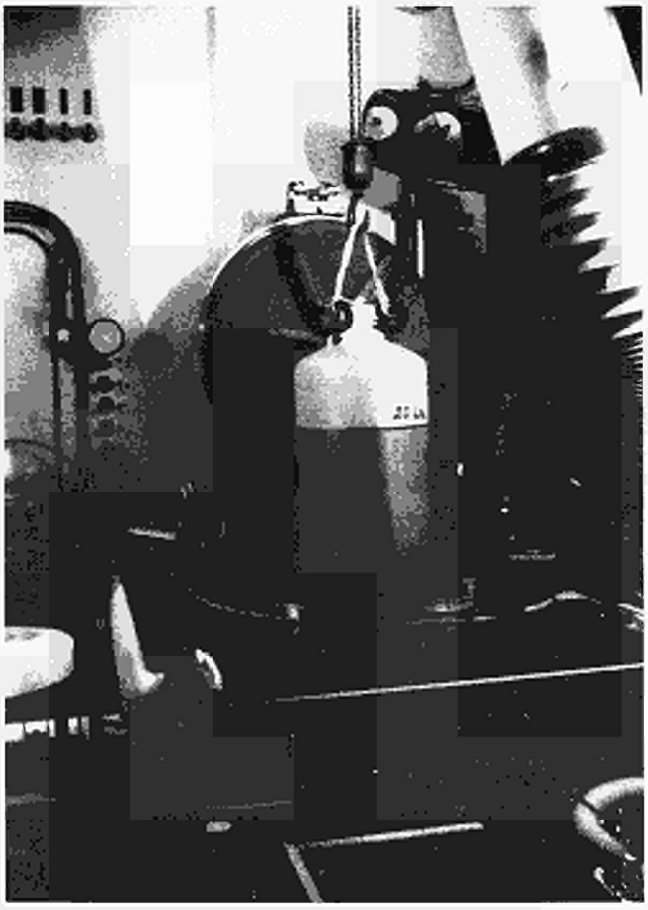

Fig. 1.18 - A view of the bottle with 20 litre MAW solution under transfer into the new hot cell

Characterization of the Solidified Product

The effects of the removal of the actinides and lanthanides from MAW by oxalate precipitation will be investigated by selected tests on solidified specimens of the mother liquor as made by cementation.

The work on cementation has been started, inactive specimens have been prepared under different conditions. The ratio water-to-cement was not varied in theses tests, but was kept at 0.5, complying with the usual practice, e.g. in KfK. These specimens will be exposed to leaching and their compressive strength will be measured. Another parameter to be followed as a function of time is the porosity of the specimen. For the analyses of Ca, Si and Al in the leachant the appropriate spectrophotometric methods have been tested.

One particular problem to be dealt with in these tests is the presence of oxalate ions in the mother liquor after the oxalate precipitation, as these ions have a pronounced delaying effect on the hardening of the cement. Experiments to quantify these effects have been started. The destruction of the oxalate ions by photochemical means is under investigation. The results of these tests will be reported upon in the next report in the frame of the waste characterization programme.

Other Activities

During this year additional studies on the suitability of leaching vessels, i.e. inserts to be used in active experiments, were carried out. Furthermore, certain quality control aspects of the leaching procedure for glass specimens were evaluated and reported upon.

As a preparation of leaching tests to be carried out on active glass specimens various metals have been tested out for their suitability as container materials in the leaching device. The vessels were fabricated seamlessly from the alloys: nickel, Hastelloy-C, Inconel, both the latter being alloys with high Ni-content, and from titanium. These vessels were used as inner containers in the usual leaching autoclaves (Berghof), the metals replacing teflon as insert material.

Demineralized water and Q-brine were used as leachants in these tests at the temperatures 150°C and 200°C. After 10 days of "blank" leaching, without glass, the leachants were analysed for metallic impurities by ICP; the results of these blank experiments at 200°C are shown in Table 1.VIII. The concentrations of all the elements are low, except in the case of Ni alloys leached in Q-brine, where the Ni concentration reaches 60 ppm. The concentrations of the alloying constituents in the leachant increase slightly as the temperature is increased (not shown in the table). A likely choice as container material for long term leaching would be titanium. Follow-up experiments on these vessels under active conditions in a hot cell are under way. Here the additional influence of irradiation will be tested.

Table 1.VIII - Results of "blank" leaching experiments with metallic inserts at 200°C

Element in leachant	Nickel insert	Hastelloy insert	Inconel insert	Titanium insert
Al	dl / 0.02	dl / 0.06	dl / 0.03	dl / 0.05
B	0.1 / 0.4	0.04 / 0.5	0.2 / 0.7	0.07 / 0.6
Ca	0.6 / 0.6	1.0 / 0.9	1.6 / 4.2	1.3 / 0.8
Ce	dl / 0.08	dl / 0.1	dl / 0.2	dl / 0.07
Cr	0.05 / 0.1	dl / 0.1	dl / 0.3	dl / 0.06
Fe	dl / 0.05	dl / 0.02	dl / 0.25	dl / 0.1
Mg	dl / dl	0.05 / dl	0.4 / dl	1.5 / dl
Mo	dl / dl	dl / 7.2	dl / dl	dl / dl
Mn	dl / 0.9	0.1 / 0.8	0.05 / 2.2	0.04 / 0.6
Ni	1.3 / 31	0.24 / 24	0.35 / 60	dl /2.5
Si	0.1 / 0.4	0.1 / 0.6	0.3 / 1.1	0.3 / 0.6
Sr	<0.01 / 0.03	0.01 / 0.03	<0.01 / 0.06	<0.01 / 0.03
Ti	dl / dl	dl / dl	dl / dl	dl / dl
Zn	0.02 / 0.1	<0.01 / 3.3	dl / 2.7	dl / 3.3
Zr	0.3 / 1.8	dl / 1.5	dl / 4.0	dl / 0.1

The results are presented in the table as the element concentration in ppm in demineralized water/element concentration in ppm in Q-brine (dl = below detection limit). The elements Cu, Eu and Nd were also determined, but were always below the detection limit.

Simple statistical tests, such as regression analysis and analysis of variance have been applied to data obtained from leaching experiments carried out under various conditions of temperature and time. The precision and accuracy of the overall leaching procedure were evaluated considering the short term within laboratory effects.

The data originated from determinations of the mass loss of leached glass specimens and from the measurements of the electrical conductivity and the pH of the leachant. The solution conductivity correlates highly with the normalized mass loss; hence it provides a consistency check on the measurements of the latter parameter. The relative precision of the overal leaching test method was found to be 5-12%, including the effects assignable to inhomogeneity of the glass specimens.

Furthermore, the conditions for the use of the teflon inserts used in leaching devices have been investigated. A modified cleaning procedure has been proposed to ascertain the absence of systematic errors by the repeated utilization of such inserts. The cleaning of the containers should include a heat treatment at 200°C after the appropriate wet cleaning. The teflon inserts should not be used in leaching at temperatures equal to or above 200°C for extended periods. For further details on the work see reference /1/.

Reference

/1/ H. BOKELUND, K. DEELSTRA — Radioactive Waste Management and the Nuclear Fuel Cycle (accepted for publication)

1.4 Characterization of High Activity Glass (M. Coquerelle)

Taking into account the development of the programmes at JRC-Karlsruhe as well as the competence and the existing infrastructure for highly active work, and the benefits of a deeper collaboration with other JRC establishments, it was decided to upgrade the future contribution to the Radioactive Waste Management programme. The future availability of fully active glasses from the PETRA installation and the need for near-field model validation by tests on actual waste forms seem to well justify an effort in the "Characterization of Nuclear Waste Forms".

Preliminary characterization tests were started on three highly active borosilicate glasses (up to 287 Ci/kg, containing 15 to 33 w/o fission products) provided from the ESTER experiment. This activity was carried out in the framework of a collaboration ENEA COMB-SVITE/JRC-Ispra. Chemical composition of these materials is indicated in Table 1.IX.

Table 1.IX - Chemical composition of ESTER glasses

	Crucible 4	Crucible 6	Crucible 8
SiO_2 (%)	36	50.9	43.4
B_2O_3	9	11.2	17
Al_2O_3	2	2.13	12.75
Na_2O	5	13	10.67
Li_2O	2	6.7	5
K_2O	3		
CaO	1		8.97
TiO_2O	6	0.33	
CuO	3		
WO_x	33	15	15

In this work emphasis has been placed on the morphology, distribution and composition of the matrix and phases precipitated within it.

As the experimental results have not been entirely discussed with ENEA experts, we will restrict ourselves to a brief description of the main experimental results giving more a picture of our experimental capabilities than a report on the characterization of these borosilicate glasses.

After checking the axial distribution of the mass and fission products of the glass crucibles by gamma scanning and radiography (Fig. 1.19) three transverse cross-sections through the crucible were cut and polished. From these, samples for microstructure examination were prepared. To this end, quantitative microscopy, scanning electron microscopy, back-scatter imaging and EDAX analysis were employed.

The more relevant analytical results can be summarized as follows :

a) Two of the glasses showed an unusual structure with precipitated secondary phases heterogeneously distributed within the matrix (Fig. 1.20); one of these glasses (57 Ci/kg, 15 w/o fission products) seems to be a two-glass system (Fig. 1.21).

b) Elemental composition of the secondary phase, given by EDAX analysis, indicates the presence of four phases composed of following elements : Cr, Ni, Fe; U; U, Pu and U, Mo compounds (Figs. 1.22 and 1.23).

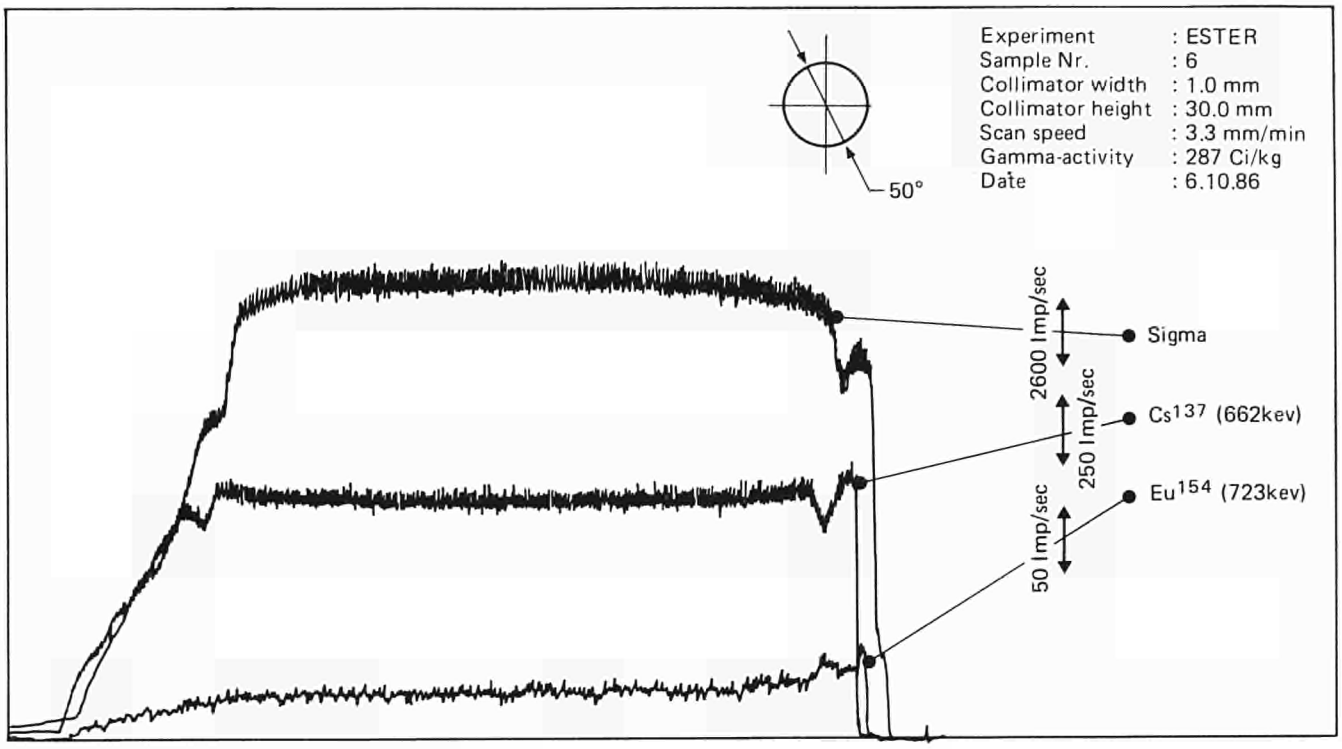

Fig. 1.19 - Gamma scanning of crucible 6

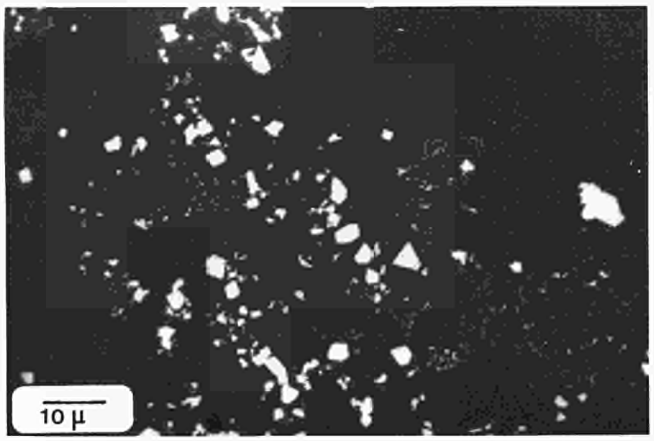

Fig. 1.20 - Glass microstructure-crucible 6

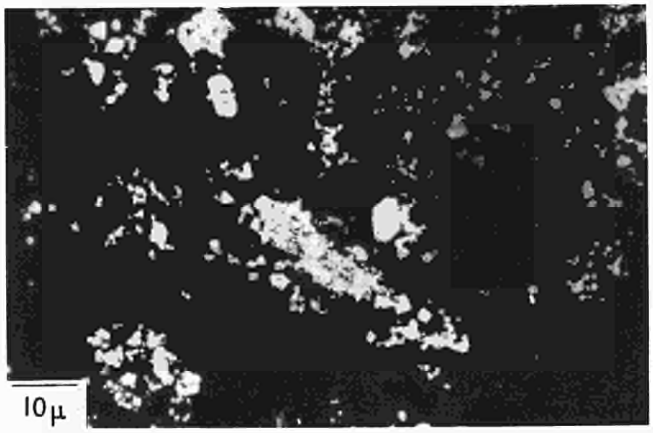

Fig. 1.21 - Glass microstructure-crucible 8

c) The glasses containing 33 w/o fission products displayed a strong devitrification process (Fig. 1.24). In the matrix, hexagonal, tetragonal, spherical precipitates but also needles or plates were observed and analysed. Compounds of the type Fe, Ni, Cr(Co) and (Gd)-Ti, Fe, Gd, Nd-Ce-Mo, Cs, (Fe) and Ti, La, Nd, Gd were found (Fig. 1.25).

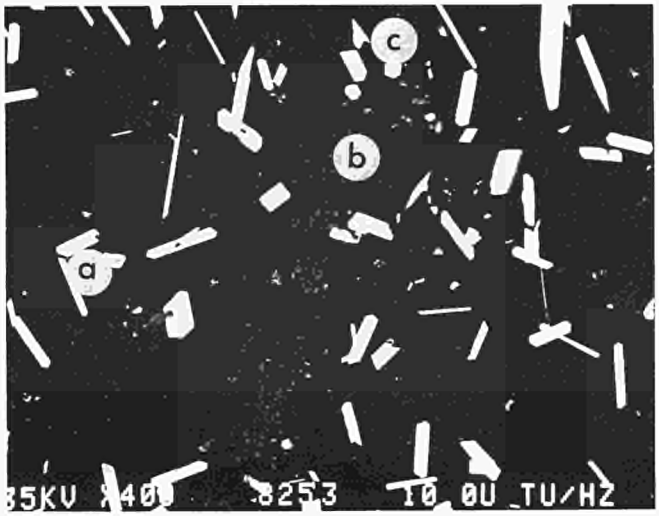

Fig. 1.22 - EDAX analysis of glass crucible 4
a) Ti, La, Nd, Gd;
b) Fe, Ni, Cr, Co;
c) Ce

Fig. 1.23 - EDAX analysis of glass crucible 8, spherical precipitate: Mo, Cs

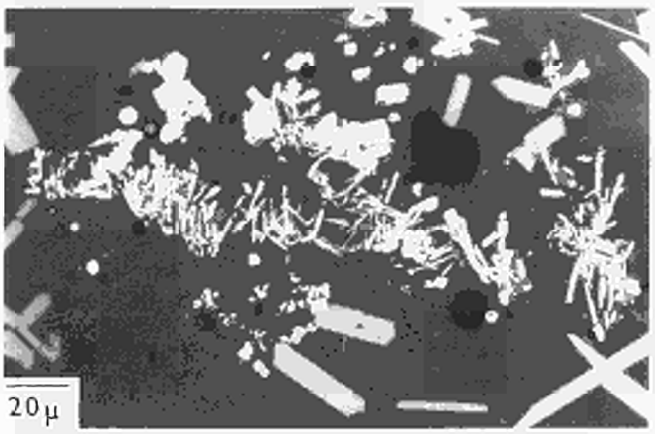

Fig. 1.24 - Glass microstructure of crucible 4

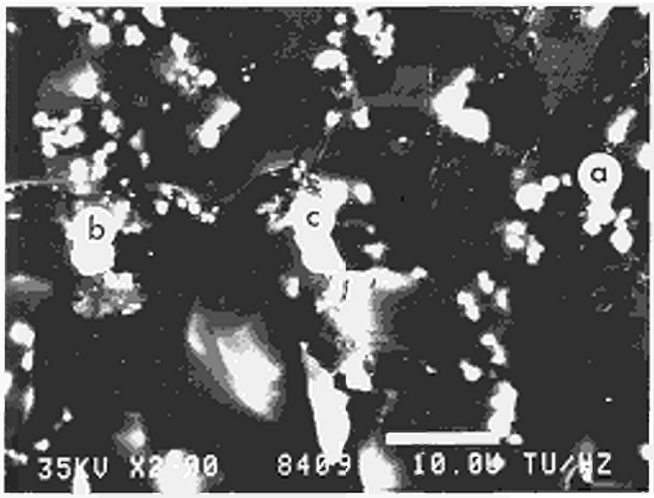

Fig. 1.25 - EDX analysis of glass/crucible 4
a) Ti, La, Nd, Gd
b) Fe, Ni, Cr, Co
c) Ce

1.5 Actinide Monitoring (L. Bondar)

The objective of this study is to develop methodologies and instruments for non-destructive analysis (NDA) of actinides in solid waste. The JRC operates as an advisory laboratory in this area.

The JRC assists in the implementation of a non-destructive assay system for plutonium waste monitoring in support of plant operators and control authorities. On the other hand, future developments of the JRC in actinide monitoring will deal particularly with test measurements in various plants applying non-destructive radiometric techniques developed at Ispra.

The activity has been concentrated on :

- *the development of a Pu monitor based on the TCA technique,*
- *the development of an actinide monitor based on gamma-ray spectroscopy,*
- *collaboration with Dounreay.*

Pu Monitor Based on the TCA Technique

Plutonium contaminated materials are generated in nearly all facilities of the nuclear fuel cycle. The accurate knowledge of the plutonium content of waste before conditioning would allow the operator to direct the waste towards one of three possible routes, which are greatly different for what concerns costs :

a) disposal in shallow land burial, if the actinide content is lower than an established threshold,
b) disposal to deep geological repositories should the threshold be exceeded,
c) recycle of the waste material, if the actinide content is high enough to justify the operation.

Furthermore, such an instrument, when applied to conditioned waste drum, would allow control authorities to inspect non destructively the waste drum and control the suitability of the waste package to the waste disposal route proposed by the operator. For this purpose, a "waste" instrument based on passive neutron assay by the Time Correlation Analysis (TCA) technique was developed at the JRC /1-3/. Firstly, a laboratory version of the "waste" instrument has been set up and then continuously upgraded to an industrial version. It is characterized by heavy duty hardware components and on-line data elaboration. The results obtained in real measurements of 200 l drums of waste conditioned in concrete show that the threshold level of 200 nCi/g can be reached by the TCA technique.

The essential features of the "waste" instrument are explained in the functional diagram below :

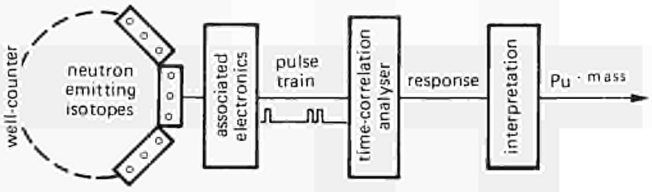

Block diagram for passive neutron assay

Neutron groups emitted spontaneously by some Pu isotopes (^{238,240,242}Pu) and detected by ^{3}He tubes generate the neutron pulse train. The time correlation analyser counts the coincidences assigned to singlets, doublets, triplets, etc. (i.e. consisting of one, two, three, ... neutrons). Using a point-source interpretation model, firstly the results are corrected for matrix effect by the relation of doublets to triplets and secondly the ^{240}Pu mass equations are determined by the total number of coincidences.

The detector head is based on a modular system each neutron detector module incorporating a polyethylene moderator, ^{3}He-detectors and Cd-cladding. Moreover, the supporting frame structure of the head can easily be adapted to specific plant conditions and measurement tasks.

The time correlation analyser permits a complete analysis of the neutron signal pulse train without any loss of information. The method was first tested at the JRC-Ispra by computer simulation. The prototype was built at the Lehrstuhl für Elektrotechnik, RWTH Aachen (FRG). Other versions of the TCA are in construction both at AERE, Harwell (UK) and at HTE/ASEM, Udine (Italy). Fig. 1.26 shows a general view of the instrument.

In addition to the two most commonly applied correlation methods (Variable Dead-Time Counter and Shift Register), the Pulse Fluctuation Analysis (PFA) and the Pulse to Pulse (PTP) time correlation analysis were elaborated at the JRC-Ispra. A coherent consideration of the various systems has been introduced. According to the developed theory, the response

Fig. 1.26 - General view of the TCA "waste" instrument

of any type of the various instruments are well defined functions of S (singlets), D (doublets), T (triplets), etc.

An assessment of the various systems for passive neutron assay has been carried out at the JRC-Ispra. The experiments show evidence that the PTP and PFA analysis techniques have an advantage over the variable dead-time counter (VDC) and shift register techniques in that they can self-correct for the non-linearity of neutron coincidence rate due either to a variations in the hydrogeneous matrix surrounding the plutonium sample, or the effect of neutron multiplication.

The verification of the plutonium content of waste items by NDA is one of the most complex tasks also in safeguards techniques. At the fuel fabrication plant Alkem, Hanau (FRG) four reference waste drums of different types were prepared by the operator and measured by the Euratom TCA /4/. The measurements were observed by both Euratom and IAEA staff with a view to future use of the four waste drums as joint working standards.

Well characterized sets of Pu standards up to 1 kg have been measured at AERE, Harwell using the Harwell high efficiency (17%) neutron wall counter /5/. The pulse train emerging from the counter was analysed by the Euratom TCA and the results interpreted in terms of the PTP and PFA models. These two models attempt to correct for the effects of neutron multiplication within the sample from the information contained in the pulse train. The results indicate that separation of the detector response into the basic ^{240}Pu mass and neutron multiplication, within the sample, appears to have been achieved with 10% accuracy on the mass figures.

This work has shown the importance of testing laboratory concepts in field conditions with large Pu masses. The importance of the dead-time corrections would not have to come to light so quickly otherwise.

Numerical procedures were developed for the determination of the source neutron multiplicity distribution caused by a fission chain and for the dead-time correction of neutron pulse train /6/.

In order to implement the alternative interpretation model /7,8/ a contract was made with the RWHT Aachen for the elaboration of a software according to flow schemes specified by the JRC /9/. The software foreseen will consist of five parts permitting

- data acquisition and reduction of measured data,
- calibration of the instrument, i.e. determination of the neutron detection probability, the decay time $1/\lambda$ of the neutron population in the detector head and a precise determination of the dead time of each individual counting chain;
- ^{240}Pu mass determination eliminating either the matrix effects and (α, n) reaction rate, or the neutron multiplication and (α, n) reaction rate or matrix effects and neutron multiplication.

A service contract with ENEA, Casaccia has been set up for scientific/technical support to the measurement of a large number of 200 l Pu-contaminated waste barrels being in store at CRE, Casaccia.

Actinide Monitor Based on Gamma Ray Spectroscopy

Segmented gamma scanning with a collimated Ge-detector and a ^{75}Se gamma transmission source is applied to measurements of Pu in 200 l solid waste drums. The γ- spectrometer has been set up mechanically including the computer controlled axial displacement of the waste barrels. A software has been elaborated permitting an automatic measurement of the γ- spectrum at each measurement step /10/. The instrument can be adapted to the requirements of plant operators. Its present detection system is based on a pure Ge γ- detector, suitable for a precise determination of U, Pu, fission or activation products (Fig. 1.27).

The scanning of such drums provides a set of count rates of γ- rays from Pu isotopes and from the ^{75}Se γ- transmission source. The computer program evaluates from these data the ^{239}Pu content per segment of the examined waste drum. The fundamental assumption of the interpretational model underlying this program is the segment wise homogeneity of the waste drum. The corrections for gamma attenuation of the observed ^{239}Pu - 414 keV γ- rays is calculated on the basis of the observed ^{75}Se - 400 keV γ- transmission /11/.

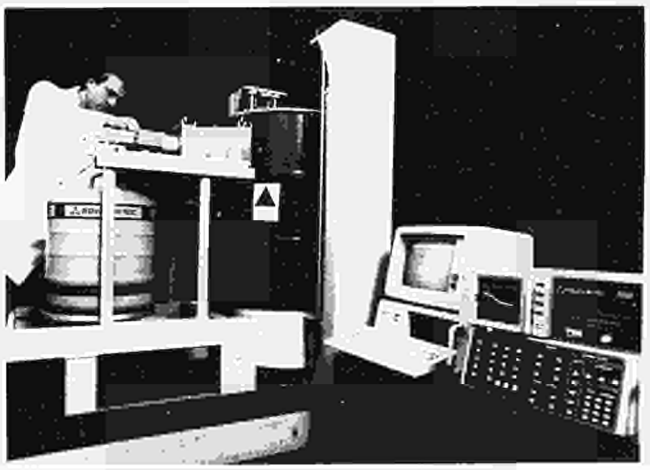

Fig. 1.27 - General view of the γ- spectrometer

Collaboration with Dounreay

The Pu-monitoring concepts proposed by the JRC-Ispra for non-destructive assay of plutonium has been firstly published during the sixties in the form of guides. At the end of the seventies, a revision of the guides has been started. The proposed methodologies have been applied and tested in the framework of a collaboration between the reprocessing plant DNPDE Dounreay and the JRC-Ispra.

The JRC has been in charge of the mathematical modelling of the Dounreay Pu-waste measurement system and the DNPDE was requested to supply calibration and real waste measurement data. Theoretical work aiming at the numerical tests has been elaborated in the framework of a series of study contracts on direct collaboration with the University of Lyon (France).

Each of the revised five chapters of the guide,

I. Planning of Monitoring Systems
II. Principles and Theory of Radiometric Assay
III. Passive Gamma Assay
IV. Passive Neutron Assay
V. Active Neutron Assay

is now completed and edited /11/. Nevertheless, each chapter is subject to continuous revision following the development of methodology for Pu-waste monitoring.

The present work is concentrated on the following items.

Multiplication and absorption corrections for passive neutron measurements of FBR fuel fabrication residues. The measurement of cans containing FBR fuel fabrication residues by NDA gives rise to some problems relating to neutron multiplication and absorption in the bulk material. There are frequent requirements for NDA verification where the physical form of the material is not known and where a mixture of several forms (e.g. powders, granules and pellets) are present.

Correction for curium emission in passive neutron measurement of head-end FBR wastes. The possibility of applying high multiple coincidence detection systems to this problem is useful and an initial basic assessment of the problem has been made at Ispra based on plutonium and curium neutron emission data supplied by DNPDE. The overall uncertainty on these measurements may be relatively high (-50-80%), but the final result might still be sufficiently precise when several hundred items are considered.

Modification of the NDA5 neutron interrogation model to allow for the use of a californium shuffler. The original sealed tube neutron generator on the NDA5 neutron interrogation system has now been replaced by a californium shuffler. The earlier mathematical modelling work will therefore require some modifications to accomodate the lower neutron energy and the change in the irradiation cycle. A new calibration has just been completed for the californium shuffler and provision has been made for the special conditions required for the measurement of separators for solid residues.
The earlier model will be brought up-to-date and a software package prepared suitable for routine application.

European Intercomparison Campaign

The aim of this exercise is to compare various NDA techniques to be used for the monitoring of drums containing Pu-contaminated wastes. It is organized by the DG XII in the framework of the shared-cost action programme on Radioactive Waste Management. This exercise groups 6 laboratories to a common action, namely CEA-Cadarache, CEN/SCK Mol, ENEA-Casaccia, KfK, UKAEA-Harwell and JRC-Ispra. The scientific secretariat of the overall exercise has been assigned to the JRC-Ispra. The configurations of the modular waste drums to be measured were defined by :

- the drum size : 220-100-25 liters
- the matrix nature : polyethylene of O.1 and 0.3 g/cm^3 concrete,
- Pu samples : PuO_2- $(Pu + Am)O_2$ of 110-200-500-1000 mg
- sample position : aluminium axial guide tubes at radius = 0 - R/$\sqrt{2}$ - R.

In addition, seven sealed drums with unknown configurations and two real waste drums have been measured.

The preparation of the final report is in course.

References

/1/ L. BONDAR — Time Correlation Analyser for Non-Destructive Pu Assay. In: Proceedings of a Meeting on Monitoring of Pu-Contaminated Waste, 25-28 September 1979, Ispra (Italy)

/2/ L. BONDAR — Passive Neutron Assay. In: Proceedings of the Intern. Symposium on Recent Advances in Nuclear Materials Safeguards, 8-12 November 1982, Vienna (Austria) IAEA-SM-260

/3/ L. BONDAR, F. GIRARDI — A Waste Instrument for Classifying of Pu-Contaminated Wastes Based on Passive Neutron Assay. In: Proceedings of an Intern. Seminar on Radioactive Waste Products, 10-13 June 1986, Jülich (FRG)

/4/ L. BONDAR et al. — Determination of Pu in Mixed Oxide Fabrication Plant Wastes by Passive Neutron Assay. In: Proceedings of the 6th ESARDA Annual Symposium, 14-18 May 1984, Venice (Italy)

/5/ L. BONDAR et al. — Experimental and Theoretical Observations on the Use of the Euratom Time Correlation Analyser for the Passive Assay of up to 1 kg of Pu. In : Proceedings of the 6th ESARDA Annual Symposium, 14-18 May 1984, Venice (Italy)

/6/ L. BONDAR — Further Developments on Pu Measurements by Passive Neutron Assay. In: Proceedings of the an Intern. Symposium on Recent Advances in Nuclear Materials Safeguards, 10-14 November 1986, Vienna (Austria) IAEA-SM-293/29

/7/ W. HAGE, D.M. CIFARELLI — Correlation Analysis with Neutron Count Distributions in Randomly or Signal Triggered Time Intervals for Assay of Special Fissile Materials. Nuclear Science and Engineering, Vol. 89 (1985) 159-176

/8/ W. HAGE, D.M. CIFARELLI — Models for a Three-Parameter Analysis of Neutron Signal Correlation Measurements for Fissile Material Assay. Nuclear Instrumentation and Methods in Physics Research, Vol. A251 (1986) 550-563

/9/ W. HAGE, K. CARUSO — A Preliminary Procedure for the Treatment of Time Correlation Analyser Measurement Data for Non-Destructive Assay on Pu. Technical Note No. I.07.C3.86.115 (Nov. 1986)

/10/ S. DONGIOVANNI — Segmented Gamma Scanning. NE.47.1550.A.002 (1988)

/11/ G. ANTONELLI — Ottimizzazione e Verifica Sperimentale del Metodo "Segmented Gamma Scanning". Tesi di Laurea, Politecnico di Milano (1986)

RESEARCH AREAS

2. Safety of Waste Disposal in Continental Geological Formations

This activity includes both theoretical evaluations and related experimental activities in order to perform long-term risk assessments of waste disposal in continental geological formation.

The scientific goals of this research area are :

a) to develop risk assessment methodologies and computer codes which can be applied to waste disposal concepts under study in the European Community. The framework of this activity is the PAGIS project which links all concerned European laboratories in a EC-coordinated effort on "Performance Assessment of Geological Isolation Systems". In this area, the JRC-Ispra has been particularly active in developping probabilistic assessment methodologies and computer codes, such as LISA, PREP and SPOP, which have been widely used in the EC. The Ispra team is also actively involved in the verification of the correct performance of probabilistic assessment codes, organizing intercomparison exercises in the framework of the NEA-PSAC working group;

b) to investigate and model the processes which, in the long term, will or could occur in waste repositories and in their neighbourhood and modify the radioactive source term. The experimental study of near-field phenomena aims at obtaining physical models of the relevant processes, which are then translated into mathematical terms for safety assessment, frequently in a simplified form. The interaction of near-field components such as buffer and backfill materials and waste package components such as steel, glass and concrete are studied. A special attention is given to surface layer formation, which is important in determining the release rate of radioisotopes at disposal;

c) to investigate and model the processes which govern the transport of radionuclides from the repository through the bulk of the geological formation and neighbouring geological strata up to the biosphere. As in the near-field studies, the final goal of this activity is the obtention of representative models for safety assessment. The geochemical conditions existing at depth are simulated in the laboratory, frequently through the use of sophisticated equipment such as anoxic boxes with controlled atmosphere, and highly sensitive analytical techniques such as laser spectroscopy. Preparatory activities for model verification by in-field experiments and the study of natural analogues are also carried out.

Contents

2.1 Risk Assessment (A. Saltelli)

The PAGIS Action

The PAGIS action (Performance Assessment of Geological Isolation Systems) was started in 1982 to investigate the general capability of selected geological formations and of the associated engineered structures to dispose vitrified High Level Waste so as to protect present and future generations and their environment. The evaluation is performed on the post operational phase through approaches and assessment methods largely common to the various options selected for the study, which are inland formations commonly found in the European countries : clay, granite and salt. The study also considers emplacement in the sub-seabed as an alternative to land based repositories.

PAGIS is a shared-cost action involving four European national institutes (CEN/SCK (B), CEA/IPSN (F), GSF/IFT (FRG) and NRPB (UK)), a coordinating group from the DG XII in Brussels and the JRC. A report covering the first phase of the action was issued in 1984 /1/.

The activity of the JRC Risk Assessment group in the PAGIS action was mainly to support the various institutes on the methodological issues and to provide a peer review for the comprehensive reports covering the four options, whose preparation has taken most of 1987.

Boxes 1 and 2, extracted from the PAGIS summary report (whose publication is expected by end 1988), illustrate a section of the PAGIS methodology : the stochastic performance assessment based on Uncertainty Analysis (box 1) and Sensitivity Analysis (box 2).

Methodologies and Computer Codes

LISA, PREP and SPOP

One of the main achievements of 1987 was the 3rd release of the LISA code delivered to the NEA data bank cf Saclay for further distribution. The code LISA (Long term Isolation Safety Assessment) has been developed at the JRC-Ispra to enable estimates to be made of radiation exposures which may affect future generations, as a consequence of radionuclide releases from nuclear waste repositories.
The code can be used to analyse release scenarios from waste repositories situated in sedimentary formations (argillaceous strata and seadbed sediments), and includes the following functions :

- decay chain evolution of the source term, as a function of time,
- radionuclide release from the repository, and migration through porous media by diffusion and advection,
- radionuclide dispersion into fresh-water or sea-water bodies,
- pathways to man and dosimetry.

The first version of LISA was prepared in 1984 and, since then, 14 different organisations have requested this code. In 1987, a new version of LISA was prepared (LISA 4) which includes the transport code TROUGH, developed from Polydynamics of Zürich. Unlike the preceeding versions, LISA 4 is not for free distribution, i.e. it is intended to be sold as a commercial product.

In the same year, two more tools related to the code LISA were issued : the PREP and SPOP codes. They are now available at the NEA data bank of Saclay. These two short computer programs tackle the problem of analysing model output uncertainty and model sensitivities. The PREP program (data PRE Processing unit) prepares the sample for a Monte Carlo simulation using the distribution functions of the input variables. The user is allowed to request any degree of correlation among the variables. Once the sample has been generated (with PREP) and Monte Carlo simulation has been performed (with a user supplied model) the utility SPOP (Statistical Post Processing unit) comes into use, performing uncertainty analysis and sensitivity analysis on the model outputs.

Boxes 1 and 2 from the PAGIS summary report in preparation show some principles of applications of these probabilistic methods.

JRC-ENRESA Cooperation

The LISA code development was the subject of a cooperation established between JRC and ENRESA (Empresa Nacional de residuos radioactivos S.A.).

One aim of this activity is to assist ENRESA in setting up all the conceptual and computational tools needed to perform a site specific risk assessment on a potential disposal site in granite. This proposal involves a transfer of know-how and of specific computational tools (such as the LISA and SPOP codes) as well as an active work of joint development needed to adapt LISA to the granite option being considered in Spain.

ENRESA shall provide a scientist for one year to work on the task agreed upon, the work being carried out with the Risk Assessment group of the JRC at Ispra. The cooperation agreement has become operative in June 1988.

Risk Quantification

An important aspect of the probabilistic performance assessment methodologies is the quantification of risk. A paper on the practical implementation of the risk computation, following the ICRP publication 46, has been prepared (Safety Assessment for Nuclear Waste Disposal. Some Observations about Actual Risk Calculations, by A. Saltelli and J. Marivoet, 1988). It deals with how to compare risks arising from different scenarios on the same risk diagrams (see box 3). This is particularly needed for the safety assessment of a disposal site, where some scenarios are certain to occur and others are of probabilistic nature. A risk diagram allows a synoptic view of the risks from the various scenarios, showing - at the same time - their probabilities and consequences.

Box 1

Uncertainty Analysis

Uncertainty analysis is aimed at quantifying the uncertainty in the output of complex model due to the uncertainty in model input parameters. In the present study, the output is generally taken to be the individual dose rate to the most exposed individual of the critical group at a certain time point (or the maximum of such a quantity over time). The complex model is the set of differential equations describing the barrier system. For any system uncertain parameter a distribution of values is defined which constitutes the input for the simulation. Uncertain parameters might be given normal, log normal or uniform density functions depending on their nature and on the amount of information available. The barrier model is then executed a large number of times, sampling, for each run, a set of parameters' values from their density function. In this way an empirical density function is obtained for the output dose. The results from Uncertainty Analysis can be visualised in a number of ways.

The probability density function (pdf) of dose at given time points. This is usually plotted as a histogram of frequency of dose in convenient dose intervals (usually logarithmic) at a given time of evaluation. It is a useful qualitative figure indicating whether the distribution is markedly skewed or has outliers. The pdf of maximum dose for each run irrespective of occurrence time can also be plotted. It should be noted that, because of the distribution form, the arithmetic mean lies close to the upper tail of the distribution.

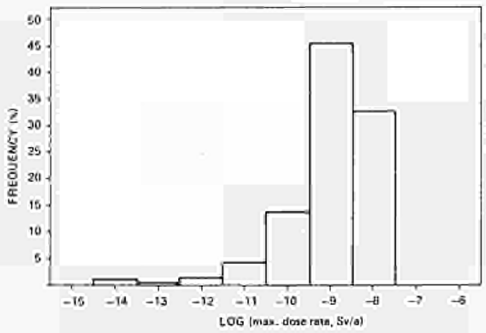

The cumulative pdf (cpdf) of dose at given time points. This is derived from the pdf histograms and can be plotted as downward or upward curve of cumulative probability against dose rate. It indicates the probability that any particular dose level will be exceeded at the time in question. In the figure, the 95% confidence bounds, computed with the Kolmogorov's statistics are also given. For any given dose level, the upper bound curve indicates the probability of exceeding that particular dose, at a 95% confidence level (see W.J. Conover, Practical Nonparametric Statistics (1980) John Wiley & Sons, New York).

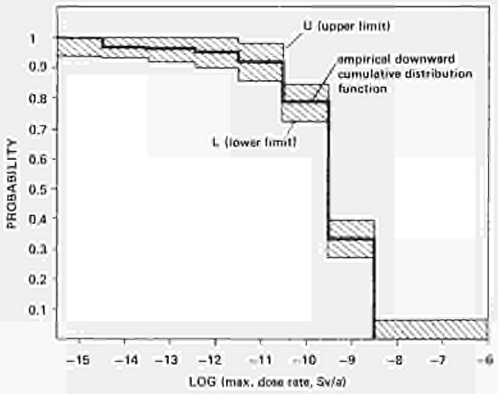

Mean, median and percentiles of the pdf of dose. The mean, median and percentiles of the pdf described above can be calculated and plotted as a function of time. The percentiles correspond approximately to the confidence limits implied from the input parameter distribution.

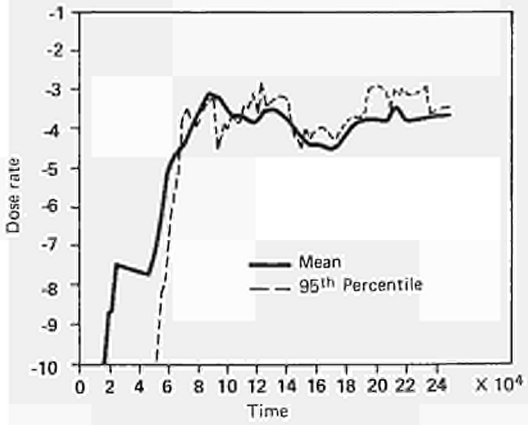

Risk curve as function of time. The mean of dose rates, when multiplied by the risk conversion factor, can be considered as an estimate of risk from the scenario being considered. A confidence bound can be computed on the mean value, using the appropriate statistics, and on the risk as well. In the figure, the risk curve as function of time is shown together with its 95% confidence bounds (see also J. Marivoet and A. Saltelli, Safety assessment for nuclear waste disposal : some observations about actual risk calculations. Radioactive Waste Managament and the Fuel Cycle, Vol. 9, 1988).

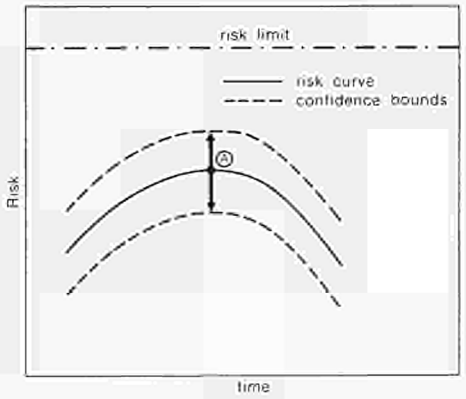

Box 2

Sensitivity Analysis

Sensitivity Analysis is the logical complement of any Uncertainty Analysis. After an empirical density function is obtained for the output dose through the Monte Carlo Simulation (Uncertainty Analysis) a Sensitivity Analysis can be made to identify which parameter was the most influential in determining the shape of the output density function. A good Sensitivity Analysis must satisfy two requisites : the sensitivity measure should weigh the entire range of parameter variability (and not just a small region around a central point); the sensitivity of a given parameter must be weighed over the entire space of the other parameters' ranges (and not keeping all the other parameters constant to their central value). The following techniques used in conjunction with the Monte Carlo analysis do the job.

Scatterplot diagrams. These provide a pictorial representation of dose at time, or maximum dose against an input parameter value. This illustrates the dependence between the two in a qualitative manner and can be used to detect non-linearities or discontinuities in dose rate to parameter relations.

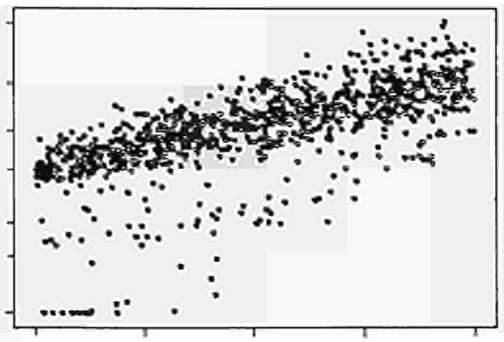

Smirnov tests. The Smirnov test, the Cramer-Von Mises test and the Mann-Whitney test belong to the same class of non-parametric statistics. In particular, they are "two-sample" tests originally designed to check the hypothesis that two different samples belong to the same population. The application of such "two-sample" tests to sensitivity analysis comes from the idea of partitioning the sample of the parameter under consideration into two sub-samples according to the quantiles of the output distribution. If the distributions of the parameter in the twp sub-samples can be proved to be different then the parameter under consideration is recognized as influential (see W.J. Conover, Practical Nonparametric Statistics (1980) John Wiley & Sons, New York).

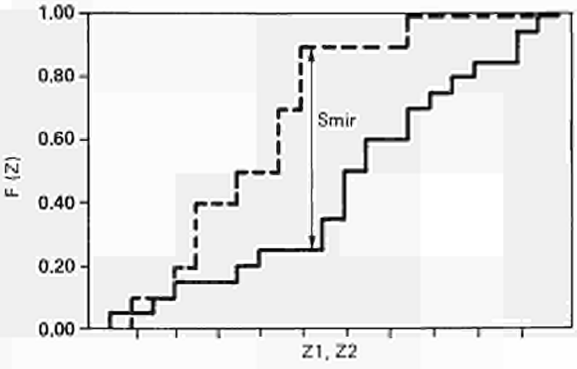

The Spearman rank correlation coefficient. This has the same functional form as the wellknown Pearson correlation coefficient but is based on the rank of the parameter values rather than on the values themselves. It is therefore more suitable for the detection of non-linear, but monotonic relations. It can be used as a test statistics to discover if the input and output variables have independent distributions (see W.J. Conover, Practical Nonparametric Statistics (1980) John Wiley & Sons, New York).

Partial rank correlation coefficient (PRCC). This is a measure of dependence between output and input after adjustment has been made for any influence due to the common dependence on any other parameter. The value of the PRCC lies between -1 and +1 and high absolute values represent a strong dependence between the two variables (see R.L. Iman, M.J. Shortencarrier, A Fortran 77 program to compute PRCCs and SRRCs. Sandia Nat. Lab. rep. NUREG/CR 4122, SAND85-0044 (1985)).

Box 3

The Risk Diagram

One point under debate in risk analysis calculations is how risks arising from different scenarios should be compared. One possibility is to sum up all the risk versus time curves to produce a single risk curve, having as confidence bounds the sum of the individual scenarios confidence bounds. One other possibility which allows a synoptic view of all the scenarios consequences is to use the risk diagram. In this diagram, isorisk curves have been drawn on H-P plane, where H is the dose rate and P is the probability of the dose being received. For doses below H^* the isorisk curves have been computed with the risk conversion factor r, taken as 0.01 $(Sv)^{-1}$, while for $H > H^*$ the isorisk curve lays on the probability horizontal axis having the same numerical value. (H^* is the dose limit for non-stochastic effects, i.e. the dose beyond which a health effect is certain to occur.)
In order to improve the readability of the diagram, the area beyond the risk curve $R = 10^{-5}\ (a)^{-1}$, taken here as the regulatory limit, has been shaded. The limiting dose for non-stochastic effects has been taken as $H^* = 1$ Sv/a for the purpose of illustration. All the isorisk curves exhibit a discontinuity in correspondence with this value. Risk arising from different scenarios can be plotted on this diagram by taking the maximum, over time, of the risk curve and placing this point, with the corresponding confidence bounds, on the proper isoline. The position of the point along the risk line can be assigned depending on the nature of the scenario.

For scenarios whose probability of occurrence is very close to one (normal evolution scenarios, in the radwaste terminology), the risk is simply given by the consequence, and the point can be positioned on the probability 1 line in correspondence to the dose value H or, if the distribution of dose has been estimated, to the expected value E(H) (point A).

- For scenarios where the probability of occurrence is significantly lower than one, and the distribution of dose has been estimated, the risk can be computed as $R = P_s r E(H)$, where P_s is the scenario probability. Even in this case the point can be positioned on the proper isoline in correspondence with the P_s, E(H) intercept (point B). The horizontal bars indicate the risk confidence bounds as computed from the dose distribution. If the probability of the scenario can itself be given a confidence bound, this can also be plotted on the same figure with vertical bars (point B).
- For catastrophic or disruptive scenarios, where only the probability of the scenario occurrence has been calculated, and consequences are expected in the non-stochastic range, the risk numerically coincides with the scenario probability and the risk point can be located on the proper risk isoline in correspondence with $H = H^*$ (point C). In this case the confidence bounds can only be given for the scenario probability.

In this way, heterogeneous scenarios can be combined in a single diagram which also gives the uncertainty on any single prediction.

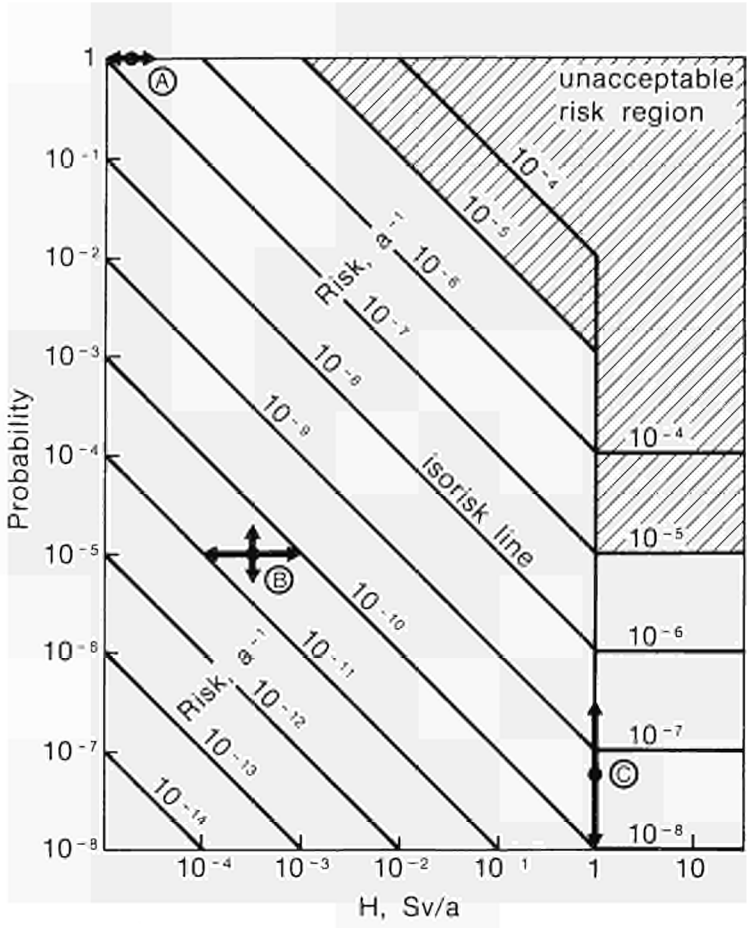

Ispra Course on Risk Analysis

During 1987, a preparatory work was carried out in order to held in May 1988 an advanced seminar on risk analysis and performance assessment in the field of nuclear waste management. It addressed different disciplines, such as Statistics, Risk Analysis, Radioprotection, Geology and Climatology, which are relevant to the analysis of the risk linked to the long term disposal of nuclear waste. The lectures cover the following issues :

- Risk perception — Reasons of the public adverse attitude toward the nuclear sector. Modelling of the risk perception. Use of psychometric studies. Risk communication to non-technical audiences.
- Probabilistic risk assessment in the nuclear sector - Analogies and differences between reactor safety and waste disposal safety.
- System Variability Analysis - use of Monte Carlo Techniques. Uncertainty Analysis, Sensitivity analysis and computation of the risk. Use of nonparametric statistics.
- Geology and Climatology - How complex climatic changes can affect the repository performance. How can they be modelled. The example of glaciation.
- Sub-seabed disposal - Specific features of the oceanic disposal. A worked example : the probabilistic safety assessment on two potential sub-seabed sites (conclusions of the international Seabed Working Group report).
- Continental disposal - The European project PAGIS (Performance Assessment of Geological Isolation System). Methodology of the study and its main conclusions. Worked examples from the Canadian concept assessment, the French deterministic approach and the UK dry run No. 2.
- Natural Analogues - Examples of natural analogues to the repository system. How can they be used in performance assessment.

The invited lecturers were B. Wynne (Centre for Science Policy, Univ. Lancaster), B.J. Garrick (Pickard, Lowe and Garrick Inc., California, USA), S. Islam (Max-Planck Institute, Munich), Bruce Goodwin (Atomic Energy of Canada Ltd., Pinawa), B. Thompson (Dept. of the Environment, London), J. Lewi (Commissariat à l'Energie Atomique, Fontenay-aux-Roses), S. Mobbs (Nat. Radiological Protection Board, Harwell), J. Fourniguet and G. Aubertin (Bureau de Recherches Géologiques et Minières, Orléans), G.S. Boulton (Grant Inst. of Geology, Univ. of Edimburgh), I. Mc Kinley (NAGRA, Baden).

The JRC contributions were be presented by A. Saltelli, M. D'Alessandro, D.A. Stanners, and F. Girardi of the Division of Radiochemistry. The course was coordinated by the Risk Assessment Group.

Code Verification : Activities at the NEA/PSAC Group

The Probabilistic System Assessment Code User Group (PSAC) was established by the OECD-NEA Radioactive Waste Management Committee in early 1985 to assist in the development of Probabilistic Assessment Codes (as LISA) by member countries of the OECD.

One of the major goals of the PSAC group is to establish a defensible basis for confidence in the capabilities of PSA (Probabilistic System Assessment) and related codes. Code intercomparisons provide evidence that different codes operated by different groups produce similar results when applied to the same problem. Such evidence contributes to the verification and quality assurance of the codes involved.

The intercomparison activity was started in 1985, with a first "level 0" intercomparison, mainly aimed at checking the executives modules of the PSA codes. Two years and four iteration of the intercomparison were necessary before an acceptable level of agreement was reached among the results from the different codes, thus showing the real relevance and opportunity of the exercise.

The JRC had an important role in the level 0 implementation contributing to both the test case specifications /2/, and to the analysis of the results /3/.

Figure 2.1 gives the flavour of the relative complexity of the intercomparison, showing the results for the third (Fig. 2.1a) and fourth iteration (Fig. 2.1b). The figures are principal component analysis projections, each letter representing globally the results of a given participant.

It can be seen that the spread in the results was much greater for the third iteration, where systematic errors were detected, than for the fourth one, where the residual error is believed to be of random nature (the codes being compared are Monte Carlo in type). The asterisk (*) in Figs. 2.1 represents a fictitious participant whose predictions equal the mean of those from all the participants. Analogously, the plus (+) and minus (-) deviate from the mean of one (inner (±)) or two (outer (±)) standard deviations. These fictitious participants helped ensuring that the residual error was of random nature.

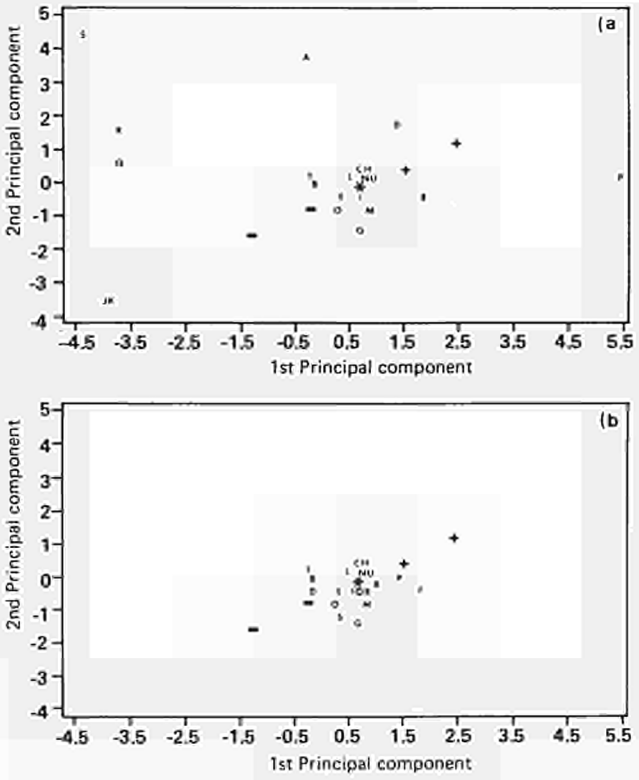

Fig. 2.1 - Results of third and fourth iteration in level 0 PSACOIN intercomparison
a) third iteration; b) fourth iteration

The main conclusions of the study can be summarized as follows :

a) **Uncertainty Analysis.** Good agreement was obtained for the estimate of the mean dose (the output being considered) for 19 sets of results, involving 12 different PSA codes, several different sampling strategies and sample sizes ranging from one hundred to one million simulations.

b) **Statistical post-processors.** Most PSA codes are designed to calculate and save a set of detailed results from many simulations. Post-processor codes are then used to analyse these results, and extract information such as mean values and standard deviations in dose at specified times, and

reorganize the data to prepare, for example, histogram and cumulative plots. Since the results actually compared were the outputs from some post-processor codes, the intercomparison implicitely includes a test of those post-processors. The consistency of the results indicates that they are functioning correctly and as expected.

c) **Sensitivity Analysis.** Most of the participants consistently identified and ranked the same set of radionuclides that contributed to the mean dose. Some participants also consistently identified the most significant parameters affecting mean dose, but there was less satisfactory agreement in the ranking of these parameters. This exercise has shown that sensitivity analysis of PSA code results is a complex and difficult task, and further work is required. The JRC was charged with the task of exploring the specifications for a sensitivity analysis intercomparison exercise using the SPOP code.

Presently, a second intercomparison is being run, which involves checking the results of PSA codes against a set of analytical results (level E PSA code intercomparison). This exercise should be finished in 1988.

References

/1/ A. CADELLI, G. COTTONE, G. BERTOZZI, F. GIRARDI — PAGIS, Summary Report of Phase 1. A Common Methodological Approach Based on European Data and Models. Nuclear Science and Technology reports, EUR 9229/EN (1984)

/2/ B. GOODWIN, A. SALTELLI — PSA Codes Level 0 Intercomparison. AECL Technical Report 1985, revised 1986

/3/ A. SALTELLI, E. SARTORI, T. ANDRES, B. GOODWIN, S. CARLYLE — PSACOIN Level 0 Intercomparison. An International Code Intercomparison Exercise on a Hypothetical Safety Assessment Case Study for Radioactive Waste Disposal Systems. OECD/NEA Publ., Paris (1987)

2.2 Near Field Evolution

This activity is intended to investigate the processes which occur in the near field of vitrified level waste and conditioned alpha waste. It is split into four tasks which are :

- corrosion of the canister
- surface layer formation and radionuclide release
- vitrified waste in clay and sea sediments
- vitrified waste in salt systems (carried out at JRC-Karlsruhe)
- alpha-contaminated waste embedded in concrete.

Corrosion of the Canister (F. Lanza)

In the framwork of the seabed disposal project (see chapter 3), a series of tests were performed in the previous year in carbonaceous oceanic sediments (CV2) in isothermal conditions in order to obtain the homogeneous corrosion rate of iron penetrators. The values obtained range from 8 to 95 μm/year for a temperature of 50 or 90°C. It has to be noted, however, that, due to the radioactive decay, the waste package will generate heat so that the sea sediments surrounding the iron overpack will not be isothermal but will be subject to a thermal gradient. As the corrosion rate depends also on diffusion of hydrogen and iron corrosion products, it is possible that the thermal gradient influences the corrosion rate.

An apparatus has been set up which allows to impose a thermal gradient on a column of sediments. Two thermostatized head allows to fixe the temperature at an upper value of 90°C and a lower one of 70°C. As the sediment column is 20 cm long, a gradient of 1°C per cm is obtained. The samples of mild steel were exposed to the sediments only on one face, namely that which was facing a decreasing temperature. Fig. 2.2 shows the assembly of ten units which has been used to perform the tests. The sea sediment was obtained from bottom of the Atlantic Ocean at the site Capoverde 2. It is a sediment rich in carbonates, around 50%. Ten similar units were mounted together in a rack, using common units which allows to keep the desired temperature at ±0.5°C. The samples were extracted successively every third week. Afterwards a new sample was introduced in the unit, to be unloaded at the end of the experiment. In this way, we have a duplication of the experimental data.

Two runs of 20 samples each were conducted. The first had to be stopped ater 112 days due to a failure of the pump on the high temperature loop. The second one, also comprising 20 samples, had a maximum duration of about 200 days.

In the previous tests in isothermal conditions, it was realised that the anoxic condition was prevalent. As a consequence, corrosion products were in the divalent state which have a certain solubility snd diffuses in the sediments. In fact, the samples did not present an adhering scale and were easily cleaned in ethanol using an ultrasonic bath. After the cleaning, the sample showed a metallic shining surface.

In the tests we have conducted under a thermal gradient, the situation is rather different. The surface is covered totally or partially by a hard adherent layer. Even in this case the samples were simply cleaned in ethanol using an ultrasonic bath.

The weight variations are reported in Fig. 2.3. It can be seen that after an initial period of about 50 days, the weight of the

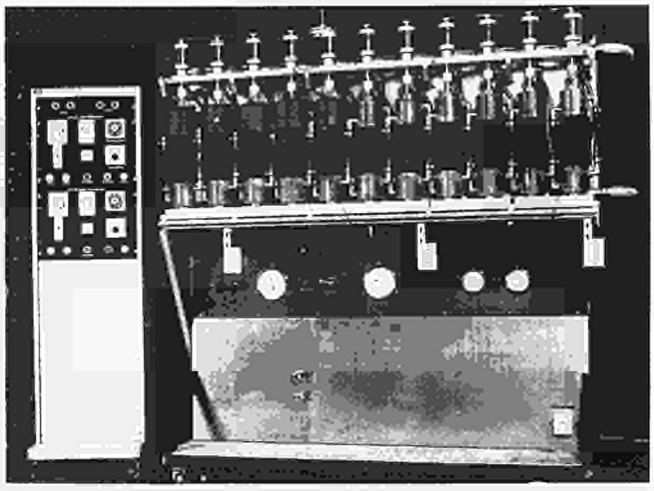

Fig. 2.2 - Assembly of the units for the study of corrosion under a thermal gradient

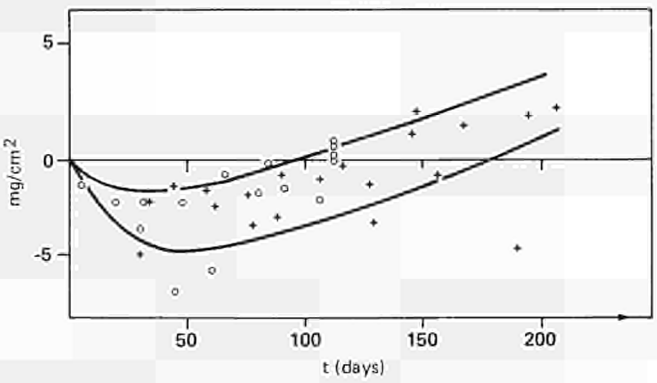

Fig. 2.3 - Variation of the specific weight of samples as a function of time

samples begins to increase reaching after about 80 days a steady increase rate of $3x10^{-5}$ gr/cm^2 day.

An analysis of the surface by XPS has shown the presence of carbon, iron, silicon and traces of calcium. The samples were etched using a solution of oxalic acid and water peroxide. A further analysis has shown the presence of calcium, iron and silicon. It appears that the surface scale is formed primarily by calcium carbonate and iron silicate.
A detailed report is in preparation.

Surface Layer Formation and Radionuclide Release

(A. Manara)

The aim of this activity is to obtain a description of the processes occurring in the surface layers of vitrified waste in different chemical-physical conditions regarding both in pH and EH. Weight loss and ESCA measurements are performed to determine concentration and valence of the different elements in the surface layers in order to have a picture of the situation after leaching in different conditions, i.e. different gas atmosphere during leaching process.

Surface and structural studies

It is commonly acknowledged that with time underground storage-deposits are prenetrated by deep water, which, after having corroded the steel containers, begins to corrode the glass. This deep water can have different chemical-physical conditions regarding both its composition and its pH and EH. In a previous study /1/, the influence of redox conditions on the leaching of elements having multiple valencies was studied. The leaching was carried out using the Sohxlet method, which foresees a continuous renewal of the distilled water used as a leaching agent. In particular, the behaviour of Fe and U was examined.

The concentration in -HCO_3 ions was added in the present study as a quantity to be investigated. It is, in fact, known that certain elements, especially actinides, form soluble complexes in presence of such ions. The tests were carried out in such a way as to define both the elements on the degrated surface of the glass itself. The tests were carried out in a static system so as to be able to compare the results obtained with those obtained during the preceding dynamic tests.

The experiments were conducted in polycarbonate vials, into which two glass samples - one large and one small - were introduced. The samples, tied with platinum wire, were immersed into distilled water with an electrical resistance of more than 2 MΩ. The ratio-leached surface/leaching solution was 0.25.

In order to obtain the different redox conditions as well as the different conditions of bicarbonate ions, the leaching solutions were balanced with different gas mixtures (Table 2.I).

The results obtained from the analyses of boron, sodium and silicon in the leaching were used to calculate normalized loss. It was observed that such data, as is also true for the global weight loss, can be fitted as a function of time according to an exponential function,

$$\Delta W_i = A\, t^n.$$

The evaluation of the parameters A and n was carried out using the least squares method for the different cases. The results are shown in Table 2.II. The standard deviations of the coefficient A, obtained assuming that the exponent n does not contain errors, are shown in the same table.

It can be seen that there is no substantial difference in the exponent in both oxidising and reducing conditions. The data can be divided into two groups. The equivalent weight losses

Table 2.I - Composition of different gas mixtures

Component	% in volume	Mixture
Oxygen	20.2	I
Argon	rest	
Carbon dioxide	0.4 ($5x10^{-5}$M/l)	
Oxygen	20.	II
Argon	rest	
Carbon dioxide	0.4 ($5x10^{-5}$M/l)	
Hydrogen	5	III
Argon	rest	
Hydrogen	5	IV
Argon	rest	

Table 2.II - Values of the coefficients A and n in the different conditions

Condition	A	σA	n
$\Delta w(B_2O_3)$ in Arg + O_2 + CO_2	$3.53x10^{-4}$	$8.6x10^{-6}$	0.42
$\Delta w(B_2O_3)$ in Arg + H_2 + CO_2	$3.00x10^{-4}$	$7.2x10^{-6}$	0.42
$\Delta w(Na_2O)$ in Arg + O_2 + CO_2	$3.73x10^{-4}$	$1.1x10^{-5}$	0.42
$\Delta w(Na_2O)$ in Arg + H_2 + CO_2	$3.27x10^{-4}$	$1.4x10^{-5}$	0.42
$\Delta w(SiO_2)$ in Arg + O_2 + CO_2	$7.73x10^{-5}$	$2.5x10^{-6}$	0.31
$\Delta w(SiO_2)$ in Arg + H_2 + CO_2	$7.26x10^{-5}$	$2.6x10^{-6}$	0.31
Δw in Arg + O_2 + CO_2	$1.30x10^{-4}$	$3.7x10^{-6}$	0.35
Δw in Arg + H_2 + CO_2	$1.17x10^{-4}$	$2.3x10^{-6}$	0.35

due to the release of boron and sodium which show a common exponent close to 1/2. The weight loss of the sample and those equivalent due to the release of silicon which show an exponent close to 1/3. It would appear reasonable to conclude that the release of sodium and boron follows a different mechanism from that of silicon.

A phenomenon depending on time according to a power of 1/2 can be identified with a diffusion mechanism. It therefore appears likely that the velocity of degradation, and consequently the release of boron and sodium, is controlled by diffusion in the surface layer. The variation in weight and the release of silicon seem, on the other hand, to depend also on a reprecipitation mechanism of some complex silicates.

A statistical analysis of the coefficients using the "Student" test shows that the difference existing for every Δw between the oxidising and the reducing conditions should be considered significant even at a confidence level of 99%. The oxiding condition, therefore, makes the weight loss as well as the velocity of degradation slightly higher. Surface analyses were carried out on silicon, uranium and iron concentration using the XPS method on the small samples with a diameter of 6 mm. The samples were examined exactly in the same way as received and after two different sputtering times, 10 and 70 minutes. The sputtering, carried out by bombarding the surface with argon ions, permits the successive removal of thickness from the surface layer. In such a way the concentration variations of the layer thickness can be revealed. In order to make the leaching processes, which cause the formation of the surface layer, more evident, the concentrations of the various element will be related back to the concentration of the base glass.

In Fig. 2.4 are shown the values of the concentration relative to silicon as a function of sputtering time. It can be seen that even

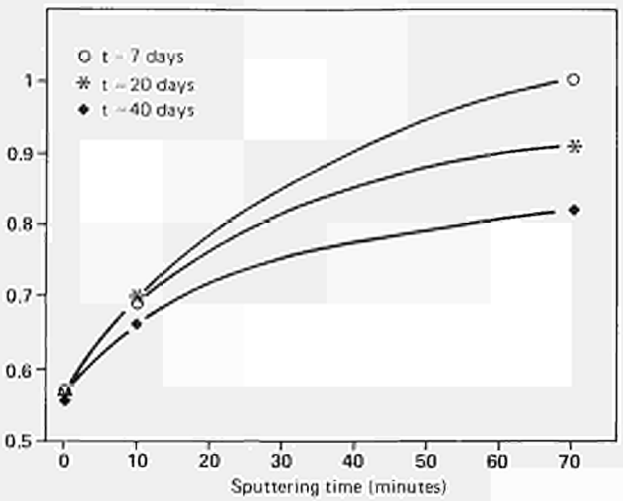

Fig. 2.4 - Relative content of Si in surface layers

though the value of the concentration on the external surface remains constant, the gradual increase in the concentration depends on the leaching time, longer times corresponding to more gradual increases.

The results of uranium analyses are shown in Table 2.III. It can be seen that on the external surface, corresponding to a null sputtering time, the relative content in uranium tends to decrease with time. It appears evident that the release of uranium is caused by a slow solubility. Moreover, it can be noted that, even in a static system, the uranium retained on the surface in oxidising conditions is less than in a reducing system. Also the presence of CO_2 helps to decrease the amount of uranium present in the layer in both oxidising and reducing conditions. Such an effect is particularly evident on the external surface of samples leached for 40 days.

Table 2.III - Relative concentration of U at the surface

Atmosphere	7 days		20 days		40 days		
	0'	10'	0'	10'	0'	10'	70'
Argon + O_2	0.89	1.42	0.57	1.08	0.43	1.08	1.17
Argon + O_2 + CO_2	0.46	1.39	0.54	1.02	0.32	0.79	1.14
Argon + H_2	0.96	1.32	0.68	1.31	0.33	-	-
Argon + H_2 + CO_2	0.87	1.49	0.68	1.24	0.29	0.78	1.38

Table 2.IV shows the results obtained for iron. It can be seen that, also in this case, the values are lower in the external surface. However, the decrease steps after 20 days, as if the phenomenon of dissolution were no longer important. Moreover, there is no effect due to the different atmospheres, neither in redox conditions nor in presence of carbon dioxide. This fact is even more surprising when taking into consideration the tests previously carried out in flowing water /1/ which had shown a very clear effect of the oxide-reducing conditions.

One possible explanation of such a difference between closed and open systems is the assumption that the iron forms a highly insoluble compound. In such a case, once a concentration in solution corresponding to the product of the solubility has been reached, there is no more release and the composition accumulates in the layer. In the case of trivalent iron the same hydroxide is highly insoluble. The difference in enrichment

Table 2.IV - Relative concentration of iron at the surface

Atmosphere	7 days		20 days		40 days		
	0'	10'	0'	10'	0'	10'	70'
Argon + O_2	2.88	4.19	1.92	3.81	1.85	3.70	3.28
Argon + O_2 + CO_2	3.07	4.90	1.90	4.08	1.88	3.95	3.49
Argon + H_2	3.14	4.34	2.84	4.23	2.28	4.24	3.55
Argon + H_2 + CO_2	3.40	4.38	2.64	4.30	-	-	-

existing in a dynamic system was attributed to the insolubility of this compound /1/. In the case of reducing atmosphere and, therefore, the release of bivalent iron, it can be assumed that the critical product is the iron silicate. From silicate (?) is slightly soluble, so that in a flowing system it is continuously removed while in a closed system it reaches rapidly the solubility limit and begins to precipitate.

Vitrified Waste in Clay and Sea Sediments

(F. Lanza)

In the tests performed in the past period, the leaching of glasses in clay and sea sediments and the resulting diffusion of the released elements was investigated. The tests were performed using simulated glasses and diffusion coefficients in clay and sea sediments of cesium, uranium, cobalt, europium and lanthanum were obtained. The amount of released elements has been evaluated and compared with the leaching rate of the sample. It appears that elements can be subdivided into two classes, those presenting a high solubility which are released proportionally to the glass degradation, and those which encounter a solubility limit and are released proportionally to the square root of the time.

Two series of tests were performed in order to verify the capability of clay and sea sediments by reducing technetium. A special glass spiked with technetium has been prepared. A first series has been conducted at 50°C up to a maximum of 56 days. It appears (Fig. 2.5) that the apparent diffusion coefficient was

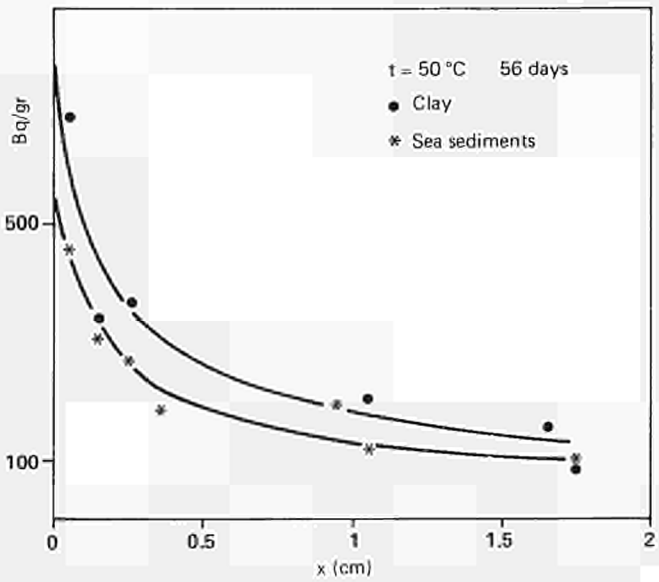

Fig. 2.5 - Distribution of the specific activity of technetium for clay and sea sediments

lower for clay which presents a lower Eh coefficient. A mathematical analysis of the diffusing species distribution is being done, assuming a simultaneous diffusion and reduction of the pertechnatate ion.

A second series of tests is being conducted at 75°C. It has to be noted that activation energy of glass degradation (~ 15,000 cal/mole K) is decidedly higher than that of diffusion in liquids (3,000 - 5,000 cal/mole K). Increasing the temperature will allow a higher release of technetium by a not very different diffusion coefficient, improving in this way the possibility to detect technetium.

A study on the effect of a thermal gradient on the diffusion of in mountmorillonite and sea sediment of cesium leached from a glass is in preparation. It is foreseen that it will begin in January 1988 and will terminated at the end of October. A detailed report is expected for the end of the year.

Vitrified Waste in Salt Systems (Hj. Matzke)

An activity to obtain a physical description of phenomena occurring in the near field of vitrified radioactive waste in a salt formation was started in 1984. This work was incorporated in the radioactive waste management activity of the JRC-Ispra and was performed at TU Karlsruhe. It was based on competence existing in TU with crystallaline waste matrices, and on experience gained in a cooperation with the Institut für Nukleare Entsorgung, Karlsruhe (KfK) on waste glasses. The decision in favour of salt systems was motivated by the fact that studies for the two alternative systems, i.e. clay and granite, were already done at other laboratories.

The first activity was the production of different waste glasses containing 0.5 and 1.5 wt% ^{244}Cm in order to study radiation damage effects with a realistic damage source, i.e. α-decay, and reaching saturation levels of damage in an acceptable time span of a few years. In 1988, the highest damage levels in theses glasses will correspond to those expected for repository conditions of vitrified HLW in more than 10^5 years. Leaching, density changes and fracture behaviour were monitored continuously through the period.

When these glasses were produced and accumulated damage, the activity was widened in two directions: measurement techniques suitable for highly radioactive glass specimens were developed (e.g. indentation methods for fracture behaviour7 and a broad parametric study was executed with simulated waste glasses in order to provide the necessary basic data for understanding the behaviour of vitrified waste in a salt system. Examples of this activity are :

- *leaching studies in water and Q-brine as functions of temperature,*
- *measurement of synergistic effects of waste glass leaching due to the presence of container materials (steel, Hastelloy and Pi/Pd alloy)*
- *studies of the diffusion of alkali ions in the glass since alkali ions are exchanged with the aqueous solution during leaching,*
- *interaction studies and interdiffusion measurements in the system : realistic repository salt/waste glasses (including fully active glasses),*
- *measurement of actinide diffusion in salt.*

To extend the number if available analytical tools, characterization work was done in the shielded microprobe and in the high resolution scanning transmissions electron microprobe of the institute, and additional techniques (Rutherford scattering, elastic recoil deflection, nuclear reactions, etc.) were adjusted to the specific case of analysis of leaded glass surfaces.

Radiation Damage Studies

Cm-containing glass

The on-going work with French, German and USA waste glasses doped with ^{244}Cm in order to realistically simulate radiation damage in an acceptably short time were continued. Damage levels corresponding to storage times of real waste glasses in excess of $\sim 10^5$ years have been produced.

The previous work has shown important damage effects in waste ceramics which, in fact, loose part of their attractiveness in the damaged state : they become amorphous (metamict), show significantly increased leach rates and swelling (volume increases) of up to 10%, etc. The effects observed for glasses are much smaller. As typical example, results for the US GLASS MCC 76-68 doped with ^{244}Cm are given in Fig. 2.6. Similar results were obtained with the French glass SON 681617 L1C2A2Z1 and the German glass GP 98/12.

Figure 2.6 shows a pronounced decrease in hardness and in crack length at Vickers indentations with increasing radiation dose. In a previous progress report (1985), the theoretically expected /1/ slope of 2/3 in a plot of crack length, c, versus indentation load, N, was observed for both undamaged and damaged glasses : an example for all three glasses at a damage level of 3.3×10^{24} α-decays/m^3 had been given. The upper part of Fig. 2.6 shows the corresponding increase in load to achieve

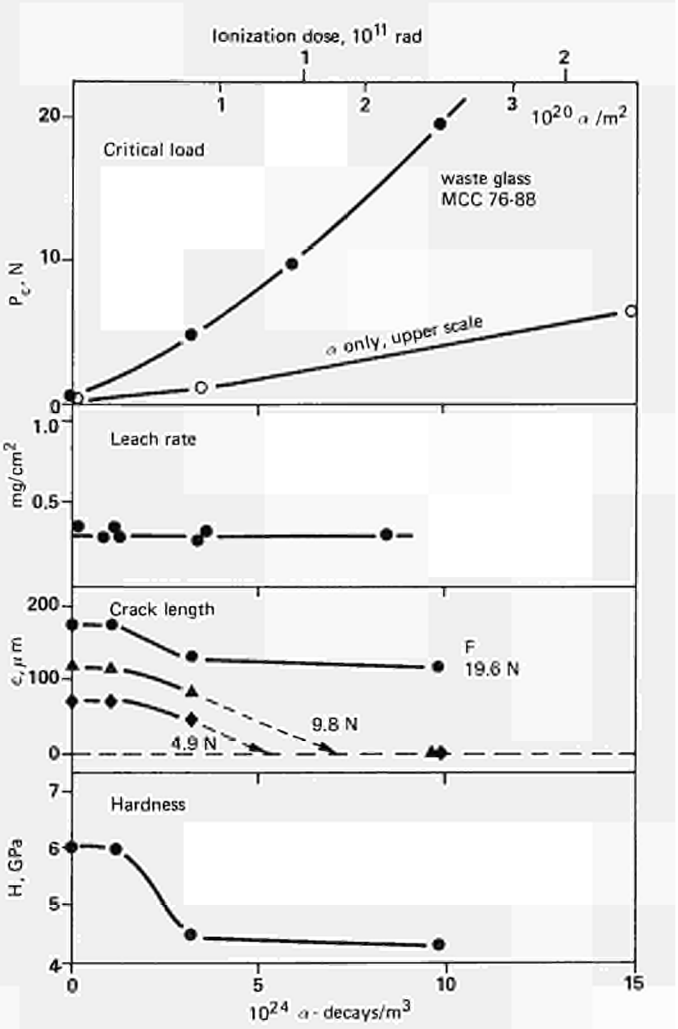

Fig. 2.6 - Property changes in Cm-doped waste glasses vs damage level. The glass is MCC 76-68. Shown are increase in critical load for fracture (included are previous data with damage by α-particles alone, open circles (2)), the lack of a significant effect on leaching, the decrease in crack length at Vickers indentation leading to a disappearance of cracks at higher damage levels, and the decrease in hardness with damage dose.

a 50% probability for fracture (critical load, P_c) as function of dose. At the same time, no significant effect on weight loss during leaching (for the conditions used, i.e. 150°C, 14 d, H_2O) is found; the lack of a significant effect of damage on leaching was also supported by ICP-emission analysis of the solutions. The upper part of Fig. 2.6 showing the drastic increase in P_c of Cm-doped damaged waste glasses includes previous results /2/ on a similar effect in the same glass bombarded with α-particles alone. In this case, the recoil particles (e.g. a 100 keV ^{240}Pu daughter atom in the decay of ^{244}Cm) with their high energy-density cascades are absent. The α-bombardment damages a surface layer of $\sim 25\ \mu m$ thickness. The corresponding number of α-decays/m^3 (which, however, include also recoil atoms) has therefore been taken as being higher by a factor of 4×10^4. If this scaling is accepted, the contribution of α-particles to the observed increase in fracture toughness is a small fraction of that of the recoil atoms. A similar conclusion can also be drawn from previous results with 77 MeV α-particles from the Karlsruhe cyclotron /3/. The density changes of all glasses were $< 1\%$ showing the absence of significant swelling (in contrast to the large swelling of the waste ceramics investigated so far).

Ion implanted glasses

The extensive work with glasses implanted at room temperature and reported in previous PRs, was continued with a study of the effect of temperature **during** damage production on properties of the nuclear waste glasses GP 98/12 and SON 681817 L1C2A2Z1. The chemically inert element Kr (energy range 50 to 200 keV) was used to produce damage in the glasses held at increased temperatures (100 to 250°C) during implantation. In a real waste glass, most damage occurs when the glass temperatures are in this range.

The fracture toughness K_{Ic} was measured as before by Vickers indentations using the equation

$$K_{Ic} = H\sqrt{a}(E/H)^{2/5}\ 0.057(c/a)^{-3/2},$$

This equation holds /1/ when the average crack length, c, is significantly larger than a, the indentation half diagonal. H is the hardness, obtained from the indentation, and E is the elasticity or Youngs modulus /4/. Five indentations were made for each load (load range 5 to 20 N). The theoretically expected slope of 2/3 in a plot of c versus load P was again observed : the increase in K_{Ic} in the damaged glass compared to the undamaged glass reported in previous PRs was still found at 100°C bombardment temperature, but not at 250°C anymore.

Leaching was done in autoclaves in distilled water at 200°C for 4 h, using a ratio of water volume V (in cm^3) to specimen surface area S (in cm^2) of V/S = 10 cm. Parallel measurements on un-implanted specimens were performed to deduce the contributions of the rear and of the sides of the glass specimens to the measured leach rates. Following leaching, Rutherford backscattering (RBS) analysis with 2 MeV He-ions was performed at the Van-de-Graaff accelerator at KfK, Na-profiles were measured with the nuclear reaction ^{23}Na(p,α)^{20}Ne at the University of Firenze, and H-profiles were measured using the nuclear reaction ^{1}He-(15_N,α)^{12}C at the University of Padova. For a description of the techniques, see a recent review published within the reporting period /5/. A large set of specimens (2 glasses, SON and GP, 2 bombardment doses and 3 implantation temperatures each) were leached. Figs. 2.7 and 2.8 show typical examples of the results. The analyses are not completely terminated yet. Fig. 2.7 shows significant enrichment of fission products, of Zr and Fe at the surfaces of leached SON glasses, and Fig. 2.8 shows hydrogen uptake in GP 98/12 due to leaching. The results available so far show an effect of temperature during damage production on leaching as well. Radiation-enhanced Na-diffusion is also affected, as was shown for fracture toughness above. More details and a discussion in terms of damage recovery during damage formation will be given in the next PR. The consequence of the present results for further damage work is to include temperature **during** damage production as an important parameter in future work.

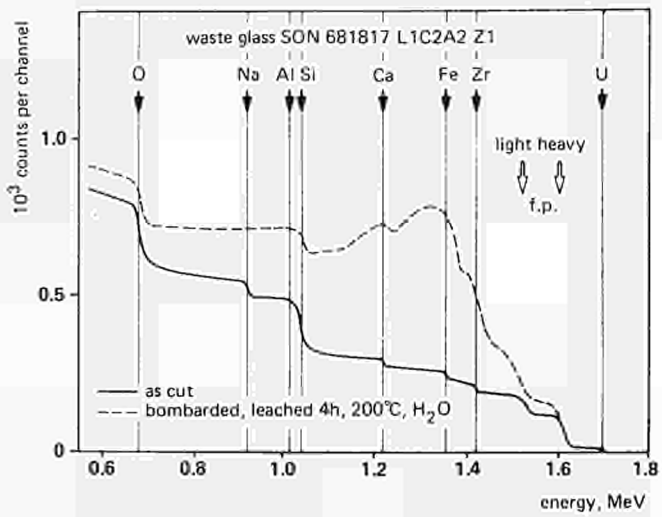

Fig. 2.7 - RBS spectrum of the waste glass SON 681817 L1C2A2Z1 leached for 4 h at 200°C

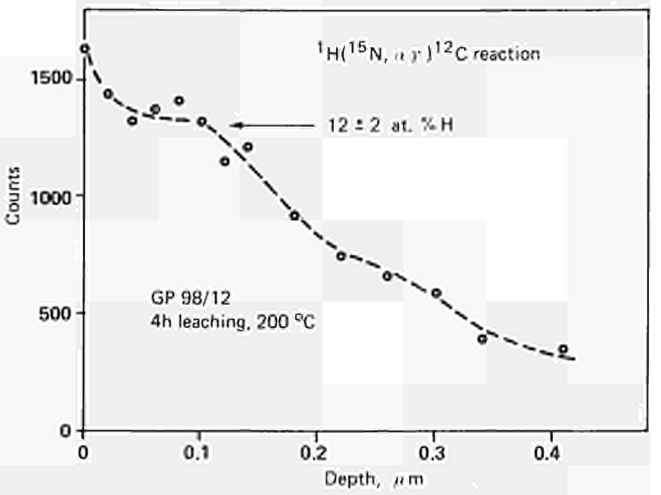

Fig. 2.8 - Hydrogen profile at the surface of waste glass GP 98/12 leached for 4 h at 200°C

Cm-doped and ion-implanted waste ceramics

The extensive study on ^{244}Cm doped host phases of actinides, i.e. on zirconolite $CaZrTi_2O_7$, on $Ca_2Nd_8(SiO_4)_6O_2$ and on $Gd_2Ti_2O_7$ and reported in previous PRs have been terminated and published /6/.

In the reporting period, the radiation stability of the complex, tailor-made waste ceramic SYNROC B was studied. Gas release measurements had indicated transformation to the amorphous state during ion implantation /5/. Further ion implantation work using high energy (570 keV) Pb-ions of the Orsay accelerator showed that the anticipated metamictization is accompanied by a large enhanced leachability. Fig. 2.9 shows RBS spectra of the implanted SYNROC either leached in the as-bombarded state or pre-annealed at 400 and 800°C for 15 min. before leaching (4d, H_2O, 150°C). Good agreement between the spectrum calculated on basis of the components added in the fabrication step and the measured spectrum is found. The typical shoulders for all components (O, Al, Ca, Ti, Zr, Ba) are seen, as indicated by arrows. Indicated is also the surface position of Pu. The Pb peak is buried to about 0.2μm depth because of the high bombardment energy (570 keV, triply charged Pb ions being

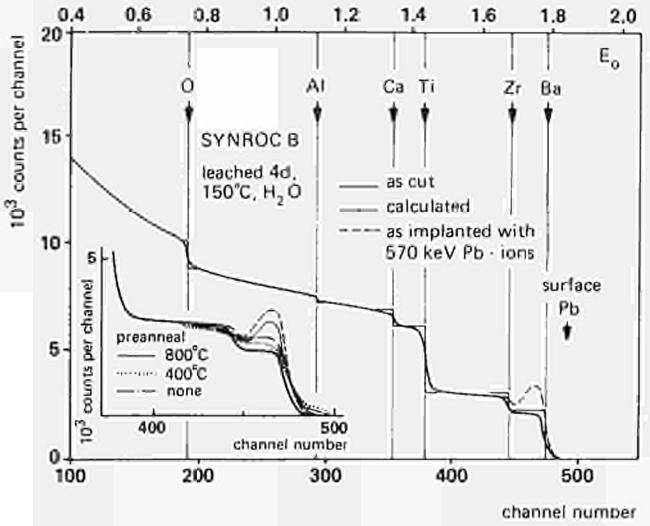

Fig. 2.9 - RBS spectrum of Pb-implanted and leached SYNROC B. The implanted damaged layer is leached away in as-bombarded SYNROC and SYNROC pre-annealed at 400°C whereas an anneal at 800°C restores the original low leaching rates of the ceramic.

used). Most of this implanted Pb-containing layer of about 0.2μm thickness is dissolved in the damaged SYNROC (not annealed annealed or 400°C, which is not sufficient given the fact that recrystallization is known to occur in the temperature range of 500-700°C). In contrast, annealing at 800°C, expected to cause recrystallization, causes the bombarded SYNROC to show the normal low leach rates of as-produced SYNROC. Continued leaching for up to 1 month under the same conditions eroded away a layer of 0.05μm thickness on the 800°C sample as shown by the Pb-peak used as a depth marker. This gives a lower limit to the enhancement factor in leaching between damaged and undamaged SYNROC of 35; the real number is probably even larger since less than 4 d may have been necessary to leach the bombarded layer away. More experiments with shorter leaching times are planned.

Prolonged leaching caused the expected preferential loss of Ca and Ba from SYNROC. This was obvious in the RBS spectra, and was confirmed by ICP emission analysis of the leaching solutions.

A ^{244}Cm doped SYNROC-B was also prepared. Gradual shrinkage of X-ray lines with increasing dose indicate onset of amorphization. No microcrack formation was sofar seen in 1000x magnification. The specimen will be reanalysed at further increase dose levels.

Alkali Diffusion in the Waste Glass GP 98/12

In the PR 1986, the reasons for this activity and extensive results for the diffusion of Rb using radioactive ^{83}Rb and ^{84}Rb of the Karlsruhe cyclotron as tracers were given. In brief, we wanted to improve our understanding of the leaching processes (basic step exchange of alkali ions by H), to explain the observed effects of alkali migration in thermal gradients (as they exist during storage) and during irradiation with external beams and also to provide data needed to decide whether the mixed alkali effect and the recent picture of a modified random network for glasses are of importance for long time storage.

In the reporting period, the Rb-tracer diffusion data given in PR 86 were confirmed with a Rutherford-backscattering (RBS) study of ion-implanted glasses. The German waste glass VG 98/12 was bombarded with Rb or Cs ions of 40 or 300 keV energy to doses of 5x10^{15} ions/cm^2. Following annealing treatments of different times at temperatures between 350 and 665°C, RBS showed diffusion profiles (see Fig. 2.10) compatible with volume diffusion only at high temperatures, whereas composite diffusion profiles were obtained at lower tempeatures. Radiation **enhanced** Na diffusion was observed **during** bombardment. In contrast, radiation damage **retarded** the thermally activated Rb and Cs diffusion : the implanted ions interacted with the damage configuration resulting from ion bombardment. Because of the complex structure of the multicomponent waste glass, the nature of the trapping defects cannot be specified yet. Damage annealing and/or dissociation of the alkalis from the damage needed annealing temperatures of about 500°C for Rb and about 600°C for the larger Cs-ions. Even following damage annealing, Rb and Cs diffusion was much slower than that of Na. The latter was measured with the boundary condition of a thin tracer layer. Fig. 2.11 shows the theoretically expected linear penetration plots typical for undisturbed volume diffusion, and Fig. 2.12 summarizes all data in an Arrhenius diagram. The Arrhenius plot for Rb and Cs is curved.

The data are of relevance for storage of waste glasses : it is now possible to predict that thermodiffusion of the (radioactive) Rb and Cs will be a minor effect during long-time storage, that the pronounced decrease in the diffusion coefficient D in the series Na-Rb-Cs will overcompensate any possible changes in

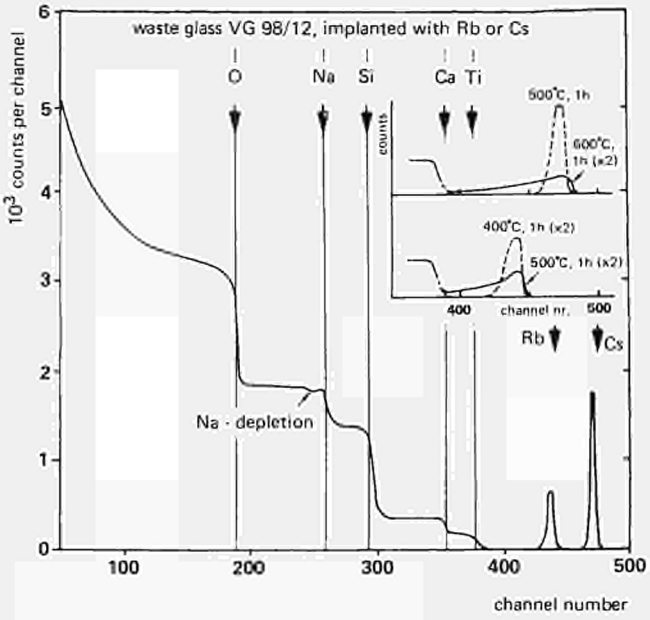

Fig. 2.10 - RBS spectrum of the waste glass VG 98/12 implanted with Rb or Cs. The inset shows the high energy end of the spectra following different annealing treatments indicating diffusion of Rb and Cs with and without trapping of a fraction of the alkali ions.

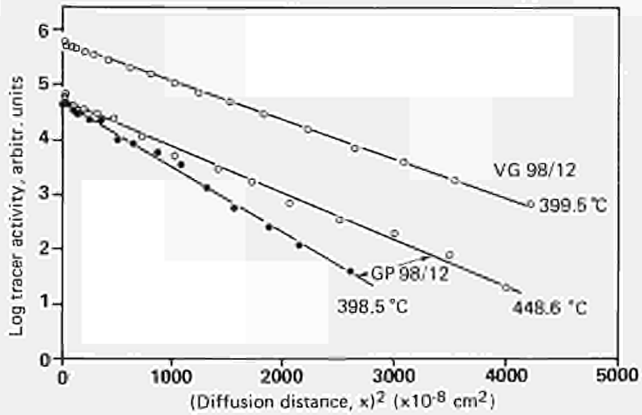

Fig. 2.11 - Penetration profiles of the radioactive tracer Na-22 in the waste glasses GP 98/12 and VG 98/12 following diffusion anneals.

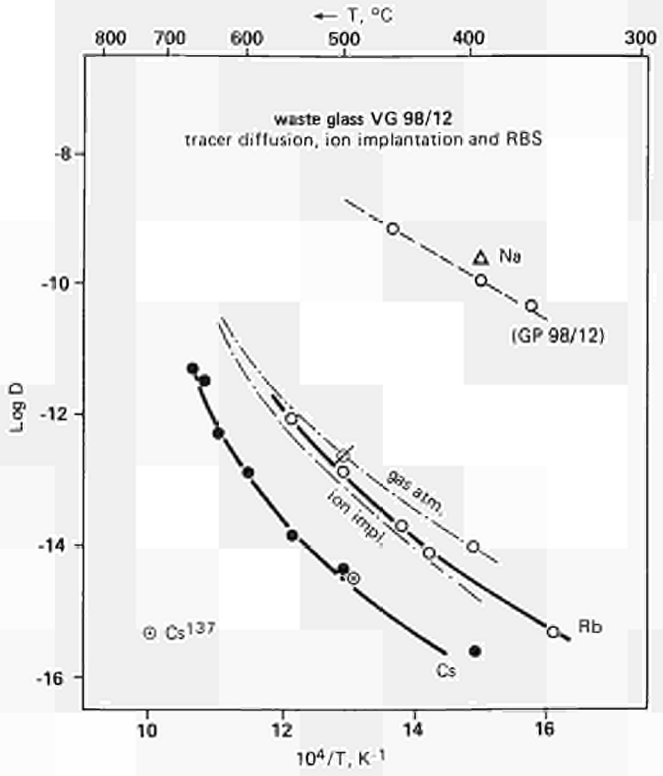

Fig. 2.12 - Arrhenius diagram for alkali diffusion in the waste glass VG 98/12.

thermally activated ion diffusion in the complex waste glass due to the mixed alkali effect if leaching, thermodiffusion or biased radiation-enhanced Na-diffusion cause local changes in the Na-content of the glass, and that radiation-enhanced diffusion will exist during storage at temperatures below ~200°C, but since there will be no biasing effect, it should not lead to any directional Na-migration but will rather contribute to maintain the glass at a homogeneous state.

This study has been concluded and the results were discussed at an international workshop on radiation effects in waste matrices organized by the Institute /7/ and held in parallel with the 4th Intern. Conference on Radiation Effects in Insulators. The proceedings containing all contributions are in print and will be available in April 1988.

Fracture Toughness of Waste Glasses

Fracture toughness, K_{Ic}, values were so far obtained with Hertz- or Vickers indentations (see previous PRs and /1-4/). A so-called short-rod fractometer has now been installed to verify the results with more conventional fracture tests. The short-rod fractometer uses chevron-notched specimens of ~6 mm diameter. The first results show good agreement with the previous data.

Vickers tests were also made in an attempt to investigate the effect of noble metal fission products and of cooling rate of the glass. The rare metals (Pd, Rh, Ru, etc.) form small metallic inclusions in waste glasses and fast cooling leaves residual stresses in the glass. Both might affect the fracture behaviour. Glasses of the types GP 98/12, either with all, with 30% or with no of the otherwise present rare metals Ru, Rh and Pd (normally 0.2 at% in the waste glass loaded with 15 wt% fission product oxides) were investigated. Different cooling times were also used (2h or 10h). Drop tests were performed at Battelle, Frankfurt (Dr. Scheibel) in a pneumatic arrangement simulating accidental dropping of glass cyclinders in mining shafts of some 100 m depth. Vickers indentations showed a very small effect only of cooling rate, but a clear effect of the rare metal inclusions and of the more complex structure of the fission product-containing waste glass GP 98/12 (see Table 2.V). This can be explained by the more distorted structure of GP 98/12 as compared with that of the base glass VG 98/12, and due to toughening and crack branching of the rare metal inclusions. These results are comparable with those of the drop tests.

Table 2.V - Fracture behaviour with Vickers indentations in waste glasses used for drop tests

glass	cooling time h	crack length		fracture toughness K_{Ic}, MPam$^{1/2}$	Vickers hardness H, GPa
		µm	relative		
VG 98/12.2	10	399.2	1.000	0.70	5.71
	2	396.8	0.993	0.71	5.59
GP 98/12.2 without rare metals	10	377.9	0.947	0.76	5.69
	2	371.7	0.931	0.78	5.70
GP 98/12.2 with rare metals	10	362.2	0.907	0.81	5.70
	3.5	362.8	0.909	0.81	5.61

Measurements performed in laboratory air (~21°C, ~50% rel. humidity). The crack length given is the sum of the average of 20 cracks each at three loads (7.84 N, 12.54 N and 22.54 N).

References

/1/ Hj. MATZKE — Indentation Fracture and Mechanical Properties of Ceramic Fuels and of Waste Ceramics and Glasses. Special Volume, Europ. Appl. Res. Reports, **7** (1987)

/2/ W.J. WEBER, Hj. MATZKE — Europ. Appl. Res. Reports, **7** (1987)

/3/ J.L. ROUTBORT, Hj. MATZKE — Mater. Sci. Eng., **58** (1983) 229

/4/ Hj. MATZKE, E. TOSCANO, J.L. ROUTBORT, K. REIMANN — J. Amer. Ceram. Soc., **69** (1986) C-139

/5/ Hj. MATZKE — Chapter 12 "Nuclear Waste Materials" in monograph "Ion Beam Modification of Insulators" (G. Arnold, P. Mazzoldi, Eds.), Elsevier, Amsterdam (1987) p. 501

/6/ Hj. MATZKE (Ed.) — Proceedings of a Workshop on Radiation Effects in Waste Matrices, Nucl. Instrum. Methods in Phys. Research B (1988)

/7/ Hj. MATZKE — Cryst. Lattice Defects and Amorphous Mater., **17** (1987) 21

Alpha-Contaminated Waste in Concrete

(E. Zamorani)

Some elements, contained in Medium Level Waste streams, present different valence states enabling difficulties in the immobilization process. The hydration of Ordinary Portland Cement, normally used in the MLW management can determine the degree of solubility of blended elements due to :

1) *the hydrolysis of inorganic metal cations represented by the reaction*

$$xM^{z+} + yH_2O \rightleftarrows M_x(OH)_y^{(xz-y)+} + yH^+$$

in which polynuclear species represent different solubilities depending on the pH values.

2) *the high solubility in alkali media ($Ca(OH)_2$ from OPC hydration) of elements in the oxidized valence state.*

3) *The syneresis effect of silica-gel observed in the hardening process, is enhanced by the presence of chemical additives influencing the rheological consistency of cement paste as well as the properties of the end product. Therefore, several parameters must be evaluated, such as*

- *water-to-cement ratio (W/C),*
- *setting and hardening period,*
- *influence of the amount and valence of elements on cement properties,*
- *leaching resistance to water.*

Changes in physical cement structure should, however, affect the matrix durability when attacked by water (representing accidental conditions in the repositories). They may result in the release of chemical impurities (added in cement) and cement constituents, leading to a degradation of the cement matrix.

Following the works on the influence of MLW streams on physical properties (density, porosity, compressive strength) and chemical behaviour (mechanism of release and matrix degradation), particular elements such as chromium and nickel have been considered taking into account :

- an MLW is of miscellaneous nature. It includes fission products and structural elements from vessel corrosion. Other than Cs, Sr and Co, as normally studies, the elements which are presenmt in an MLW stream will influence the properties of the matrix;
- these elements concern with hazardous industrial wastes as well;
- the amount and the valence state (Cr^{3+} and Cr^{6+}) can modify the physical properties and the retention capacity of cement matrix. Several elements (Cr, Cu, Fe, Mn, Mo, Ru, Zr) contained in an MLW stream from reprocessing plant, exhibit different valence state determining an influence on the redox potential in the cement matrix.
- in analogy with the multiple valence state, the leaching behaviour of actinides can be predicted.

An estimation of the amount of these elements in aqueous solution amounts to $1.2x10^2$ kg/$1.2x10^2$ kg/1000 t HM for chromium and nickel compared to $2.6x10^3$ kg for cesium and $2.4x10^3$ kg for Ru/Rh. Two different states of chromium (3+, 6+) corresponding to $CrCl_3.6H_2O$ and CrO_3 giving rise to different chemical behaviour in cement medium and $NiCl_2$ have been selected. The selection of these compounds is also based on the following :

1. varying degree of solubility depending on the pH values. According to the previous results (Pourbaix, 1966), the solubility of Cr^{3+} in solution containing chloride is $\sim 10^{-6}$ moles/l, whereas it is $\sim 5x10^{-11}$ moles/l in solutions not containing chloride. The solubility of Cr^{6+} is very high in the pH range 6-14;
2. different hydrolysis products of chromium (3+ and 6+ states) in aqueous solutions. The behaviour of Cr^{3+} is characterized by the slow kinetics of its polymerization reaction;
3. the ability of chromium (3+, 6+) to form a variety of polynuclear complexes in aqueous solutions;
4. the ability of chromium to form a variety of chromates and chromosilicates with metallic cations (Ca, Si, Na).

Preparation of Samples

OPC 325 powder, the chromium and nickel compound and water are mixed in a predetermined ratio in order to obtain the solid element-to-cement ratio, SE/C, in the range 0.013 - 0.068. The water-to-cement ratio (W/C) plays a prominent role in determining the physical characteristics of the cement matrix. A value od W/C = 0.35 is generally considered the best compromise between workability, strength and porosity of neat hardened cement samples. In these experiments, however, it was seen that W/C = 0.65 represents the best amount of water for use in the preparation of cment samples containing chromium compounds. Cylindric samples, prepared following the procedure described in the previous annual reports, have been used for physical properly measurements and leaching experiments.

Physical Characteristics Determination

Physical tests have been carried out taking into account :

- the cement samples were prepared and aged under the same conditions;
- physical properties such as compressive strength (CS) and apparent (bulk) density (AD) were measured in sample specimen of average cylindrical dimensions H = 35 mm, ϕ = 20 mm;
- pycnometric density (PD) and pore size distribution were measured on cement granules (2.8-3.2 mm), dried at 120°C and maintained in silica gel containers for 24 hours.

Static Leaching Experiments

Static leaching tests on cement samples (H = 35 mm, ϕ 20 mm), containing $CrCl_36H_2O$, CrO_3 and $NiCl_2$ were performed at a solid surface-to-liquid volume ratio S/V_L = 0.071 cm^{-1}, in a closed system maintained at 50°C. The choice of the temperature has been dictated by a possible repository location. The cement samples, prepared for leaching experiments, incorporated maximum amount of each compounds corresponding to SE/C = 0.068 of element. The leachate samples taken after a fixed time were analysed to determine pH, chromium(III), chromium(VI), nickel and chloride.

Physical Properties Results

The mechanisms of strengthening cement by adding salts depends principally on the interference in the hydration process forming a calcium silicate hydrate (CSH) gel. Salts such as calcium sulphate and chloride and sodium chloride deliberately added to cement, influence the setting which depends on the type and concentration of the salts.

Compressive strength. The rapid set properties of chromium and nickel chloride (and to a lesser extent of CrO_3) is given by the increase of the value of W/C = 0.65 (instead of 0.35 as normally used for neat cement) to obtain a workable paste. About 5 wt% of elements improve the compressive strength of cement samples as reported in Fig. 2.13. Beyond this limit, the setting

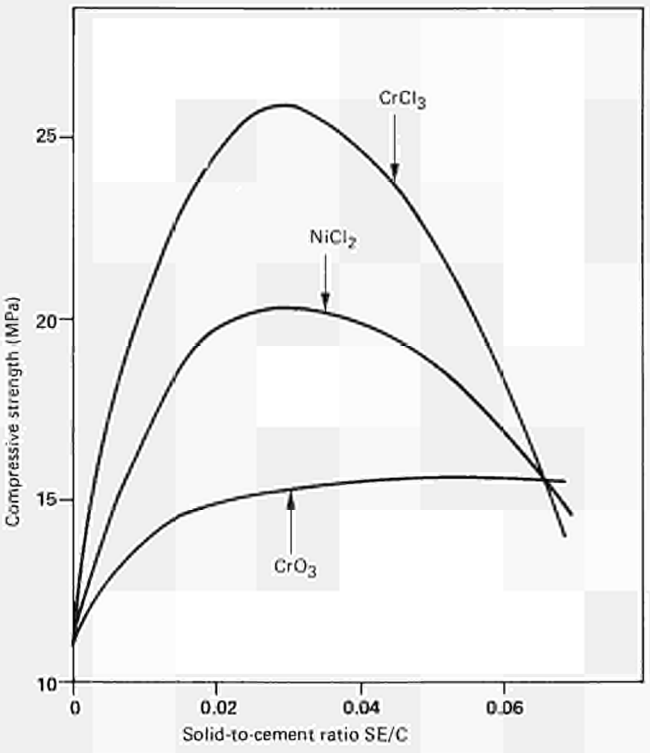

Fig. 2.13 - Variation of compressive strength (CS) vs solid element-to-cement ratios for cement containing $CrCl_3$, $NiCl_2$ and CrO_3

properties of chloride compounds counteract the beneficial effects of hydroxide gel $Cr(OH)_3$ and $Ni(OH)_2$ (presenting properties similar to CSH gel), which contribute to the increased mechanical strength of cement samples.

Density and porosity. The strengthening effect of added materials should equally be confirmed by the values of density and porosity (by Mercury Intrusion Porosimetry) reported in Table 2.VI. These values indicate an increase in density and a decrease in porosity following the trend of the values of the compressive strength.

Table 2.VI — Physical properties measurement on cement samples doped with chromium and nickel compounds (W/C = 0.65)

SE/C	Density AD (g/cm^3)	Density PD (g/cm^3)	Pore volume (cm^3/g)
Chromium chloride $CrCl_3.6H_2O$			
—	1.76	2.374	0.272
0.0133	1.76	2.390	0.208
0.0267	1.80	2.308	0.164
0.0533	1.84	2.422	0.125
0.0677	1.87	2.302	0.1555
Chromium anhydride CrO_3			
—	1.76	2.374	0.272
0.0133	1.78	2.421	0.269
0.0267	1.75	2.580	0.264
0.0533	1.77	2.491	0.250
0.0677	1.81	2.880	0.257
Nickel chloride $NiCl_2$			
—	1.76	2.374	0.272
0.013	1.80	2.333	0.218
0.026	1.80	2.397	0.175
0.040	1.80	2.332	0.156
0.068	1.81	2.280	0.165

AD = Apparent (bulk) density
PD = Pycnometric density

Leaching Results

The high alkali media in the cement hydration contribute to the formation of insoluble hydroxide in the reduced state of Cr^{3+} and Ni^{2+}. Low concentrations in the leachate were observed for chromium = 10^{-6} M/L and nickel = 6.8×10^{-8} M/L, confirming the values reported in the literature. The formation of chromium and nickel hydroxide takes place by the following stoichiometric reactions :

$$xCa(OH)_2 + y\,M\,Cl_x + nH_2O \rightleftarrows yM(OH)_x.nH_2O + CaCl_y$$

in which M = Cr^{3+} or Ni^{2+}.

The formation of $CaCl_2$ is confirmed by the release of chloride in the leachate; nearly all of it is released in the first days of leaching, compared to the low amount of chromium and nickel.

On the other hand, chromium in the 6+ valence state presents very high solubility probably due to chromate formation.
The fractional release C/Co of chromium 6+ vs time can be represented by the equation :

$$C/Co = B\,t^n \qquad (1)$$

A straight line is obtained for the first 30 days of leaching. A value of n = 0.25 appears to suggest that chromium can be released by one of the following mechanisms :

1. The kinetic release of chromium(VI) follows a double diffusion mechanism similar to that observed for calcium which is unlike the release of cesium and strontium which diffuse from the bulk to the external surface and follow the simple diffusion mechanism predicted by the slope n = 0.5 in eq. (1).
2. The release of chromium(VI) seems to depend on the kinetic release of calcium because of the formation of chromates with calcium. In this case the release of both calcium and chromium appears to be controlled by the CSH gel. The slope n = 0 in eq. (1) after 30 days of leaching can be assumed to depend on the high solubility of calcium chromate (1.5×10^{-1} M/L) resulting in a depletion of the external layer of the samples during leaching.

When the amount of chromium (6+) leached out is plotted as a function of pH on a standard predominance diagram for Cr(VI)-OH^- species at 25°C (Baes, 1976), the data points are scattered in a region with dominant chromate ions (CrO_4^{2-}), so chromium in this case is leached out mainly as Cr(VI).

Remarks

From the results of our works and from those published elsewhere, we can distinguish the behaviour of elements or compounds conditioned in cement :

1) elements forming insoluble hydroxide (such as Act, Cr^{3+}, Ni^{2+}) for which the cement represents a good host material;
2) elements forming compounds with calcium and presenting a double diffusion kinetic release similar to that of calcium (CrO_4^{2-}, SO_4^{2-});
3) soluble elements or compounds (such as Cs, Sr, NO_3^-) presenting a diffusion kinetic release for which a matrix structural modification will contribute to increase the retention capacity.

In the light of the present results, cement composites represent a good material for immobilization of elements in reduced valence state (Cr, Ni, Act). A beneficial effect on physical characteristics has been observed by blending chromium and nickel compounds almost at the concentration limit of about 5 wt% in cement.
The results of the physical properties and leaching experiments suggest the feasibility of cement as a favourable confinement matrix (but Cs and Sr) for immobilization of MLW streams.

2.3 Far Field Studies

(G. Bidoglio, M. D'Alessandro)

A groundwater flow through the repository may lead to the mobilization of radionuclides from waste forms. Contaminated groundwaters could then be discharged into surrounding aquifers and reach surface waters. A thorough understanding of the role of the surrounding geologic body in ensuring an adequate nuclide containment is therefore needed. Progress in this direction is limited by the extremely low concentrations involved and the complex chemistry of radionuclides in multicomponent natural systems. Analytical results from radio-ecological measuring procedures alone are of little help for the interpretation of natural events. Additional information is needed on the nature of solid-liquid interactions, the solubility limits of radionuclides, the presence of inactive carriers and competing ions, the rate of geochemical reactions, the hydrodynamic of groundwater flow.

The goal of the geochemistry research activity is to provide input data for models describing radionuclide migration. Probabilistic calculations for risk may only involve a lumped approach with recourse to global Kd coefficients. Nevertheless, more sophisticated deterministic models are needed in field and laboratory experiments aiming at the identification of phenomena which may result in the underestimation of risks. The approach followed involves three different research areas : simulation experiments, speciation studies and barrier modelling. The laboratory simulation of events resulting in the release and migration of radionuclides is a necessary step to bring about first indications on the variables affecting the transport processes. This task involves leach tests of the matrix containing the radionuclide under investigation, batch Kd measurements, continuous flow experiments with soil columns, measurements of diffusion rates. The goal of speciation studies is the quantification of phenomena observed with simulation experiments. This task entails the development of analytical techniques working at very low concentration levels. All these experimental data used in conjunction with transport models will then yield predictions of path lines and travel times of radionuclides. Site-specific porous materials representative of geological systems surrounding possible repositories in Europe are being used. These include the aquifers overlying the clay formation in Mol (B), and the salt dome in Gorleben (FRG).

Radionuclide Release Studies

Dynamic leach studies were performed to simulate the accidental intrusion of groundwaters in a repository and their interactions with 1000 yr cooled vitrified highly active wastes. Borosilicate glass (code I 117) beads containing 20% simulated fission product oxides and the radionuclide under investigation were used. The major glass constituents were SiO_2 (48 wt%), B_2O_3 (15 wt%), Al_2O_3 (5 wt%) and Na_2O (16 wt%). Labelling of the glass was done by melting the glass components and the radionuclide in a graphite crucible at 1200°C under argon atmosphere. Portions of ground glass were introduced into teflon containers percolated with the leachant serving as a source term in the column experiments described in the following section. The values of relevant leaching parameters are shown in Table 2.VII. The leachants used (Table 2.VIII) were : (1) a bicarbonate groundwater simulating that found in an aquifer overlying the Boom clay formation in Mol; and (2) a brine of high ionic strength typical of salt brine aquifers close to halite deposits (Gorleben). The effect of the redox environment was studied by tests under normal laboratory atmosphere (oxic conditions) and in metallic glove-boxes purged with nitrogen (anoxic conditions) /1/.

The average values of normalized leach-rates are reported in Table 2.IX. The rate of matrix dissolution was measured by using ^{22}Na doped glasses of the same composition. This value was found to be $\sim 10^{-6}$ g.cm^{-2}d^{-1} both in the bicarbonate groundwater and in the brine solution. It is interesting to observe that Np and Tc release rates in the air saturated solutions compare with those measured for Na. This suggests that no solid alteration products involving Np(V) and Tc(VII) were formed at the glass-water interface and that these soluble nuclide species follow alkali release. Results given in Table 2.IX. indicate that for redox sensitive nuclides leach-rates under anoxic conditions are lower than those determined in air-saturated solutions. Accordingly, the steady state Am(III) leach-rate in the bicarbonate water was found to be virtually unaffected by the oxygen concentration.

Figure 2.14 shows that the Am release rate in the brine solution initially decreases as a function of time. Interactions of Am with a growing gel layer were postulated. A periodic cycle of decreasing/increasing Am concentrations was then found over the 550 days of the test. If the corrosion products forming the surface layer are not in equilibrium with the flowing solution, the gel layer will be progressively dissolved from the outside. The consequence of this removal will be a steady rise with time of the Am leachate concentration until the layer builds up again. The oscillating trend reported for Am(III) in brine was observed also for Np in the low redox potential brine. Under oxic

Table 2.VII — Experimental values of leaching parameters

Parameter	Value
Flow rate (cm^{3}h^{-1})	1.5
Glass surface (cm^2)	~ 14
Glass volume (cm^3)	~ 0.3
Doping level (wt%) :	
^{99}Tc*	0.6
^{237}Np	2.4
^{238}Pu	0.01
^{241}Am	0.04

* Nominal value, initially added to the glass components before melting

Table 2.VIII — Water composition (mg/l)

Constituent	Bicarbonate groundwater	Salt brine
Sodium	55.2	1.26×10^5
Potassium	7.8	78.2
Iron	0.1	7.0×10^{-2}
Calcium	3.1	164
Magnesium	3.2	26.7
Chloride	6.4	1.94×10^5
Sulphate	0.5	538
Bicarbonate	158.6	6.1
pH	8.35	6

Table 2.IX — Normalized leach rates (g cm^{-2}d^{-1}) at 25°C (1.5 ml h^{-1})

	Bicarbonate groundwater		Salt brine	
	Oxic	Anoxic	Oxic	Anoxic
^{99}Tc	1×10^{-7}*	2×10^{-8}*	1×10^{-6}	—
^{237}Np	1×10^{-6}	6×10^{-8}	1×10^{-6}	2×10^{-7}
^{238}Pu	4×10^{-7}	9×10^{-8}	3×10^{-7}	1×10^{-7}
^{241}Am	3×10^{-7}	3×10^{-7}	3×10^{-8}	—

* Normalized to the ^{99}Tc activity initially added to the glass components before melting.

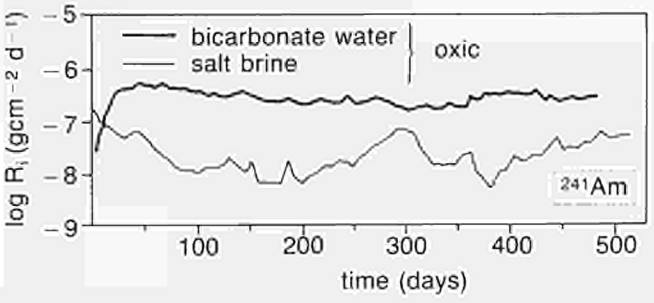

Fig. 2.14 - Normalized release rate R_i of Am(III) as a function of time

conditions, where Np(V) is the dominant oxidation state in solution, a constant Np release was instead measured. This ascribes the leach behaviour to the redox state of Np, rather than to a de-aeration effect on the brine/glass interactions. The same behaviour was observed with a ^{238}Pu doped glass.

Radionuclide-Soil Interactions

The migration rates of actinides were investigated using geologic materials from Mol (quartz sand containing 25% of glauconite) and from Gorleben (Gohy 263 : ~95% of quartz with minor amounts of magnetite, rutile and argillaceous material). The glass leachates obtained as described in the previous section were continuously pumped through glass columns (20 cm x 2.5 cm i.d.) packed with soil to a bulk density of ~2 g cm^{-3}. Column effluents were analysed during the loading period. The columns were then cut into thin sections and the distribution profiles measured. The focus of this activity during the reporting period was addressed towards the migration chemistry of Pu and Np under reducing conditions /2/. The percolation experiments were performed in anaerobic chambers containing a gas mixture of N_2 + CO_2 (Fig. 2.15). Measurements of the redox state of the groundwaters were carried out using Pt electrodes. Eh values lower than -200 mV were found.

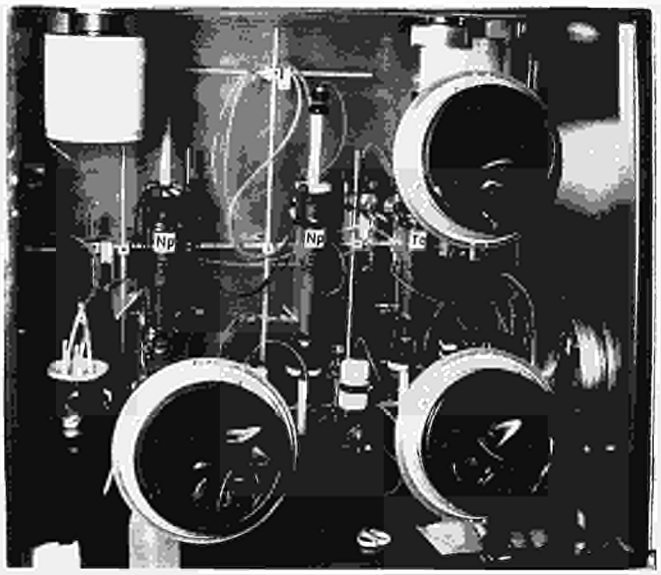

Fig. 2.15 - Metallic glove-boxes containing a nitrogen atmosphere for use in laboratory migration studies

Table 2.X compares the retardation factors, R_f, measured for Pu and Np under oxic and anoxic conditions. Analytical and thermodynamic considerations suggest Pu(V) to be the more stable oxidation state in oxigenated natural waters. If the same applies in the oxic columns of this study, R_f should approach the value obtained for Np, which was determined to be present as Np(V) under the same conditions. However, the R_f data given in Table 2.X are not consistent with this model. Pu sorption may follow a non-linear isotherm where the rate of movement is dependent on its solution concentration. This is supported by the lower initial Pu concentrations used, compared to the Np(V) experiments. Alternatively, adsorbed Pu ions may evolve to a more strongly bound form.

The contamination profiles of ^{238}Pu under anoxic conditions for the Mol and Gorleben soil samples are shown in Figs. 2.16 and 2.17. For both systems, a small peak can be observed on the front of these profiles. This may relate to possible chromatographic separation of two species. Further experimental

Table 2.X — Retardation factors of ^{237}Np and ^{238}Pu

		Np	Pu
Bicarbonate water/clayey sand (Mol)	oxic	$2x10^3$	10^4
	anoxic	$>5x10^3$	$6x10^4$
5.4 M NaCl brine/Gohy-263 sand (Gorleben)	oxic	39	$9x10^3$
	anoxic	162	$4x10^4$

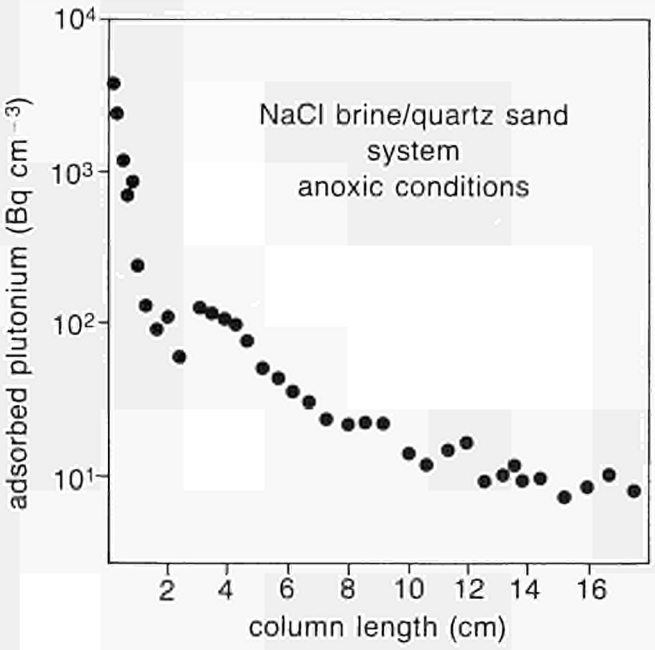

Fig. 2.16 - Contamination profile of the Gohy-263 sand column loaded with ^{238}Pu glass leachate

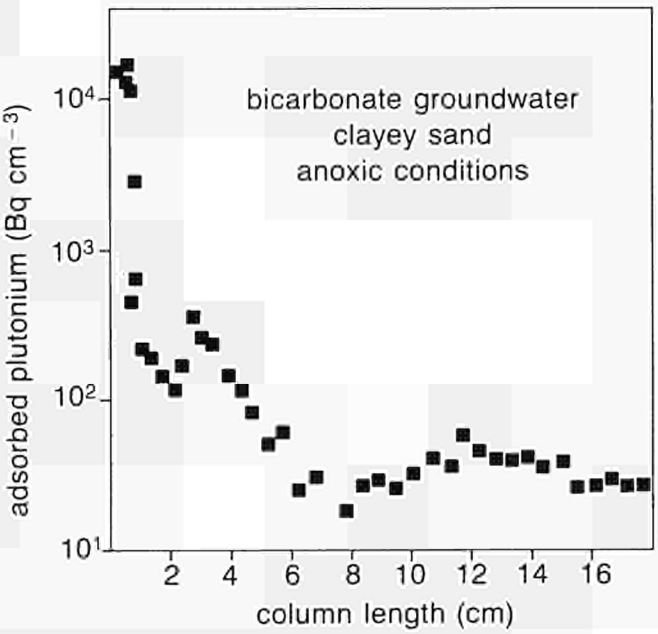

Fig. 2.17 - Contamination profile of leached ^{238}Pu in the glauconitic sand column

and modelling activities are underway to get more information on the migration mechanism.

A report on the ^{237}Np migration in oxidizing clayed sand from the Mol site was published /3/. It shows the validity of a multispecies exchange model for the description of Np migration. Rapid sorption reactions and slow interconversion between soluble Np species were included in the model. Because time constants of rate determining steps are in the order of only a few hours, chemical equilibrium between dissolved Np species will be attained in the long run and the simple Kd concept is still useful in Np(V) transport calculations.

An additional activity performed in collaboration with the Hahn-Meitner Institut, Berlin, investigated the retention properties of mined salt as backfill material. Modelling of integrated experiments (see previous Progress Report) using simulated HAW glass and pressed salt from the Asse mine as column material (Fig. 2.18) was completed during the reporting period. Results were presented at the Migration '87 Conference in Munich /4/. An effective retardation was found for Am and Pu, but almost no retention was measured for Tc and Np under oxic conditions. The influence of low redox potentials is being investigated. As the adsorption capacity of natural salt is very low, the use of high concentrations close to the solubility limit will be necessary in future work. An approach to more realistic conditions is possible using leachates obtained at elevated temperatures.

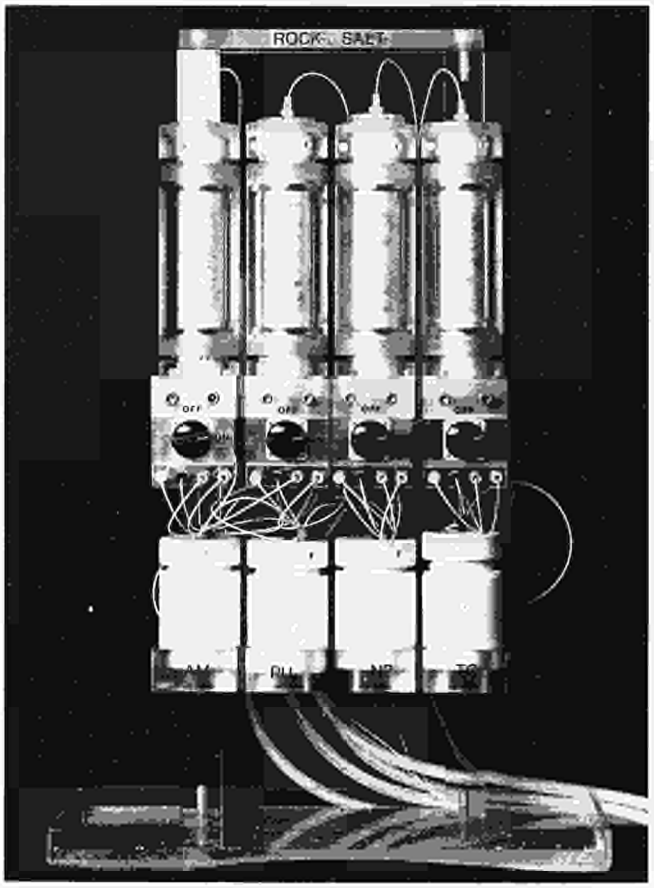

Fig. 2.18 - Experimental set-up for radionuclide percolation through columns of pressed salt

Role of Colloids

Adsorption onto natural colloids is generally considered to dominate the chemistry of trace contaminants in natural waters. Most of our efforts were focused on the identification of physico-chemical conditions controlling the formation of actinide pseudo-colloids /5/. Part of this work was carried out under contract with the University of Milan /6/. Because of their different surface characteristics, amorphous silica and γ-alumina in the colloidal state were selected as models of particles present in repository environments. The uptake of Am(III), Th(IV) and Np(V) on these model colloids was investigated as a function of pH, humic acid and carbonate concentration. Fig. 2.19 shows that surface interactions with alumina are oxidation state dependent, with adsorption edges shifting towards high pH in the order (IV), (III), (V). The addition of humic acids (extracted from Boom clay samples) was found to increase the actinide uptake at low pH and lower the adsorption by the colloidal particles in the neutral to alkaline pH range (Fig. 2.20). Similar results were obtained for colloidal silica. Modelling of the adsorbent-water interface for the identification of adsorption mechanisms will be performed in the course of next year.

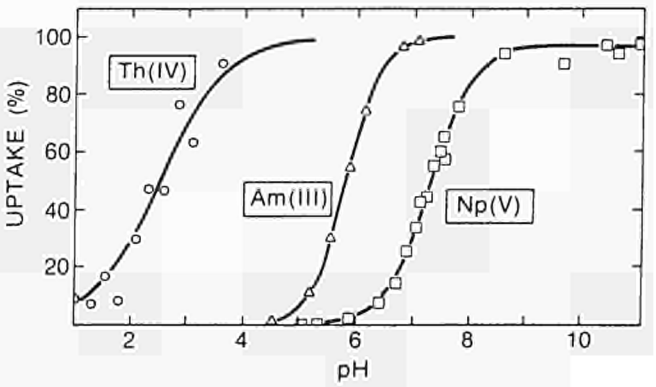

Fig. 2.19 - pH effect on actinide uptake onto γ-alumina

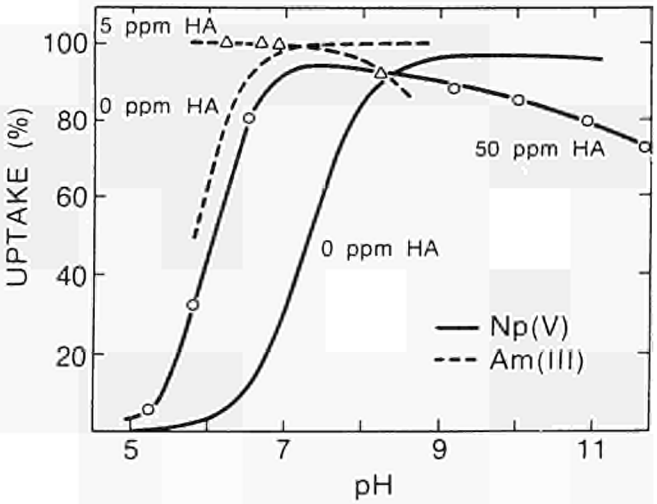

Fig. 2.20 - Influence of humic acids (HA) from Boom clay on actinide uptake onto γ-alumina

Development of Analytical Techniques

The suitability of laser spectroscopic techniques for the identification of chemical species in very dilute aqueous solutions is being investigated. Work in the reporting period concentrated on Thermal Lensing Spectrophotometry (TLS). The heat-induced refractive index change caused by absorption of a pulsed dye laser radiation by solution species, was used to investigate the conversion of U and Nd free ions to complete complexation in neutral and carbonate solutions /7,8/. A He-Ne laser was used as a probe beam in a conventional dual beam configuration where the beam waists are independently adjusted (Fig. 2.21). Fig. 2.22 shows the recorder tracings of the laser energy (dye

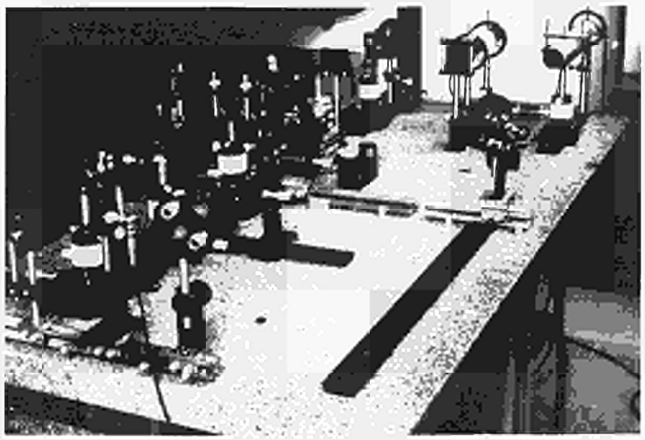

Fig. 2.21 - View of the tunable dye laser excitation system used for thermal lensing spectrophotometry

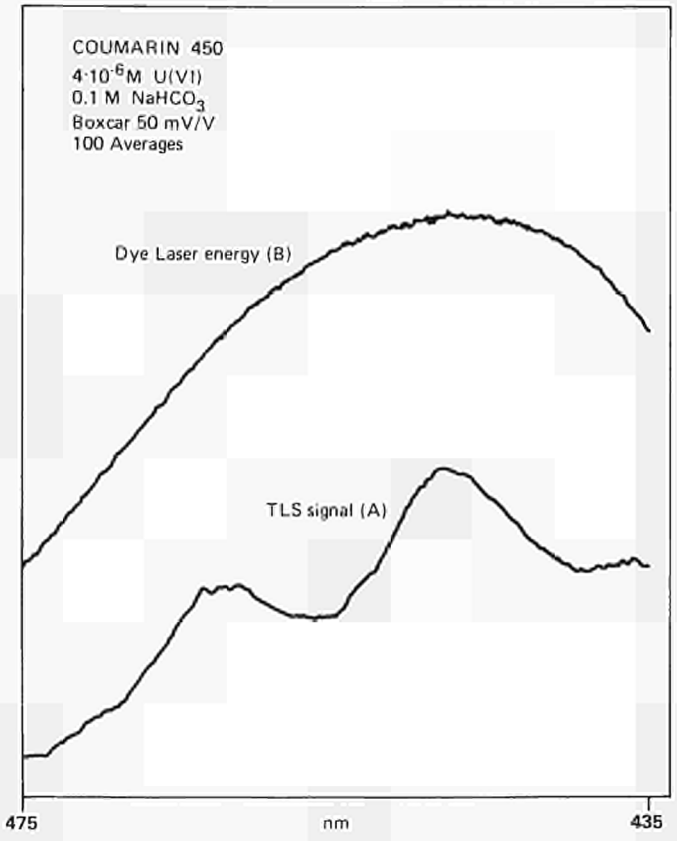

Fig. 2.22 - Recorder tracings of the laser energy and the thermal lens signal

Coumarin 450) as measured by the pyroelectric detector, and the uncorrected spectrum of the species $UO_2(CO_3)_3^{4-}$ in the region 435-475 nm. Fig. 2.23 gives the same spectrum after the correction procedure, together with the TLS spectra of $UO_2(CO_3)_2^{2-}$ and $UO_2CO_{3(aq)}$ recorded at total U concentrations below the solubility limit of the solid UO_2CO_3 ($\sim 10^{-5}$ M). TLS was also used to get information about the mononuclear hydrolysis of U(IV), information that is difficult to obtain with more traditional solution chemical methods /8/. The TLS measurements were made by using a reactor vessel which was connected via glass tubings and a piston burette acting as a pump to a cuvette placed in the TLS equipment. The presence of a Pt-net covered with H_2-saturated Pd-sponge and bubbling of H_2(g) in the reactor vessel were necessary to prevent U(IV) oxidation. The TLS data were obtained at 25°C in the concentration range $0 \leq -\log[H^+] \leq 2.8$ using a 3M $(Na,H)ClO_4$ ionic medium. The data were described with the following chemical model :

$$U^{4+} + H_2O \rightleftharpoons UOH^{3+} + H^+$$
$$\log^* \beta_1 = -1.65 \pm 0.05$$

$$U^{4+} + 2H_2O \rightleftharpoons U(OH)_2^{2+} + 2H^+$$
$$\log^* \beta_2 < -4.5$$

Part of this work was performed during a visiting period of a scientist from the Royal Institute of Technology, Stockholm.

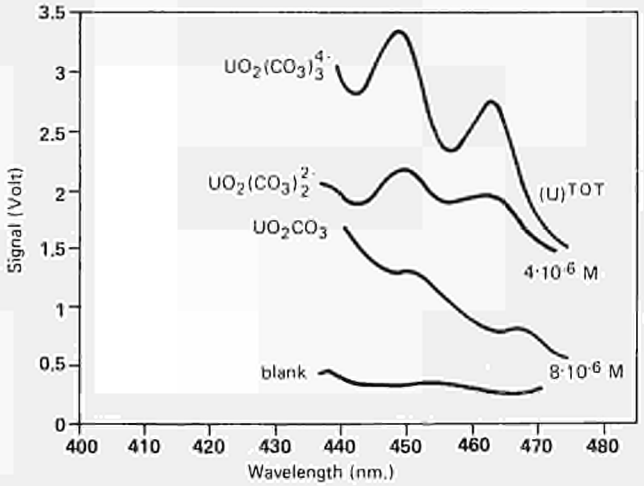

Fig. 2.23 - TLS spectra of uranium species in the U(VI)/H_2O/CO_2 system

Field Activities

Studies concerning the hydrogeochemical characterization of the Ispra site are going on in co-operation with the Polytechnic Institute of Milan, with the objective of fully understanding the hydrodynamics of the groundwater system at the test site (near the Radiochemistry building) in view of its possible use for the verification of transport models for both radioactive and chemical toxic compounds.

After the completion of four boreholes, fully equipped for hydrological and geochemical tests, most activities were devoted to set up a more efficient system for hydrodynamical data acquisition. A more powerful submersible pump was installed, aiming to enable high flow rates to be reached in both variable and constant discharge abstraction tests. Furthermore, an automatic data acquisition system was installed to facilitate the detection of dynamic levels simultaneously in different piezometres during pumping tests. This makes use of an EPSON HX-20 microcomputer as central unit, which is connected to an analog-digit converter. The system may receive up to 16 different signals simultaneously, following a procedure which could be adapted to specific needs through a suitable software.

The detectors, which consist of pressure transducers of different sensitivity, were installed within the piezometres at a depth which is consistent with the expected water level lowering; this depends on both the distance of pumping well and the rate of water abstraction.

A demonstration of this operative system for automatic data acquisition was requested by the "Service d'Etudes et de Recherches sur l'Environmment" of Cadarache, in the frame of a collaboration contract between the JRC-Ispra and the CEA-Cadarache. The demonstration will be performed in the second half of '88 within an experimental site near Limoge, which is being prepared.

One test at constant abstraction rate was performed as far, which has given excellent results. The pumping was performed with a flow rate of 2.08 l/sec over 93 hours. The depth of the pump was 62 m, allowing the abstraction to be done from both upper and lower aquifers. Subsequently, the recovery of rest water level was followed for other 139 hours.

The main parameters of the test were the following :

- rest water level : -12 m below ground level
- depth of submersible pump : -62 m below ground level
- constant discharge rate : 2.08 l/sec
- distance of the piezometres (m) : 4, 22, 38 m, 4(P_2), 22(p_3), 38(P_4)
- drawdown in pumping well : 29.38 m
- drawdown in piezometres : 3.21, 0.46, 0.71.

The curves of borehole No. 3 (Fig. 2.24a) confirm its anomalous behaviour already shown by a piezometric head 3 m higher than the average in static conditions. His drawdown, in fact, reaches 0.5 m only, while borehole No. 4 (Fig. 2.24b), having twice the distance from the pumping well, shows a 0.9 m lowering. It appears that the water body crossed by borehole No. 3 has a poor connection with the other piezometres, being possibly a perched aquifer.

These data, however, are being confirmed by other tests performed with different abstraction rates and pumping from different depths. Unfortunately, the high sandy content in the aquifer causes serious problems when the abstraction rate exceeds 2.5-2.8 l/sec. The strong water attraction towards the well mobilizes large quantity of sand which enters the pump's rotors causing a sudden block of the abstraction device.

The stratigraphy based on core examination of borehole No. 1 suggests the presence of a multilayered aquifer lying on the clay bed. The size distribution analysis performed in the laboratory confirmed the existence of some silty levels up to the clay's depth, likely acting as semi-impermeable sheets (Fig. 2.25).

The sediments below the clay bed, where the sandy component is more important, present a different hydrological situation due to the higher homogeneity. That is a thick aquifer lying either on the silt bed of -150, or on a deeper aquiclude. The sandy level at about -140 m could constitute a preferential channelling for such an aquifer.

The 10 m thick clay bed shows in its lower parts sandy intercalations. It cannot be excluded that this interstratification acts as a confined aquifer, possibly squeezed by the surrounding rock. In fact, a slight ground water rise in the deep boreholes is the more likely cause of the rather homogeneous geochemical composition of water column in wells 1 and 2, against the evident geochemical stratification in shallower boresholes 3 and 4; this aspect will be further checked.

The above described configuration seems to be consistent with the hydraulic conductivity (K) measured in the laboratory on core samples. A comparison between the log of sediment coarser fraction (which is thought permeable) and the log of K values obtained by the laboratory tests is shown in Fig. 2.26.

A calculation of the correlation coefficient (PEARSON) was made. The results show that the correlation on the whole log is fair, but it becomes excellent neglecting two shallow points (-6.8 m and -30 m). The conclusion is that in the shallow portion, where sand-

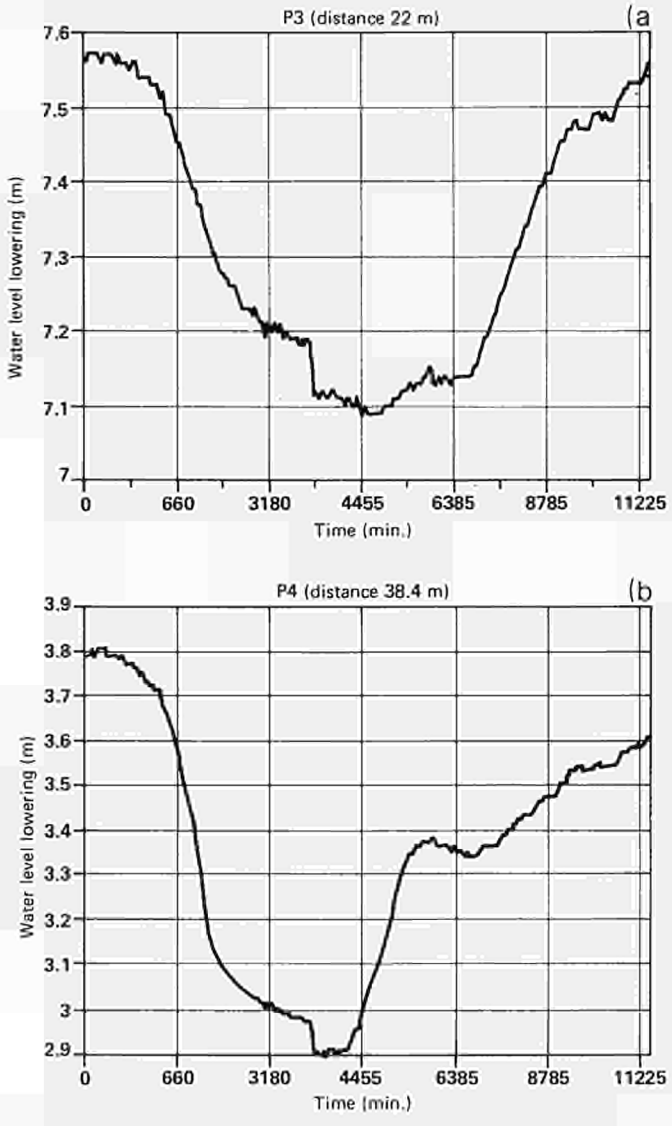

Fig. 2.24 - Drawdown and recovery curves in piezometers P_3(a) and P_4(b)

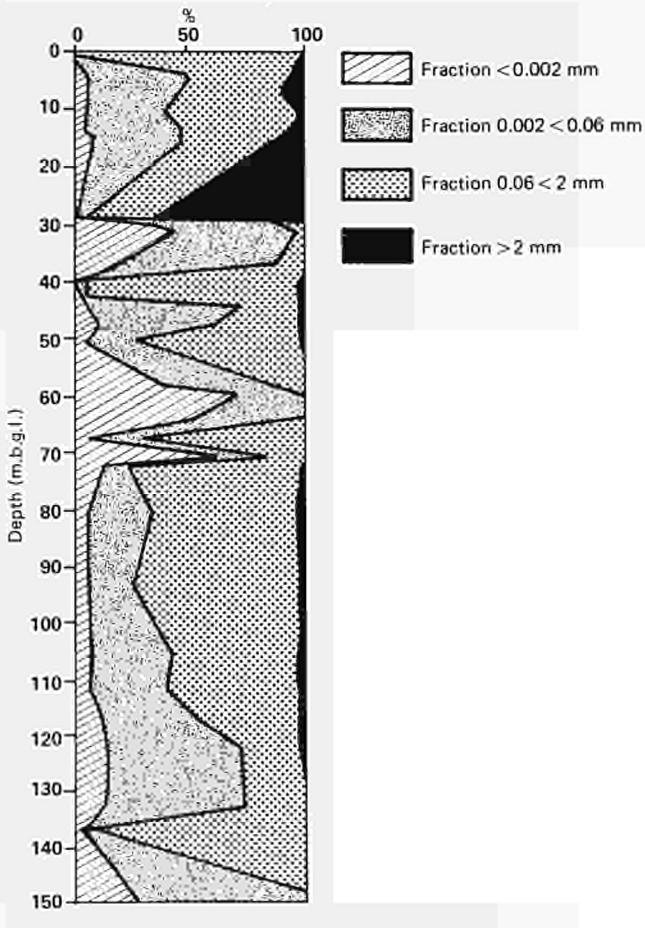

Fig. 2.25 - Total cumulative size distribution vs depth (borehole No. 1)

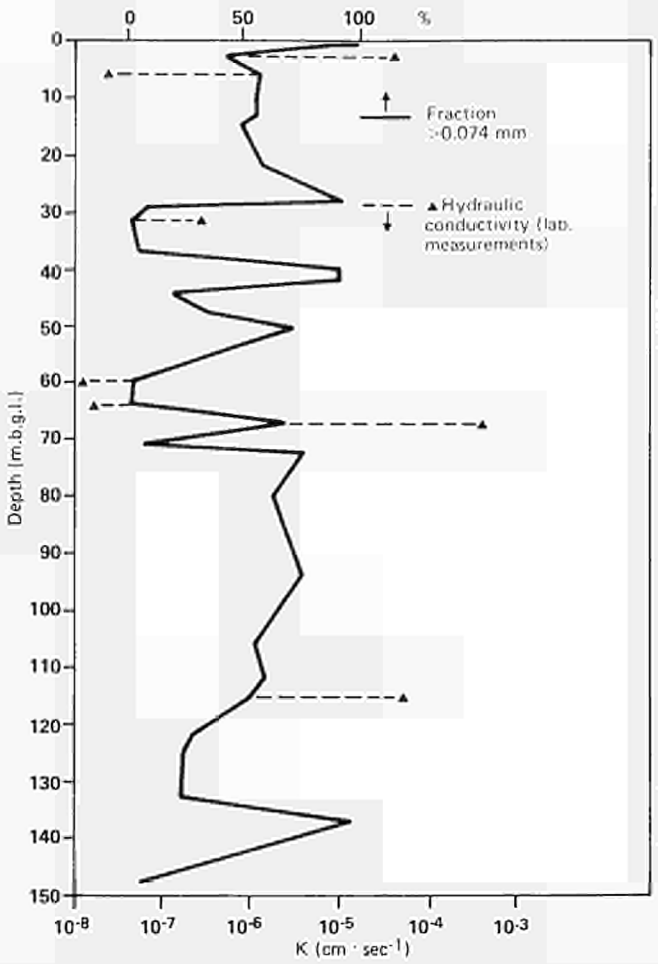

Fig. 2.26 - Fraction >0.074 mm vs depth (borehole No. 1).
▲ : Hydraulic conductivity from laboratory measurements.

silt alterations are frequent, the K values measured on the samples do not represent the actual permeability of the examined layer, as it often occurs. Conversely, the K values of deeper levels, showing more homogeneous size distribution, can be accepted as the actual hydraulic conductivity of the examined sediments.

A geochemical campaign is going on with survey of boreholes 3 and 4, both 60 m deep. In-situ measurement of geochemical parameters was performed by using a well-logging probe. Precautions were taken to maintain the undisturbed character of the water.

Geochemical data were acquired after several months of equilibrium. The data of boreholes 3 and 4, crossing the upper aquifer only, revealed a strong variation of redox potential from shallow levels to the bottom. Values of relevant parameters are given in Table 2.XI. These data were checked with those obtained during a previous survey on boreholes 1 and 2, 150 m deep, where constant chemical parameters were found: Eh ~ +300 Mv, ph ~ 7, conductivity: 0.36 mS cm^{-1}. Thus, oxidizing conditions are present down the whole depth of the deepest wells, indicating different geochemical conditions.

Table 2.XI — Main geochemical characteristics of ground water at the Ispra test site

Well	Depth (m)	Eh (mV)	pH	Conductivity (mS cm^{-1})
P_3	-10	+389	6.01	1.22
	-50	-390	6.27	1.23
P_4	-10	+295	7.23	0.34
	-46	-414	7.37	0.34

Natural Analogues: The OKLO Case

The discovery in 1972 of the existence of natural nuclear reactors which were "in operation" at Oklo (Gabon) about two billions years ago, has rightly excited the scientific community and over hundreds papers have been published up to now on the various scientific aspects of the phenomenon.
The fact that it is possible to reconstruct the geometry of the reactor cores from the presence on the site of the stable daughters of the fission products and actinides is undoubtedly a strong point in favour of the possibility of disposing of nuclear waste by emplacement in properly selected geological formations.
"Natural analogues", such as Oklo, may also serve the more ambitious task of validating the models which have been developed for safety assessment, although with obvious important limitations. With this objective in mind, we are reviewing the literature on the Oklo reactor, in co-operation with the University of Pavia (Italy), in order to see whether the present knowledge of the phenomenon can be utilised also for the validation of some models developed for safety assessment of present concepts of waste disposal in the European Community.

A preliminary literature screening shows that the nuclear physics aspects of the phenomenon and the dynamics of evolution during reactor operation are the aspects which have been more widely studied. Conversely, little effort seems to have been done in order to investigate the geochemical aspects of radionuclide migration in the surrounding geological media during and after the reactor working.

As far as the chronological and geometrical aspects are concerned, the spontaneous fissions began about 1.8 billion years ago at a depth ranging between 4,300 to 3,300 m, within a detrital level composed of sandstone lenses alternating to conglomerates (Figs. 2.27 and 2.28). The affected area covers some tens of thousands of square metres in which 9 reaction zones have been identified. The criticality appears to be due to a remove of silica, which, in turn, has been trigged by tectonic stresses. In fact, the hypothesis suggesting the sedimentary origin of the uranium enriched material appears to be inadequate for explaining uranium content up to 60%, allowing the criticality.

The nuclear reactions lasted for a time span ranging 100,000 to 500,000 years during which the reactor depth diminished of about 1000 m. This time spreads between two diagenetic events the first of which formed the silica further removed by tectonic stresses.

Concerning the radionuclide mobility, the preliminary investigations showed that the uranium and the rare earths have not been removed during the reactions. The concentration of different nuclides found out in the reaction zones were consistent with the development of fission reactions governed by the well-known nuclear parameters.

Further, more accurate examinations showed that more or less important discrepancies were detectable near the borders of the cores, where uranium migration during nuclear reactions cannot be excluded.

The review of the behaviour of transuranics as well as fission products other than rare earths, is still being carried out; nevertheless, some preliminary conclusions might be drawn.

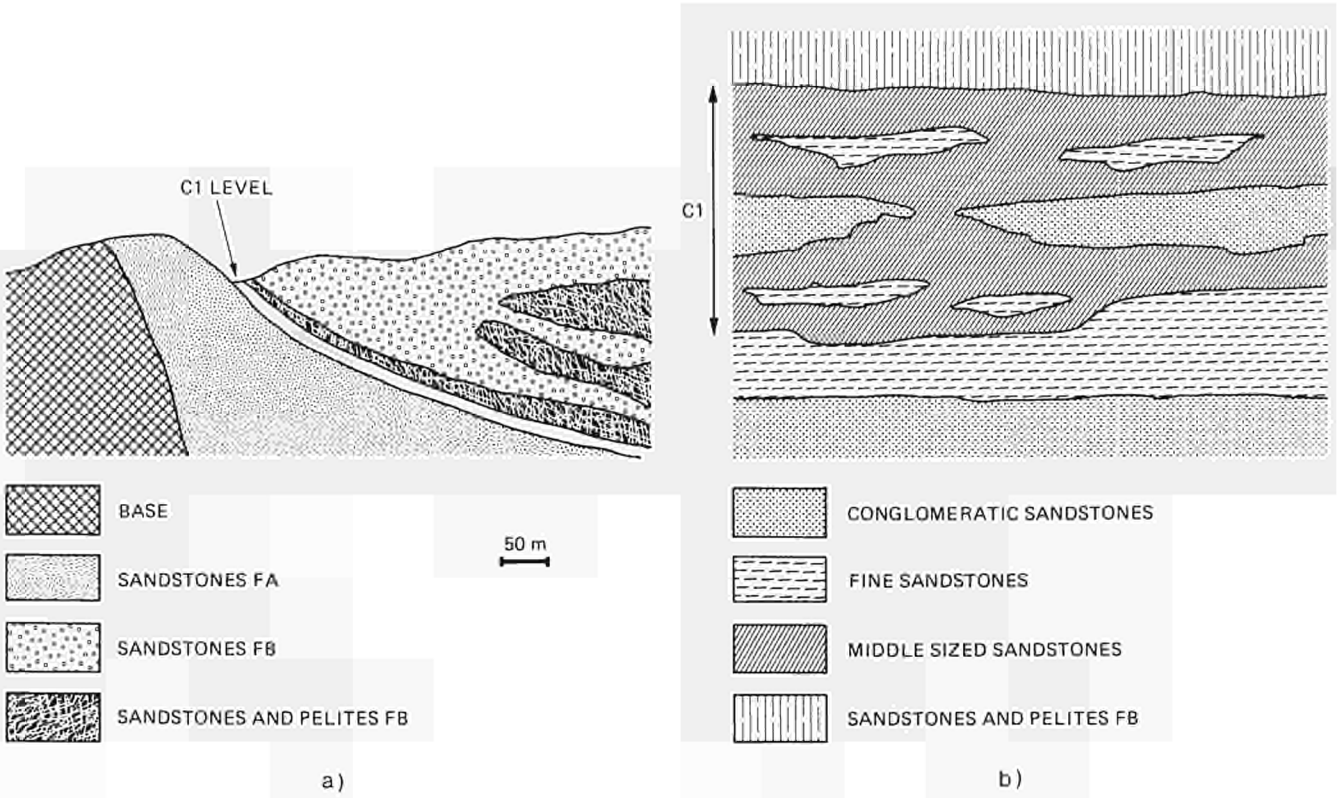

Fig. 2.27 - a) Geological view of the Franceville basin at Oklo
b) Geological cross-section of the level C_1
(from R.J. Chauvet, 1975)

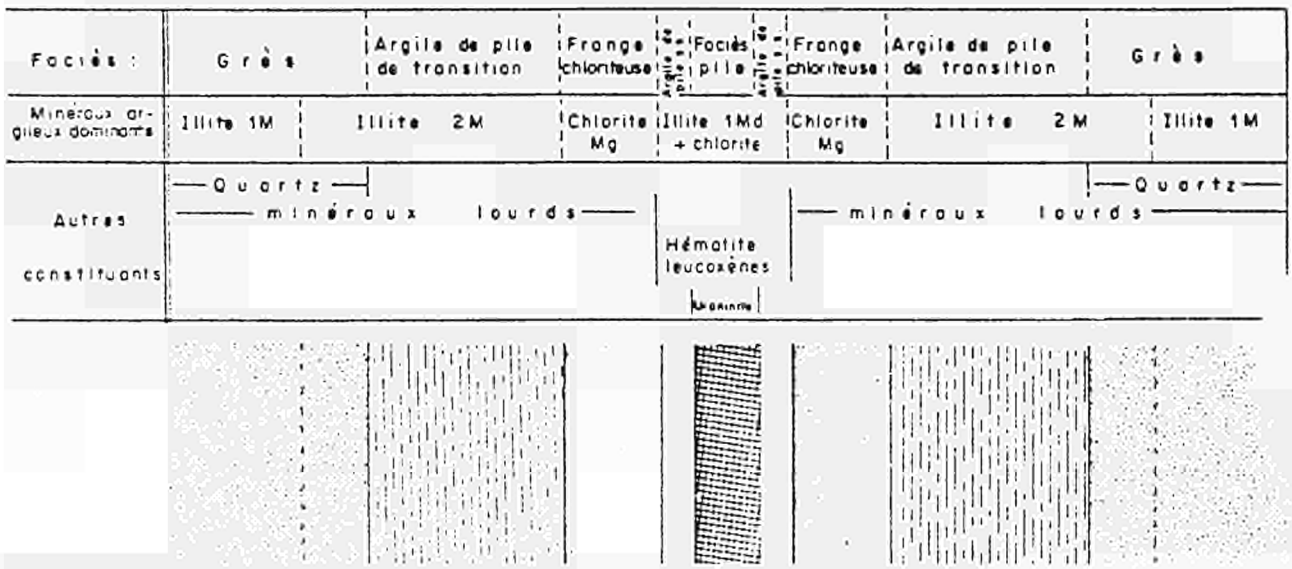

Fig. 2.28 - Distribution of different minerals near the reaction zone (from Gautier and Weber, 1977)

It is almost certain that the totality of ^{239}Pu formed during the reactions has been trapped within the uraninite grains until its complete decay. The ion probe showed that on a micron scale, ^{238}U and ^{235}U occupy the same position. Thus no movement of ^{239}Pu occurred, since almost half of the remaining ^{235}U is a decay product of ^{239}Pu.

Equally no migration has been observed for ^{232}Th, which is present only in negligible amount outside the reaction zone, being totally confined within the uranium mineral lattice.

Concerning the fission products, some conclusions can be drawn about the behaviour of some alkali and alkali-earth elements. The Rb moved few metres only, the migrating fraction accounting for no more than 60% of the total. Concerning Sr, 5% only has been retained in the uraninite, the remaining fraction being redistributed near the borders of the reaction zone. A more important retention has been advocated for Cs, during both the criticality period and the following 20-30 Ma.

In the light of these considerations, it appears quite clear that the Oklo example should be rather addressed to the concept of spent fuel disposal than to the burial of conditioned waste, since major retention capability has been exhibited by the uraninite lattice than by the surrounding geological environment.

A further item of interest is the possibility of modelling the radionuclide migration in the "near field" of the Oklo reactor. This activity has been tentatively planned as conclusion of the review. A further survey of the quantitative data available in the literature will determine whether such a modelling is feasible.

International Co-operative Projects

Within the CEC co-ordinated project MIRAGE, the JRC-Ispra participates in the working group on COlloids and COmplexes (COCO club). Work concentrated on :

1. characterization of humic substances,
2. characterization of natural colloids in groundwaters from reference sites.

The purpose of the first exercise was to evaluate the reliability of available analytical methodologies to provide information on the composition and the structural chemistry of humic acids. Accordingly, the investigations during this phase focused on reference products : two commercial humic acids from Aldrich and a natural humic acid extracted from a Gorleben groundwater (Gohy-573). Investigations made include : major and trace element analysis (with a contribution from the Dalhousie Univ., Halifax, Canada), functional group analysis (spectrophotometry in the visible and UV region, infrared spectroscopy, NMR, potentiometric titrations), molecular size measurements (ultrafiltration and ultracentrifugation). The ultrafiltration results of the Gorleben humic acid reported in Table 2.XII, indicate a polydispersed system with particle size below 3 nm. In parallel, attention is paid to the identification of natural colloids (exercise No. 2). Groundwater samples from the Markham Clinton (UK) sandstone aquifer were analysed. The same exercise is underway with groundwaters from Gorleben and Grimsel (CH). A meeting of participants in the COCO club was organized in Ispra in October 1987.

Table 2.XII — Ultrafiltration data of the Gorleben humic acid (Gohy-573) in 0.1 M $NaClO_4$

Nominal MW cut-off*	Porosity nm	pH 5.5 % retained	pH 8.5 % retained
$1x10^5$	5	2.6	2.7
$3x10^4$	2	14	36
$1x10^4$	1.5	55	61
500	1	96	99

* Amicon membranes

Within the OECD/NEA project TDB (Thermodynamic Data Base), the JRC-Ispra is contributing to the development of a data base for Am. Aim of the TDB is to compile and critically review literature data for a number of elements of interest to safety analysis.

A joint project, ENRESA-CIEMAT (Spain)/JRC, on the investigation of radionuclide migration in crystalline rocks was established. The study will involve the following activities : groundwaters and rock materials characterization, evolution of natural colloidal fractions in granitic groundwaters, laboratory migration experiments through intergranular pores and permeable fractures.

References

/1/ G. BIDOGLIO, P. OFFERMANN, A. DE PLANO, G.P. LAZZARI — Influence of Groundwater Composition on Glass Leaching and Actinide Speciation. In: Scientific Basis for Nuclear Waste Management XI (M.J. Apted, R.E. Westerman (Eds.), Materials Research Soc., Pittsburgh (1988) in press

/2/ G. BIDOGLIO, A. AVOGADRO, A. DE PLANO, G.P. LAZZARI — Reaction Pathways of Pu and Np in Selected Natural Water Environments. Radiochimica Acta (1988) in press

/3/ G. BIDOGLIO, P. OFFERMANN, A. SALTELLI — Neptunium Migration in Oxidizing Clayey Sand. Applied Geochemistry, **2** (1987) 275-284

/4/ P. OFFERMANN, G. BIDOGLIO — Rentention Properties of Pressed Salt for Tc, Np, Pu and Am. Radiochimica Acta (1988) in press

/5/ L. RIGHETTO, G. BIDOGLIO, B. MARCANDALLI, I.R. BELLOBONO — Surface Interactions of Actinides with Alumina Colloids. Radiochimica Acta (1988) in press

/6/ I.R. BELLOBONO — Indagini su Reazioni di Interfaccia in Acquiferi Chimicamente non Saturi. Contract report, EDISPI 2677-85-04 (1987)

/7/ N. OMENETTO, P. CAVALLI, G. ROSSI, G. BIDOGLIO, G.C. TURK — Thermal Lensing Spectrophotometry of Uranium(VI) with Pulsed Laser Excitation. J. of Anal. Atomic Spectrometry, **2** (1987) 579-583

/8/ G. BIDOGLIO, G.TANET, P. CAVALLI, N. OMENETTO — Uranium and Lanthanide Speciation by Thermal Lensing Spectrophotometry. Inorganica Chimica Acta, **140** (1987) 293-296

/9/ I. GRENTHE, G. BIDOGLIO, N. OMENETTO — On the Use of Thermal Lensing Spectrophotometry (TLS) for the Study of Mononuclear Hydrolysis of Uranium(IV). Submitted for publication

RESEARCH AREAS

3. Feasibility and Safety of Waste Disposal in Deep Oceanic Sediments

The technical feasibility and environmental acceptability of disposing high-level nuclear waste in geological formations under selected zones of the oceans is presently being investigated by the International Seabed Working Group (SWG) of the NEA. Several countries of the EC participate in the study and the Commission is an official member of the SWG, and joint programme co-ordinator (with Sandia National Laboratories, USA).

The SWG is at the moment completing an evaluation of feasibility and safety of sub-seabed disposal. A first evaluation should be completed within 1988.

In the framework of the feasibility and safety assessment of this option, two main emplacement technologies have been identified; those of free-fall penetrators and deep ocean drilling. An initial emphasis is being placed by the JRC on the study of the penetration option due to the lack of information on its feasibility compared with that of drilling. Deep drilling has been practiced, over at least the last 15 years, in many parts of the world's oceans, although not as yet as the scale envisaged for nuclear waste disposal.

The approach of the JRC is to develop all the mathematical models necessary to undertake an initial assessment of the option. These include the use of the JRC probabilistic code LISA for radiological dose calculations, the application of models for sediment radionuclide dispersion under the influence of diffusion or caused by migration due to pore water movement and the development of models for the prediction of the mechanisms controlling penetration and hole closure.

The application of the above range of models for the feasibility and safety assessment will require the support of a realistic data base and model validation. It is intended that these will be obtained essentially by in-situ tests and laboratory simulation experiments.

In-situ tests have been carried out in international campaigns, to which the JRC has participated both directly and by extensive geochemical studies of the sediment cores taken in these campaigns (namely, for 1987, the ESOPE cruise). Advanced instrumentation for long-term in-situ tests, with direct data transmission to the laboratory via satellites, has also been under development for several years at the JRC.

Laboratory simulation experiments are carried out at the JRC in conditions as close as possible to those of deep oceanic sediments, under controlled pH and Eh. The influence of the high pressure existing at sediment depth (over 500 bars) is also being studied.

Contents

3.1 Risk Assessment of the Penetrator Option

The probabilistic risk assessment of the sub-seabed option, including sensitivity analysis, has now been completed. The results have been written up and included in the final report of the Radiological Assessment Task Group (RATG) of the SWG. This is the culmination of the assessment work underway for the past four years and of a 16 month visit of a modeller under contract from the University of Liège (B). Preparatory to conducting the assessment itself, close contact was maintained with our colleagues of the RATG, especially those from the Ecole des Mines, Paris (F), to ensure and maintain compatibility between the models and data being used by different groups.

Introduction

The probabilistic analysis of the sub-seabed option was conducted on the basis of the normal evolution scenario. This consists of the successful emplacement of the waste package at its prescribed depth (mean value 50 m) in the two selected areas. This is followed by the slow corrosion of penetrators and canisters eventually leaving the vitrified waste exposed to the sediment pore water. As the glass gradually dissolves, radionuclides are released to migrate by diffusion into the surrounding sediment. The nuclides undergo interactions with the sediments leading to varying degrees of retention and hence retardation in their movement. The radionuclides arriving at the sediment-ocean interface are released into the water column where they are slowly dispersed and mixed. By way of marine food chains they eventually become available to man by ingestion and inhalation.

To perform the stochastic-uncertainty analysis, the LISA code, developed at the JRC, was used. The work of adaption and modification to render the code applicable to this assessment has, up to the last year, formed the bulk of the exercise. The sensitivity analysis was conducted using the SPOP code, also developed at the JRC, which applies four different non-parametric statistical techniques to the sample.

Results

Simulations using 500 runs and an integration time of up to 10^6 years were performed for the Great Meteor East (GME) and South Nares Abyssal Plain (SNAP) sites. Individual dose rates were calculated for two separate pathways.

For **pathway 1**, the following sub-pathways were considered :

- the ingestion of seafood (fish, crustaceans, molluscs and seaweed), desalinated water and sea salt taken from surface water;
- the inhalation of marine aerosols.

Pathway 2 is the same as 1 except that mid-depth ocean concentrations were used.

For each site and both pathways, similar results were obtained. The small differences found between the results for the GME and SNAP sites do not influence the conclusions, and consequently, only the results obtained for the GME site with pathway 1 are discussed.

In LISA the dosimetry model provides for each run a curve of the individual dose rates versus time, each one representing the sum over all the radionuclides. From these curves, the mean dose rates versus time are computed and in Fig. 3.1 the values obtained are represented by a curve which reaches a maximum mean value of 2.9×10^{-9} Sv/a at 1.5×10^5 years and afterwards decreases due mainly to radionuclide decay. These mean values have been obtained from one sample of 500 runs and another sample would probably produce different empirical mean values. To obtain the true mean values, a simulation with an infinite number of runs is required but impossible to realise in practice. Fortunately, from the empirical mean values it is possible to define bounds and make the statement that the true mean values lie within those bounds, with a probability $1-\alpha$ that the statement is correct. The level of significance α is the maximum probability of rejecting the above statement. In practice, the confidence bounds on each of the mean values are estimated using the Tchebycheff's Theorem for a significance level $\alpha = 0.05$. The results are represented in Fig. 3.1 by the upper (U) and lower (L) curves which thus define the confidence interval for the mean dose rates. From this analysis there is a probability of 0.95 that the maximum value of the true mean dose rate ranges between 2.2×10^{-9} Sv/a and 2.7×10^{-9} Sv/a.

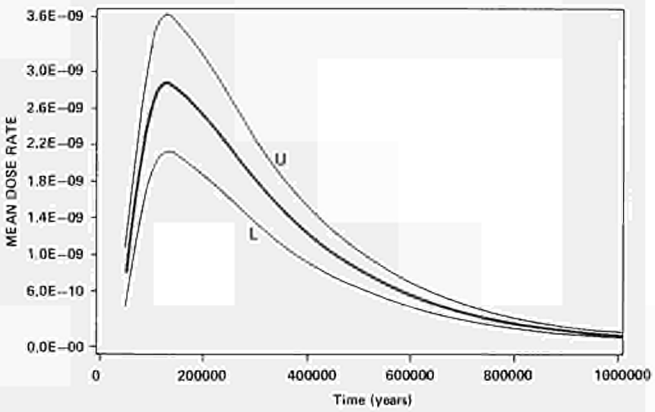

Fig. 3.1 - Mean dose rates (Sv/a) vs time for the GME site, base case scenario and pathway 1. The upper (U) and lower (L) curves define a 95% confidence interval.

Figure 3.2 illustrates the frequency histogram for the maximum dose rate found (irrespective of the time of occurrence) for each of the 500 curves defined in the dosimetry model, and Table 3.I gives for each histogram unit represented in Fig. 3.2 the contributing radionuclides. From the figure we see that no dose rate value appears above 3.2×10^{-8} Sv/a. More accurately, the highest dose rate reached over the 500 runs was 2×10^{-8} Sv/a after 110,000 years with the ^{99}Tc as the most important contributing radionuclide. The arithmetic mean of the maximum dose rates is 3×10^{-9} Sv/a (equivalent to -8.5 on the log scale in Fig. 3.2) with confidence bounds of $\pm 7 \times 10^{-10}$ Sv/a for $\alpha = 0.05$.

The downward distribution function computed from the frequency histogram shown in Fig. 3.2, is given in Fig. 3.3. The purpose of this distribution is to show the probability of exceeding particular dose rates. For the same reason as previously mentioned for the mean values, confidence bands should be drawn which are defined by the region between the upper (U)

Table 3.I - Percentage of runs in each histogram in Fig. 3.2 where the given radionuclide is the main contributor

Histogram unit	Percentage						
	Tc99	Se79	Zr93	Pd107	Sn126	Cs135	I129
1	50	50	–	–	–	–	–
2	75	–	–	–	25	–	–
3	76.9	–	7.7	–	15.4	–	–
4	72	4	–	–	16	8	–
5	58.6	20	7.1	–	14.3	–	–
6	75.8	0.4	1.8	–	22	–	–
7	86.9	–	–	–	13.1	–	–

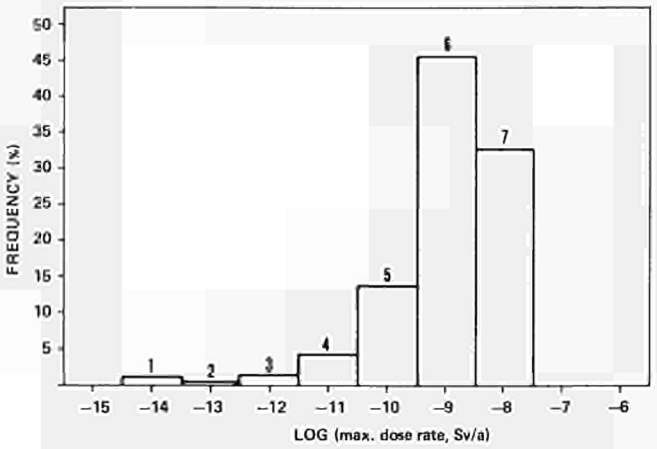

Fig. 3.2 - Maximum dose rate frequency histogram for GME site, base case scenario and pathway 1

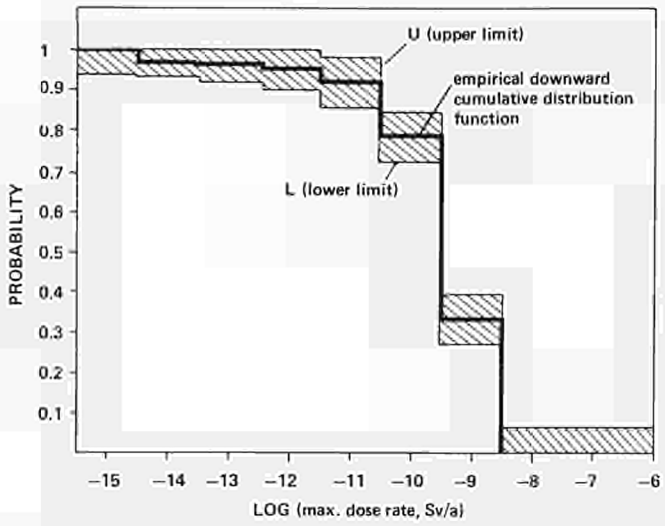

Fig. 3.3 - Downward cumulative distribution of the frequency histogram represented in Fig. 3.2. A 95% confidence band is defined by the dashed zone.

and lower (L) downward distribution functions. These two limit distributions have been obtained by using the Kolmogorov's statistic with α = 0.05 (95% confidence level). Whereas the simple downward cumulative curve gives an estimate of the probability of exceeding particular dose rate values, the upper confidence bound curve (U) gives the highest value of such a probability at the given confidence level. These bounds now enable an estimate to be made of the probability of exceeding the dose rate of 3×10^{-8} Sv/a (the upper limit of the highest bin of the frequency histogram in Fig. 3.2). This is shown in Fig. 3.3 by the upper bound value of probability at 10^{-8} Sv/a, of 0.06. This can be interpreted that with a confidence level of 95%, the frequency of doses above 10^{-8} Sv/a (Fig. 3.2) will not be higher that 6%, which corresponds to 30 out of 500 runs. From this it is not possible to calculate by how much this value of dose might be exceeded; however, by increasing the number of runs, the distance between the simple downward cumulative and the U curve can be reduced (doubling the number of runs reduces U by a factor 1.4).

Results of the Sensitivity Analysis

To perform the stochastic sensitivity analysis (SA) for the normal evolution scenario with the LISA code, the basic data files for both sites were simplified. Decay chains beginning with the following radionuclides were omitted since they were shown not to significantly contribute to the results : ^{246}Cm, ^{245}Cm, ^{243}Am, ^{240}Pu. This facilitates the interpretation of the sensitivity results and enables a greater number of runs to be performed improving the quality of the analysis. The sensitivity analysis was finally performed for pathway 1 with 1000 runs which is double that made for the base case analysis of the normal evolution scenario.

For the GME site, the sensitivity analysis enabled the most important variables to be divided roughly into three groups : i) those important over the whole simulation time span; ii) those important only over the initial transient phase; and iii) those parameters whose influence increases with time.

The first group includes almost all the ^{99}Tc related variables, such as :

- the distribution coefficient KD(Tc) in the mildly reducing sediment zone;
- the concentration factors for crustacea CF2(Tc), molluscs CF3(Tc) and macro-algae CF4(Tc).

These results are in agreement with the fact that for pathway 1, ^{99}Tc was detected as the most important radionuclide over almost all the simulation time (10^6 years), i.e. it is the main dose contributor.

Figure 3.4 shows one possible representation of the SA results for the variable KD(Tc). In this figure, the rank values versus time are plotted for each estimator considered for the SA studies. The upper horizontal dashed straight line represents the maximum rank value (i.e. the number of input variables) while the lower one represents an estimated threshold for the identification of influential parameters.

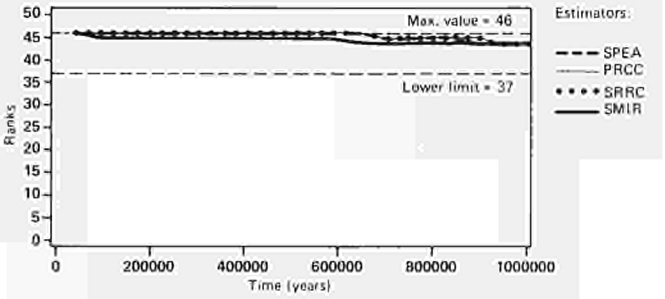

Fig. 3.4 - Non-parametric sensitivity analyses (1000 runs/ 46 variables). Rank values vs time for the variable KD(Tc). GME site - base case scenario - pathway 1

The first group of important parameters also includes RLEACH, being significant over almost all the simulation time. Generally, RLEACH has no influence whenever the radionuclide migration time through the sediment column is long enough to spread the input pulse to such an extent that the shape of the peak leaving the near-field (governed by RLEACH) is lost. For this specific assessment, however, the appreciation of the reducing environment found in the sub-seabed sediments has led to the selection of leach rate values extending up to a total waste dissolution time of 10^5 years.

The shape of the nuclide pulse leaving the sediment column is particularly important since the maximum nuclide concentration in the ocean is governed by the competing actions of the release from the sediment and the scavenging in the ocean. This latter process is slow compared with the time needed to disperse the activity in the various boxes, so that a much higher concentration in the ocean is obtained when the release rate from the sediment is fast. If, on the contrary, the radionuclides are released at the sediment-ocean interface at a slower rate, the scavenging effect succeeds in keeping concentrations in the ocean at lower levels.

The last varibale which can also be considered in the first group is the porosity of the mildly reducing sediment zone (POR). This variable is influential over most of the simulation time (10^6 years), but its importance decreases slowly after about $7x10^5$ years. In the base case scenario, the advective velocity in the sediment column has been assumed equal to zero. Therefore, only the diffusion process, which is governed by the variable POR, can move the radionuclides retained in the sediment column up to the sediment-ocean interface. Obviously, if after a certain period of time all the radionuclides were released into the ocean, the porosity would no longer be important. In the present case, however, the results suggest that some radionuclides are still in the sediment column after 10^6 years.

The decrease in the influence of POR after about $7x10^5$ years appears to be related to that of KD(Tc), which also decreases slightly after about the same time period. This shows that the influence of the porosity on the output is mainly conditioned by the presence in the sediment column of the most important dose contributor (i.e. ^{99}Tc).

The second group of parameters, those which are only important for the initial transient phase, includes the sediment column length XPATH, the canister mean lifetime CMLT, and variables related to the nuclide ^{126}Sn, such as the distribution coefficient KD(Sn) in the mildly reducing sediment zone and the concentration factor for fish CF1(Sn). The sensitivity plot for XPATH is illustrated in Fig. 3.5, which clearly illustrates the decrease in influence of this parameter with time. The relationship between the radionuclide migration time through the mildly reducing zone and the input variables XPATH and POR shows that for the dominant radionuclides having KD values close to zero, the variable XPATH is very important in determining the migration time values. Furthermore, in this case, the shape of the pulse leaving the sediment column depends only on the XPATH value. The shorter the sediment column length, the higher and narrower will be the pulse at the sediment-ocean interface, and thus the higher will be the output doses. Therefore, once the bulk of the dominant radionuclides is released into the ocean, the input variable XPATH becomes unimportant. This effect occurs after about $2x10^5$ years.

When KD values are significantly greater than zero, the influence of the variable XPATH on the output is cancelled by the variable POR. This result can be explained by a combined effect of the type of probability function associated to the input variables (XPATH and POR) and the influence of POR on the migration time. In fact, when the KD value chosen changes from close to zero to a value significantly greater than zero, the importance of the variable POR on the migration time increases (the dependence of migration time on porosity changes from $(POR)^{-1.5}$ to $(POR)^{-2.5}$). Furthermore, because of the normal density function used for XPATH, its sample value will not be much diffierent from the mean value (i.e. corresponding to the maximum of the normal density function), while the uniform probability function used for the variable POR allows more important variations of its value. Consequently, the shape of the output pulse will also depend on the POR values.

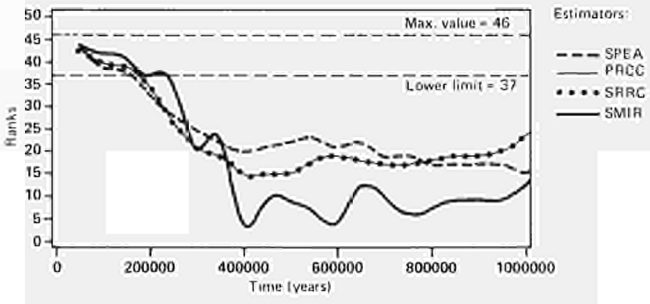

Fig. 3.5 - Non-parametric sensitivity analyses (1000 runs/ 46 variables). Rank values vs time for the variable XPATH. GME site - base case - pathway 1

^{126}Sn can only contribute to the output results at short times in the initial transient phase because the scavenging effect for ^{126}Sn is more pronounced than for ^{99}Tc (the sediment partition coefficient or distribution coefficient in the water column for ^{126}Sn is five hundred times greater).

The canister mean lifetime CMLT, which falls into the second category of parameters, is significant initially but, as would be expected, its importance is very short-lived. With the gaussian density function defined in the data base for CMLT, the maximum canister lifetime is $4x10^4$ years. Since the maximum lifetime of the glass block in the canister is about $7x10^4$ years, all the radionuclides will be released into the sediment after a maximum time of about 10^5 years and, consequently, after this, CMLT cannot have any further influence.

The last group of variables are those whose influence increases with time. Since scavenging is a slow process it might be expected that this influence would become evident after very long times. Thus, the parameters describing concentrations (CS and CL) and setting velocities (SS and SL) of small and large particles would be expected to become influential at large simulation times. In fact, this is only observed for the settling velocity of large suspended particles, SL (Fig. 3.6), which is clearly always negatively correlated.

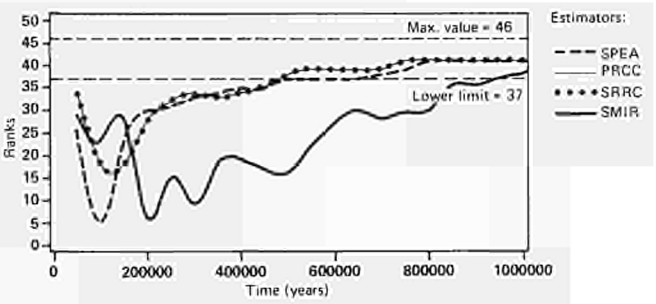

Fig. 3.6 - Non-parametric sensitivity analyses (1000 runs/ 46 variables). Rank values vs time for the variable SL GME site - base case scenario - pathway 1

The reason why SL is the most important of the scavenging parameters relates to the size of the ranges used for their parameter distributions. The sedimentation flux of small or large suspended particles in the water column depends on the product CS x SS x CL x SL. The values of these products are comparable, but the range of the SL values is the most important. Consequently, this variable appears as the most influential.

Other parameters which fall into the last category of important variables include concentration factors for caesium and iodine. The fact that they only become important after long time periods is linked to the long half-life of ^{129}I and ^{135}Cs, compared with the other important contributors (about 100 and 10 times greater than ^{99}Tc or ^{126}Sn, respectively).

The main features of the sensitivity analysis presented above are duplicated for the SNAP site. Since the geographical location of the site does not much influence the output dose values, the main differences observed are due to the existence at the SNAP site of a second sediment layer representing the surface oxidized zone. In this second layer, new input variables such as the thickness and distribution coefficients were introduced. The probability functions associated with the distribution coefficients are generally the same in the mildly reducing and oxidized zones; this is except for the radionuclides U, Ra and Tc for which the

corresponding probability functions generally provide distribution coefficients which are smaller in the oxidized zone. Porosity values are normally equal or higher in the oxidized zone.

As a consequence of these differences, the sorption capacity, or barrier effect, of this second upper layer is generally weaker than that of the lower mildly reducing zone, particularly for ^{99}Tc, the radionuclide most influencing the dose. The thickness of the oxidized layer is, therefore, positively correlated with the output doses (for a given total sediment column length, the increase of this variable reduces the thickness of the first layer and, therefore, the total barrier effect of the sediment column is reduced).

Conclusions

A stochastic radiological assessment of the sub-seabed option has been completed which forms part of the JRC's contribution to the work conducted by the Radiological Assessment Task Group of the OECD (NEA) International Seabed Working Group.

No significant differences in the results were found between the two sites considered (GME and SNAP), although the quality of their sediments is slightly different. For the base case scenario the peak of the mean dose rates over time for the maximally exposed group of individuals is in the order of 2.9×10^{-9} Sv/a, for the complete repository of 10^5 metric tons of heavy metals waste equivalent, occurring 150,000 years after disposal. This is more than 10^5 times smaller than ICRP recommended limits (10^{-4} - 10^{-3} Sv/a), and also about 3.4×10^5 times smaller than background levels; such very small doses are negligible and insignificant. The uncertainty range of maximum dose rates, independent of time of occurrence, falls between 3×10^{-15} and 4×10^{-8} Sv/a. The highest dose calculated by the stochastic analysis, in a sample of 500 runs, was 2.5×10^{-8} Sv/a which is still more than 4×10^4 times smaller than ICRP limits. These results correpond well with the values obtained by the deterministic and bracketing exercises. The radionuclides contributing most to these doses are those which are long-lived and poorly sorbed, principally ^{99}Tc, but also with contributions from ^{79}Se, ^{126}Sn, ^{129}I and ^{135}Cs. The major pathway is the consumption of fish, molluscs, crustaceans and seaweed.

3.2 Instrumentation for In-Situ Experiments: The SOFT LANDER

(C.N. Murray)

As has been reported in earlier Programme Progress Reports as well as in the present one, section Laboratory Simulation Experiments, the Joint Research Centre has been investigating the geochemical characteristics of selected marine sediments from sites of interest (Great Meteor East and Southern Nares Abyssal Plain) in the North Atlantic. Studies have been carried out in the laboratory on the mechanisms controlling the migration and diffusion of long-lived radionuclides through sediment samples obtained from the above sites as well as in the development of models to investigate the dispersion of the elements with time in these materials.

Results from the radiological modelling work have shown that the sediments under study are extremely capable of retarding the migration of nuclides and that they represented a very good barrier against their dispersion into the water column. It has also been shown, however, that for certain of the nuclides which formed soluble non-absorbed chemical species, the migration rate would be highly dependent on pore movement within the sediment column.

The detection of fault like structures in certain areas of the study sites in the North Atlantic lead to the possibility that vertical pore water movement might be occurring along the fault lines and that preferential pathways to the sediment surface could exist.

In order to investigate this possibility more closely, the Seabed Working Group undertook an International Long Core Cruise during June-July 1985 (see PPR 1985). On this cruise core samples of up to 34 m in overall length were obtained for detailed geotechnical and geochemical study. A second approach to this problem was investigated; this was the feasibility of undertaking long-term experiments in the sediment column and to obtain the data in real-time at a European based laboratory. The availability of the data during the actual investigation would allow a control of the correct execution of the experiment as well as permitting real time model verification to be undertaken. Tests carried out from the M.V. Marion Dufresne during the cruise showed that an acoustic link could be set up between instrumentation emplaced within the sediment column and that data could be transmitted from the sea surface via the European Space Agency's Meteosat geostationary communications satellite to Darmstadt (FRG).

These encouraging results lead to the development of a surface platform, which has continued during 1987, for data reception and transmission and a retrieval deployment vehicle. For a detailed description of surface platform, see PPR January-June 1986.

Design work on the deployment vehicle, a "Soft Lander", as it became to be known, was started in 1987 with the definition of the performance requirements in relation to its operational objectives.

Operation Objectives

In view of the importance of the top few metres of the sediment column, where active biological and geochemical processes are occurring, a vehicle was required that could be easily deployed and recovered, inexpensive and capable of emplacing various types of instrumentation in and on the seabed.

The operational objectives of the Soft Lander were thus defined as being : to deploy a reasonable load of specialized instrumentation within the first few metres of the sea floor; to carry sufficient power for the emplaced sensors so that they could undertake their experimental investigation for a period of several months up to one year; to transmit the data obtained from within the seabed back to the surface via a low frequency acoustic transponder and after completion of the study period to return to the sea surface with the instrument load for collection and redeployment.

Previous investigations had shown the feasibility of emplacing instrumentation deep sea within the ocean bed using free fall penetrator technology. However, the drawbacks to this technique are that the instrumentation cannot be recovered; depths of penetration are in order of several tens of metres, and that data can only be recovered while the surface ship is on station.

These studies had, nevertheless, demonstrated the effectiveness of this deployment technique and it was realized that by decreasing the penetrator's velocity sufficiently, it should be possible to emplace the instrumentation within the upper sediment layers at a pre-determined depth.

Using a model developed for the prediction of the depth of free fall penetration, as a function of their density and shape, it was

calculated that values of 1-3 m/sec as a descent velocity for the vehicle would produce a penetration of 2-5 m for the Great Meteor East site.

To achieve this low velocity and at the same time enable the recovery of the vehicle, a number of low density floats were added to the penetrator. This was done in such a manner that on separation of a predetermined section of the penetrator, the positive buoyancy of floats would bring the instrumentation section back to the surface.

Vehicle Design

The characteristics of the prototype vehicle were finally defined as follows :

- effective retrievable instrument (including batteries) load of around 400 kg in air,
- descent rate to be 1-3 m/sec depending upon depth of penetration required into sediment column,
- maximum deplayment depth 6000 m,
- overall weight of vehicle to be less than two tonnes in order for it to be easily handled from a standard oceanographic vessel,
- a two way acoustic link to enable real time data transmission and interrogation,
- sensors to be deployed within the penetrator section (within the sediment column) or within the instrument package section (on the seafloor).

A schematic diagram of the vehicle is given in Fig. 3.7. The vehicle consists of twelve independent cylindrical floats made of syntactic foam having a density of ≈ 0.62 gm cm^{-3} and dimensions, height 1340 mm, diameter 308 mm being conical at each end. The central structure of the Soft Lander consists of two aluminium discs of 1650 mm diameter into which the twelve floats are fitted. The two discs are attached to a central aluminium tube to give structural rigidity to the vehicle and are welded 620 mm apart. The assembled module can be seen in Fig. 3.8.

Attached to the lower disc is a section where batteries and instrumentation can be placed. The size of this section can be varied according to instrument requirements. In order to transmit data back to the sea surface a 3.5 kHz transponder is fitted between the floats and is connected to the instrumentation by pressure cables (see following section, Acoustic Link - Data Transmission). An accelerometer and tilt package is also placed in the upper float section to monitor the behaviour of the vehicle during its descent and landing on the seabed. This has been provided by the Building Research Establishment, U.K.

Underneath the instrument section is a solid disc which is designed to act as a brake and give stability to the Soft Lander once it has arrived at the seafloor. On the basis of the required penetration this disc comes to rest on the seafloor in such a way as to stop the instrument section entering the sediment.

Attached to this disc is a 2-5 m long penetrator. In the present prototype this is 2 m in length and comprises of two sections. The upper section, 0.5 meter in length will house geochemical sensors and the control unit. The section is pressure resistant with the sensor heads recessed in the penetrator wall against

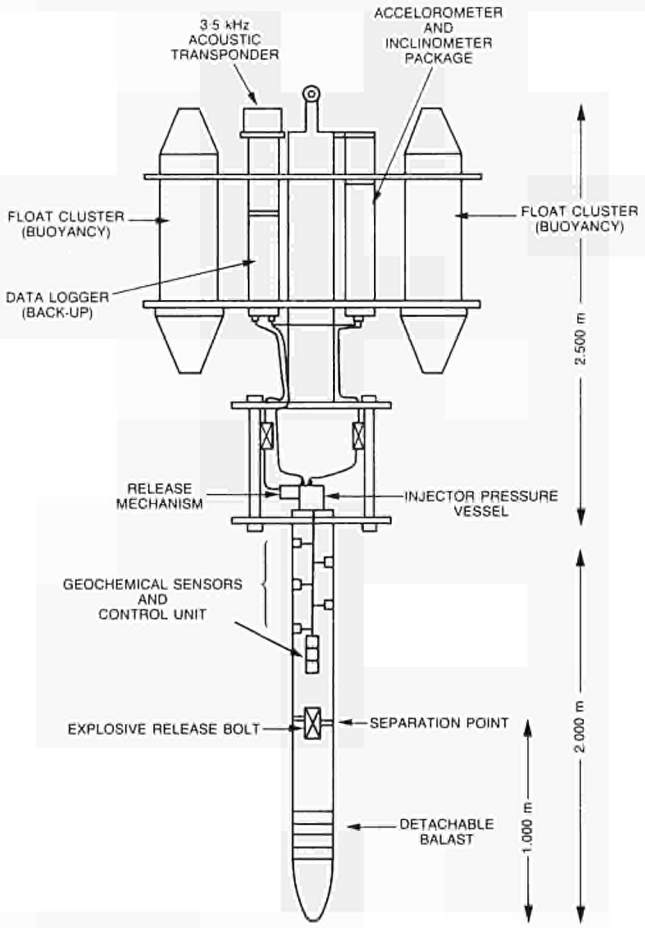

Fig. 3.7 - Soft lander

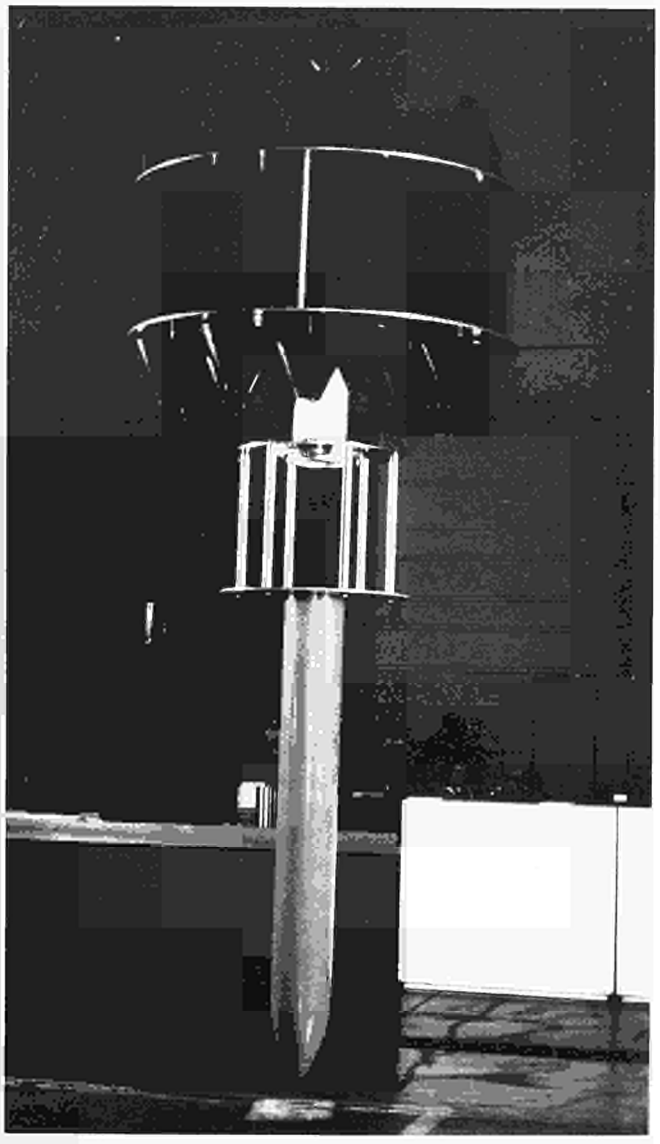

Fig. 3.8

metal O-rings. The sensors have been pressure tested to 500 atmospheres and measure pH, Eh, dissolved oxygen and temperature. The instrumented part of the penetrator is modular in construction and can be attached at any pre-determined length along the penetrator providing sufficient buoyancy is available to extract the section from the sediment after release of the ballast.

Ballast is provided by the lower section of the penetrator which is shaped to allow easy insertion into the sediment as the Soft Lander comes to rest on the seabed. The two sections of the penetrator are attached via an explosive bolt. This bolt is controlled from the transponder computer unit and should be fired either after a pre-set time or on command from the surface through a special acoustic signal. The separation of the bolt releases the lower ballast section, the positive buoyancy of the floats of several hundred kilograms will cause the module to return to the surface for collection and re-deployment.

Acoustic Link - Data Transmission

A general scheme of the 3.5 kHz acoustic transponder is shown in Fig. 3.9. The system comprises of an electro-acoustic transducer connected to a central processer unit and an instrument package. The system has been developed by the Institute of Oceanographic Sciences with financial support from the U.K. Department of the Environment and the JRC-Ispra (Italy).

During descent and penetration data are collected at 500 Hz using a frozen buffer system. Up to eight channels of data can be collected with approximately 10 bit resolution. Data are telemetered using pulse interval modulation of a 3.5 kHz carrier frequency and can be by free pinging or by transponding.

Use of the transponding mode allows a two way communications link to be set up and the power consumption to be reduced to a minimum as transmission only occurs when the ocean surface platform requests the data. Initial tests of the communication system were carried out in 1984 and demonstrated that acceptable signal to noise ratio were possible through 6 km of water and 20-30 m of sediment. Further tests on the 1985 Marion Dufresne and 1986 Tyro cruises succeeded in transmitting accelerometer data, from a free fall penetrator, collected during penetration and inclinometer and pore pressure data collected post emplacement in 40-50 m of sediment.

Figure 3.10 shows the testing of the acoustic transponder unit for the Soft Lander vehicle. The pressure housing is designed for deployment in over 6 km of water.

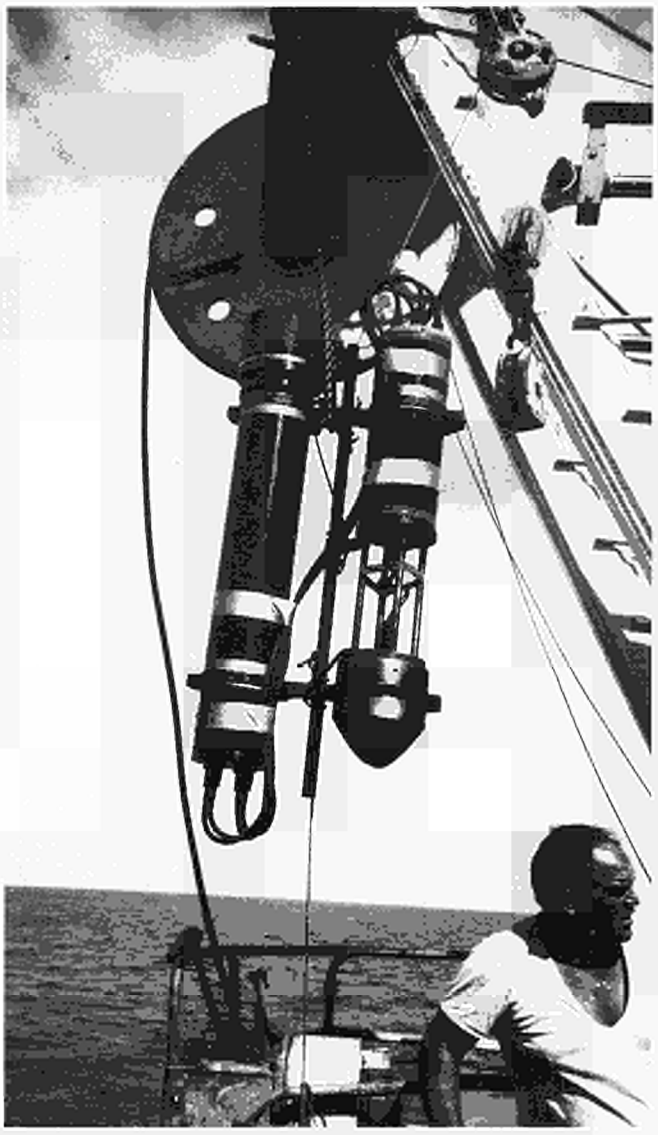

Fig. 3.10

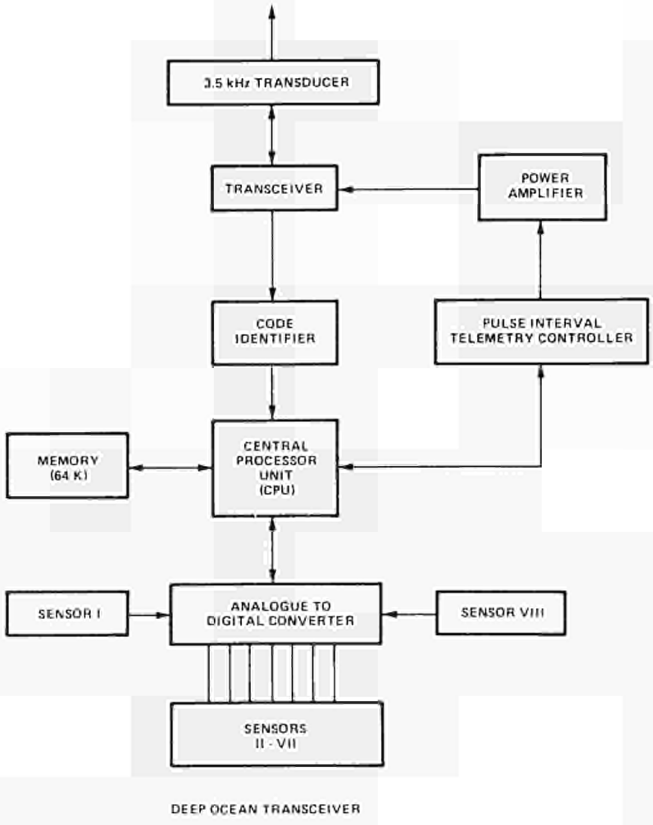

Fig. 3.9

Testing

At present the Soft Lander module has been constructed and the acoustic link tested. A geochemical sensor package has been defined and a commercial unit tested in the laboratory up to a pressure of 500 atmospheres. It is planned that during 1988, the electronic control system will be interfaced with a specially designed geochemical unit and that tests can be carried out on Lake Maggiore to investigate the stability and recoverability of the vehicle and the long-term reliability of the acoustic link. Testing of the overall communications link via a surface platform will eventually allow a demonstration of the system.

3.3 Participation in Joint In-Situ Experiments

Geochemical Results from Post-Cruise Research on ESOPE Samples

As part of a continuing co-coperation with participants of the International Long Core Cruise (ESOPE cruise), that took place in 1985 under the auspices of the Seabed Working Group, a programme of research and analysis has continued utilising the sediment samples that were collected at the two study sites from depths down to 35 m in the sedimentary column, at water depths of over 5 km. The purpose of these investigations is to obtain more detailed information on the geochemical conditions prevalent at the actual depths of interest in the sediments. This will enable a better understanding to be gained of the geochemical processes active in the sediments to help in the experimental and modelling work and in site suitability assessment.

Results are now available on the solid phase partitioning of a series of elements in core MD10 from the Madeira Abyssal Plain (eastern North Atlantic) and how this varies with depth. These results complement those already obtained for core MD48 discussed in the last PPR.

Figure 3.11 summarises the partitioning results for core MD10 illustrating the average fractionation of nine elements in the sediments amongst six solid phases, calculated from the whole length of the 34 m core. From this data a number of general observations can be made : (1) most of the authigenic Fe, Cu, Mg, Ni, Zn and Pb is associated with the moderately reducible fraction (fraction 4); (2) most of the authigenic Ca and Mn is associated with the carbonate fraction (fraction 2); (3) calcium, manganese and magnesium have appreciable amounts (i.e. between 10-19%) of their total concentration associated with the exchangeable fraction; (4) of the authigenic aluminium most is associated with the moderately reducible fraction, although aluminium, with 83% in fraction 6, is essentially detrital in nature.

In general, the main effect of the presence of calcium carbonate is as a diluent, thus complicating the interpretation of the data. However, this does not apply to manganese and calcium since they are both strongly associated with the carbonate fraction (83 and 47%, respectively). Since these two elements are most dominant in the non-detrital sediment fractions, this renders them more sensitive to the different geochemical environments found down the core. It is precisely the understanding of these processes more fully for the purpose of long-term prediction of the behaviour of artificial radionuclides in such an environment, that these studies have been undertaken. It is, therefore, useful to investigate the behaviour of these two elements in greater detail.

The down-core partitioning profile obtained for manganese is illustrated in Fig. 3.12. Considering firstly the results of fraction 2, the "carbonate phase", it would appear that between approximately 1500 and 2700 cm down the core the concentration of manganese in this fraction increases. The percentage contribution of manganese also appears to increase from a mean of approximately 45%, between 0 and 1500 cm, to 55% between 1500 and 2700 cm. The mean contribution of fraction 2 manganese to the total concentration for the entire core is 47%. This increase in fraction 2 between 1500 and 2700 cm is tentative evidence that manganese carbonate is precipitating in this region of the core. Additionally, this may also be a consequence of a higher calcium carbonate content in this part of the core.

Unlike core MD48 very little manganese is found associated with the "easily reducible" fraction 3. Most of this is confined to a very sharp surface peak (Fig. 3.12). This distribution can be explained by the post-depositional mobilisation and migration of manganese below approximately 300 m. Manganese is mobilized because the reducing conditions in the core at this depth cause manganese to dissolve into the interstitial water. A diffusion gradient is set up and the manganese diffuses upwards until it is re-precipitated as manganese oxide in the oxidised zone (between 69 and 300 cm). This explains the peak in concentration of fraction 3 manganese at this point. This increase in concentration is great enough to make fraction 3 the predominant host for manganese in this zone, accounting for approximately 40% of the total manganese compared to < 10% in the rest of the core. Other elements probably also take part in this process, the most likely candidate being iron. Moreover, fraction 4, the "moderately reducible" phase, also appears to be involved in this process, exhibiting sub-surface concentration peaks.

In conclusion, therefore, it is probable that two active geochemical processes are operating in core MD10. The first is the precipitation of manganese oxide in the upper oxic zone. The second process is the precipitation of manganese carbonate down the core.

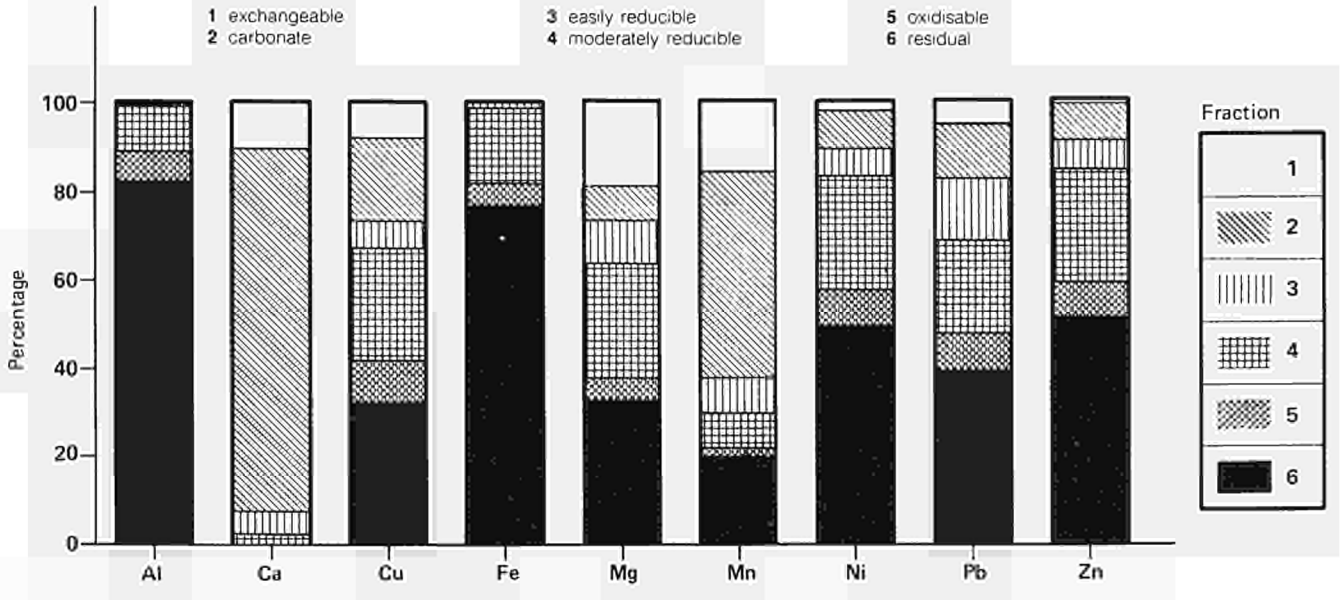

Fig. 3.11 - Mean percentage partitioning signatures of Al, Ca, Cu, Fe, Mg, Mn, Ni, Pb and Zn : Core 10

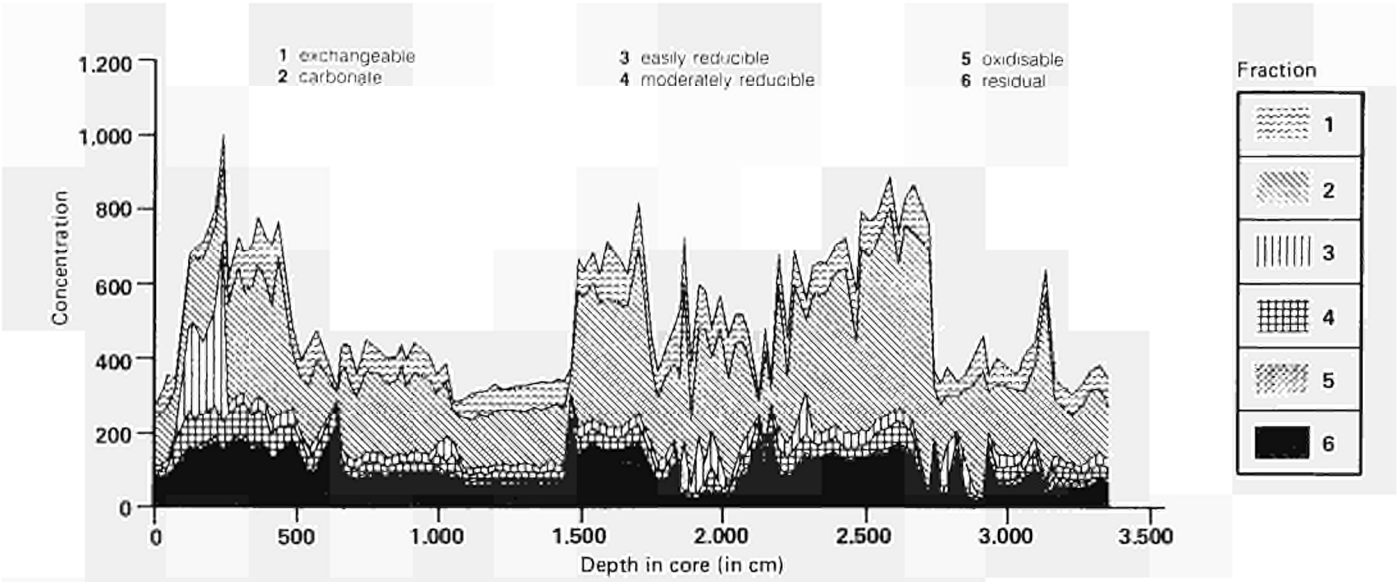

Fig. 3.12 - Downcore profile for manganese concentration partitioning: Core 10 (units, $\mu g\ g^{-1}$)

Despite the mineralogical and geochemical differences between this core and the one discussed in the previous PPR, MD48, there are similarities in the findings. First of all, in both cores elemental partitioning is not correlated with particle size. Secondly, metal enrichment is observed in both oxidized surface layers, and carbonate phases, particularly of manganese, appear in the mildly reducing zones of both cores. In addition, the organic fractions of copper (fraction 5) correlate very highly in both sediments with their respective organic carbon contents. This underlines the importance of the role of organic material in the fate of particular elements in such sediments.

The greatest difference between the partitioning results of the two cores concerns the large quantity of calcium carbonate present in core MD10 and the consequent existence of a large "carbonate" fraction. In result manganese is dominantly associated with this fraction in MD10 in place of the "easily reducible" phase as exhibited by core MD48. Furthermore, the evidence found in core MD48 of a diagenetic manganese fraction of low solubility, slowly forming in the core and becoming more pronounced with depth, is not repeated for MD10.

The study of these two cores has, therefore, highlighted the significance of the different mineralogies of the sediments found at the two study sites and how this might influence the behaviour of migrating species. The application of the same solid phase partitioning techniques used in these investigations to similar sediments contaminated under controlled labratory conditions, with artificial radionuclides, are underway. Results concerning the partitioning of americium are presented below under section 3.4 (Low Pressure Tests).

3.4 Laboratory Simulation Experiments

(D. Stanners)

The development of laboratory simulation experiment is essential to gain an understanding of the main processes controlling the immobiliation of radionuclides in sediment columns; one of the principal barriers to the dispersion of emplacement wastes over the long term. Data obtained from such investigations allow the development of more realistic models for the long-term assessment of the sub-seabed option.

Three major parameters have been identified as of potential importance in the interaction of vitrified wastes with the sediment column. These are the redox potential of the media effecting the geochemical behaviour of the waste radionuclides, the transient thermal field during the initial few hundred years altering the near field environment around the emplaced canisters, and the high ambient pressure (500-600 bars) existing at 5-6 km water depth.

The objectives of the laboratory simulation experiments are thus to investigate these parameters through a number of studies increasing in complexity. Initially a physical description of the processes affecting the long-term containment of waste material are made, using low-pressure tests. The results of these investigations support the assessment of key parameters affecting the migration of radionuclides.

Two specific potential mechanisms of transport are studied, diffusion in a sediment column with or without the presence of a transient temperature field, and migration of radionuclides under the influence of induced pore water movement. Pressures studied range between 500-1000 atmospheres and temperatures 2-250°C.

Low Pressure Tests

Results are now available from long-term column migration experiments conducted with seabed sediments and the following radionuclides: ^{99}Tc, ^{241}Am, ^{237}Np, ^{137}Cs and ^{113}Sn. The experiments conducted cover most of the important radionuclides (as identified by sensitivity studies), sediment types and conditions studied by the SWG. The configuration of the experiments was the same in each case, where a preconditioning column, about 20 cm in length, followed by a shorter (10 cm) migration column are used. Water is pumped slowly (ca. 5 ml/day) through the columns, which, on entry to the migration column, passes through a container holding the doped glass of interest. Some experiments were temperature controlled and others conducted in inert atmospheres to preserve the original 'redox' conditions of the sediments. Most tests were conducted over extended periods of greater than 200 days, after which time the migration columns were sliced and analysed.

Americium

Americium migration experiments were performed using seabed sediments collected from three different study sites, two from the North Atlantic (GME, Great Meteor East in the Madeira

Abyssal Plain, and SNAP, the South Nares Abyssal Plain) and one from the central North Pacific (PAC). The water depths at these sites are between 5 and 6 kilometers. The sediments used in the experiments were selected for their varying calcium carbonate mineralogies in order to study the influence of sediment type on the processes of migration and adsorption. The tests were all carried out under laboratory oxic conditions and were maintained at real in-situ temperatures of 4°C.

During 1987, the three columns were dismantled and the sediments analysed. Initially, a gamma scanning was carried out to obtain a first impression of the distance over which the americium had managed to migrate into the sediment over the two and a half year migration periods. Following this, the columns were sectioned and sub-samples taken for sequential leaching analysis to obtain information on the solid phase partitioning of the americium in the sediments. The development of this analysis technique and its application to radionuclide contaminated sediments formed part of a collaboration with the University of Liverpool which has been underway for a number of years. For this phase of the work a research assistant from the University spent a period of four months at Ispra applying the analytical scheme to the active sediment samples. Results on the application of the same techniques to the partitioning of natural non-radioactive elements in deep sea sediments of a similar nature are presented and discussed in this PPR under section 3.3 (Participation in Joint In-Situ Experiments).

The results from the gamma scanning of the columns clearly showed that the majority of the ^{241}Am was confined to the bottom few centimetres of the sediment at the point of entry of the glass leachate. After slicing and analysis of each segment this observation was confirmed with the resulting cumulative profiles (Fig. 3.13) showing that, no more than 10% of the total americium entering the columns during the course of the experiment progressed further than the first centimetre of sediment. The amount of activity found in each of the columns was, however, very different (Fig. 3.14). The GME column, the richest of the three in calcium carbonate (50%), contained the least activity, while the Pacific sediment column, poorest in calcium carbonate (< 1%), contained the greatest quantity of americium. Despite these differences, the activity was spread along the columns in the same relative proportions.

Since large differences between the sediments are not expected in the americium K_ds (they are all in the order of 100,000 g/l), this cannot be used to explain the differences in total activity measured in the columns. This is instead related to the differences noted between the glass leach rates in the three separate experiments (0.68×10^{-8} g cm^{-2} d^{-1} for GME and 2.2 or 2.5×10^{-8} g cm^{-2} d^{-1} for SNAP and PAC respectively). This directly affected the total quantity of americium delivered to each of the columns during the course of the experiments which is reflected in the quantity of americium found to pass through the columns

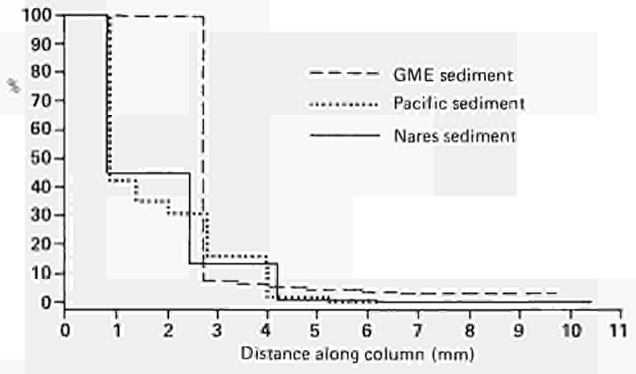

Fig. 3.13 - Final ^{241}Am profiles in the three migration columns expressed as an inverse cumulative distribution (%)

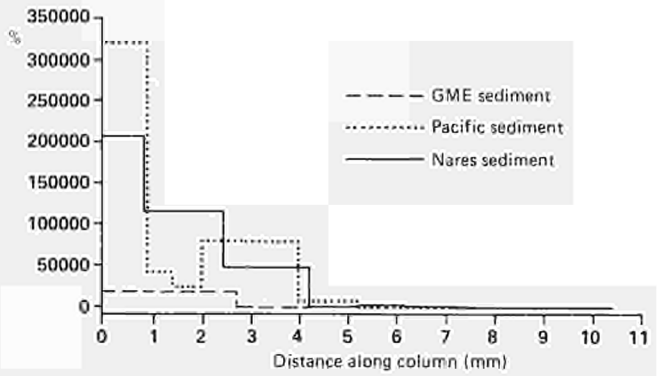

Fig. 3.14 - Final ^{241}Am profiles in the three migration columns expressed as concentrations per slice (pCi/g weight)

in each case; the concentration of americium in the Pacific column eluate was one order of magnitude greater that the GME column (see previous PPR).

Why the three experiments exhibited different leach rates when the glass in each case was from the same batch and the temperature and flow rates were very similar still needs to be clarified. However, the explanation is expected to involve the different leach fluid chemistries (especially the silicon and dissolved organic matter contents) caused by the individual pre-conditioning of the pore waters used in each test. Additionally, in the case of the GME core, localised precipitation of calcium carbonate in the leach container might reduce the glass surface area available for leaching.

The percentage solid phase partitioning of americium in the active 10 mm zone of each of the three sediment columns is shown diagramatically in Figs. 3.15 to 3.17. The average partitioning of the ^{241}Am over the same 10 mm zones for the "carbonate", "easily" and "moderately reducible" fractions are shown in Table 3.II, for the three cores. In each case these three fractions account for more than 90% of all the americium present in the migration columns. Table 3.II also includes results of the partitioning of three indicator elements (Ca, Mn and Fe) also analysed in these sediments to illustrate the contrasting geochemistries of the three sediments.

These data reveal distinct differences in the distribution of americium among the sediments fractions. The "carbonate" phase dominates the americium distribution in the carbonate rich

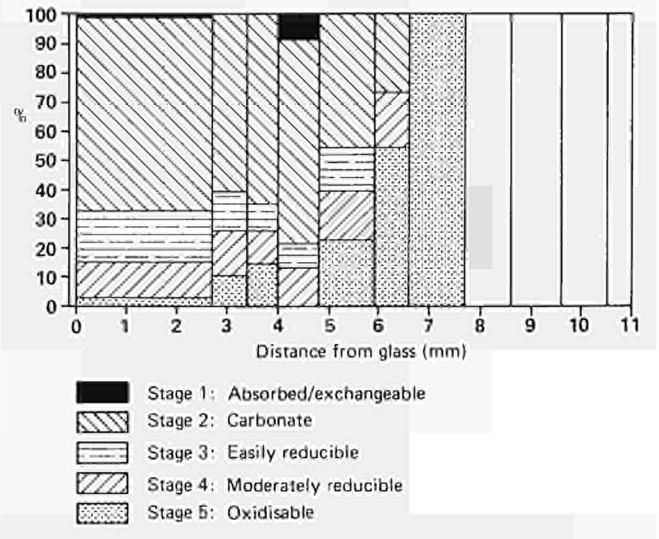

Fig. 3.15 - GME sediment migration column: partiniotning of ^{241}Am among solid fractions (%)

Table 3.II - Average partitioning of americium, manganese and iron between the three most important sediment fractions in the first 10 mm sections of three migration columns (percentage contribution to each column shown in brackets)

Extracted fraction	Element analysed		GME column	SNAP column	Pacific column
Carbonate (2)	Am	nCi	38 (67%)	118 (23%)	17 (3%)
	Ca	ppm	3016 (86%)	56 (37%)	8 (14%)
	Mn	ppm	3.4 (51%)	0.33 (0.4%)	0.06 (0.7%)
	Fe	ppt	0.1 (0.1%)	0.01 (0.01%)	0.01 (0.01%)
Easily reducible (3)	Am	nCi	10 (18%)	265 (51%)	379 (63%)
	Ca	ppm	81 (2%)	10 (7%)	6 (10%)
	Mn	ppm	0.9 (14%)	87 (92%)	5.4 (52%)
	Fe	ppt	1.3 (2.2%)	34 (18%)	24 (22%)
Moderately reducible (4)	Am	nCi	7 (12%)	97 (19%)	160 (26%)
	Ca	ppm	14 (0.4%)	17 (11%)	11 (19%)
	Mn	ppm	1.2 (17%)	5.5 (6%)	4.2 (40%)
	Fe	ppt	41 (68%)	132 (71%)	53 (50%)

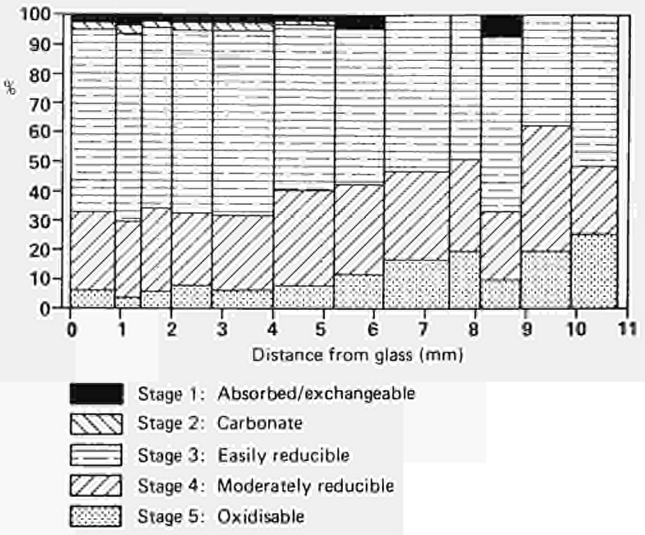

Fig. 3.17 - Pacific sediment migration column: partitioning of ^{241}Am among solid fractions (%)

GME sediment while the "easily reducible" phase associations of americium are more significant in the SNAP and Pacific sediments. The presence of a large carbonate fraction in the GME sediment, attested by the high calcium concentration in fraction 2 (Table 3.II.), is the greatest influence on the distribution of americium in this column.

If the americium lacks any preference for "adsorption" sites, then the partitioning of this radionuclides would simply reveal the relative proportion of active mineralogical phases present in the different sediments. To a large extent the partitioning results do tend to show this; the Mn and Fe analyses conducted on the separate fractions (Table 3.II) indicate that the GME sediment is impoverished in the manganese and iron hydroxide phases as suggested by the smaller fraction of Am found in fractions 3 and 4 (total 30%) compared with fraction 2 (67%). The opposite is the case for the SNAP and Pacific sediments. In fact, the three sediments progress from calcium (carbonate) dominant (GME) through manganese (SNAP) to iron dominant (Pacific), which is reflected in the dominant americium fractions for these columns (Figs. 3.15 to 3.17).

Despite this apparent lack of selectivity on the part of americium for adsorption sites, a full picture can only be obtained when account is taken of the relative proportion of effective adsorption surfaces in the three sediments. Although data specific to these columns is not available at the present, it is well known that sediments rich in calcium carbonate usually have significantly smaller surface areas compared with those which are clay rich. Also, the relative americium retention capacities of the three sediments were not found to be significantly different, after accounting for the different leach rates in the three experiments. It follows therefore, that since the "carbonate" fraction contributes no more than 60% by weight to the GME sediment, the fact that 67% of the americium is associated with this fraction, strongly suggests preferential association with carbonate particles. This result suggests that the immobilisation of americium in these sediments is not strictly related to "adsorptive" and surface area effects.

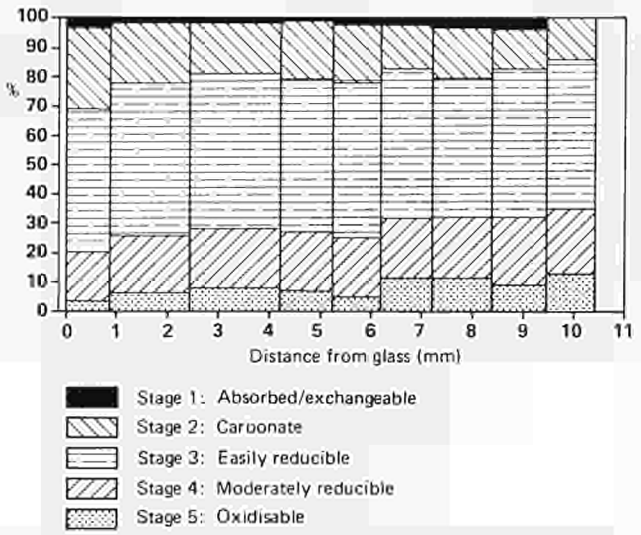

Fig. 3.16 - SNAP sediment migration column: partitioning of ^{241}Am among solid fractions (%)

Technetium

The results of the column migration experiments conducted with ^{99}Tc dopes glass under oxic and anoxic conditions are currently being worked up. Both experiments were performed with the carbonate rich 'CV2' sediment from the Cape Verde abyssal plain in the north-east Atlantic having an average water depth of 4750 m. The oxic experiment lasted for 250 days while that under anoxic conditions lasted over 800 days.

Table 3.III compares the average concentrations of ^{99}Tc in the leach fluid and at the exit to the migration columns for both experiments. The first thing to note from these data is that under anoxic conditions the leach rate is lower by one and a half orders of magnitude. Comparing the input (leach) concentrations of the water entering the migration columns with those at the column exit an impression can be obtained of the amount of technetium retained on the sediment column. At oxic conditions the range of column effluent concentrations is the same as the leach values and it follows therefore that little if any technetium was retained

Table 3.III - Comparison of technetium concentrations in the leach fluids and interstitial waters leaving two migration columns under oxic and anoxic conditions

	Oxic conditions	Anoxic conditions
Leach value	$0.8 - 2.4 \times 10^{-8}$M	$2.6 - 5.3 \times 10^{-10}$M
At column exit	$0.7 - 3.0 \times 10^{-8}$M	$0.7 - 2.2 \times 10^{-10}$M

on this column. The results under anoxic conditions, however, show that ^{99}Tc concentration in the fluid leaving the sediment migration column was on average 2.5 times smaller than the input value. This suggests that under anoxic conditions some reduction of the pertechnetate species is occurring, forming the less mobile Tc(IV), retarding the migration of this radionuclide in the sediment column. Confirmation of this will have to await solid phase and speciation data.

Mixed Nuclide Tests

During the first half of 1987, the active leaching-migration phase of these column migration experiments was begun. The sediments used in these tests were taken from the undisturbed full-round core sections sampled from between 25 and 32 metres deep in the sediments at the GME site during the ESOPE International Long Core Cruise in the summer of 1985 (see PPR July-December 1985).

Two parallel experiments are being conducted : one under an inert atmosphere, in a specially controlled glove box and the other without atmospheric control under normal laboratory oxic conditions.

For the first time in these types of experiments the glass used in these tests contains a mixture of radionuclides. Despite the increased analytical difficulties that this causes this significantly increases the productivity of each experimental column, which is particularly important due to the small quantities of sediment of the same quality available.

The glass is doped with the following radionuclides, which for the first time includes an isotope of tin; ^{113}Sn, ^{137}Cs, ^{237}Np and ^{241}Am. The choice was made balancing the requirements arising from the expected radiological importance of each isotope and the complications inherent in successfully analysing a mixture of radionuclides. A typical gamma spectrum of the glass leachate is shown in Fig. 3.18. The characteristic peaks for each of the nuclides can be seen which are sufficiently independent from each other to facilitate individual analysis.

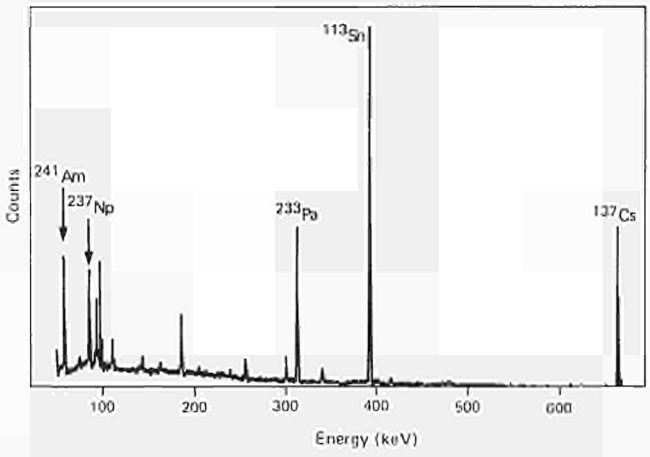

Fig. 3.18 - Typical gamma spectrum of mixed glass source

High Pressure Tests

Following the completion of a series of experiments investigating the geochemical behaviour and stability of sediments at high pressures, a new phase of tests were begun using active radionuclide tracers. These tests are aimed at investigating the influence of pressure and temperature on the diffusion of important nuclides in deep ocean sediments in order to check whether measurements of diffusion made under atmospheric pressures can truly represent the behaviour of these species in the deep sea environment. A post-doctoral research assistant began working on this project during 1987.

Experiments have now been completed with technetium (^{95m}Tc), plutonium (^{238}Pu) and neptunium (^{237}Np) in two different experimental configurations : a column method involving generation of a diffusion profile, and a half-cell technique involving measurement of the total activity transferred from a spiked to an unspiked side. An accurate definition of the diffusion coefficient for technetium in the deep sea environment is particularly desirable since the low affinity of technetium for sediment surfaces in oxic conditions results in a low retardation of this element in the 'Far-Field'. This behaviour facilitates short term experiments and allows a rapid comparison of the two methods. For the strongly retarded actinides diffusion profiles cannot be generated in a reasonable timescale and only the half-cell technique is applicable. The latter allows a considerable reduction in the required run-time for diffusion tests enabling actinide diffusion coefficients to be obtained rapidly but by a tested method. Using Tc, and with both experimental configurations, the first tests were conducted to establish suitable run-times for diffusion.

For the column method with the following boundary conditions

$$C(x,t) = 0 \qquad x > 0 \qquad t = 0$$
$$C(x,t) = C_o \qquad x < 0 \qquad t = 0$$

the solution is :

$$C(x,t) = 0.5\, C_o\, \mathrm{erfc}(0.5\, x/\sqrt{(D.t)})$$

where, C - concentration of diffusing species
x - distance along diffusion medium
t - diffusion time
D - diffusion coefficient
and erfc - complementary error function.

At a fixed time t, the graph of ierfc($2C/C_o$) against x is a straight line through the origin with gradient ($0.5\sqrt{(D.t)}$), where ierfc is the inverse complementary error function, i.e. the solution of the equation.

An alternative solution, mathematically simpler but less accurate, is :

$$\ln(C) = \text{constant} - x^2 / (4D.t)$$

and D can be obtained from a least squares fit to this equation. (The graph of ln(C) versus x^2 is a straight line with slope $1/(4D.t)$.)

The half-cell technique is a special case of the column method from which the following explicit expression for D is obtainable :

$$D = \pi h^2 f^2 / t$$

where, h is the length of the spiked half of the cell
f is the fraction of the total activity transferred to the unspiked half.

Mathematically, the two methods are similar and in neither case is the diffusing species allowed to breakthrough at the low-concentration boundary (unspiked end) of the cell, if their solutions are to remain valid.

Diffusion coefficients obtained to date for Tc, including the initial tests (Table 3.IV), suggest the absence of a significant pressure effect. Small variations evident in the D values are the result of certain tests not satisfying the mathematical boundary conditions. This is apparent from the profiles illustrated (Figs. 3.19 and 3.20) and the 'f' factors (Table 3.IV). For the hald-cell experiments 'f' should be less than or equa to 0.15 so that the following relationship should be satisfied:

$$h/\sqrt{(4D.t)} \geq 2.$$

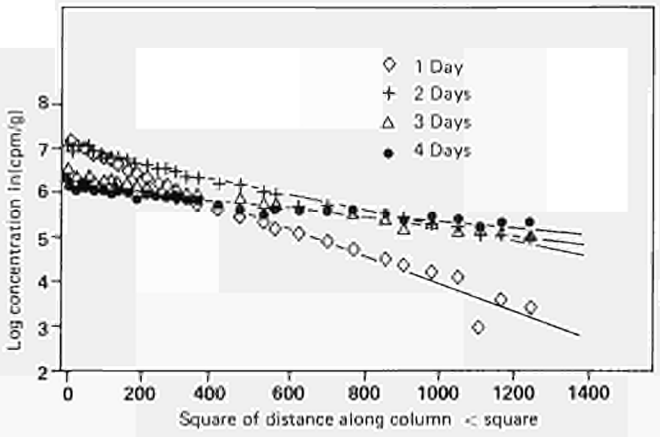

Fig. 3.19 - Log concentration plots. ^{95m}Tc diffusionn profiles: atmospheric pressure

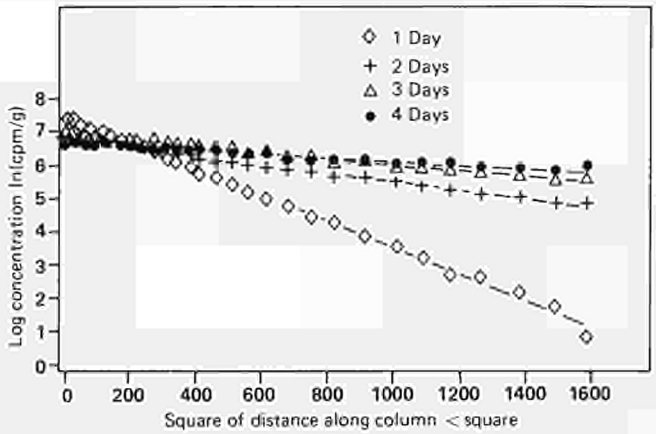

Fig. 3.20 - Log concentration plots. ^{95m}Tc diffusion profiles: 55 MPa pressure

Table 3.IV - Apparent diffusion coefficients for ^{95m}Tc measured at ambient temperature (20°C) in sea sediment (GME) by two different techniques and at two hydrostatic pressures

	Half-cell method		Column method	
	Atmospheric pressure	55 MPa	Atmospheric pressure	55 MPa
Da	3.90	6.10	8.17	7.66
t	2.00 h	0.75 h	1 d	1 d
f	0.14	0.15	—	—
Da	6.10	5.86	8.77	7.86
t	3.50 h	1.13 h	2 d	2 d
f	0.20	0.20	—	—
Da	4.95	5.66	8.52	8.14
t	4.00 h	1.38 h	3 d	3 d
f	0.20	0.21	—	—
		Da	11.10	10.30
		t	4 d	6 d
		f	—	—

Da apparent diffusion coefficient, 10^{-6}cm^2/s
t diffusion time
f fraction of total activity transferred to unspiked half
— not applicable

More reliable definitions of run-times and cell dimensions required to satisfy the mathematical solutions fully, now established, will permit further refinement in subsequent experiments.

Patent Applications

From the results of the research carried out over the last four years, a number of systems have been developed which appear innovative. Applications have thus been made for the following inventions. To date patents have been awarded by the Luxembourg Patent Office for inventions 1-4 inclusive.

1. High pressure sediment corer. Description given in Marine Geotechnology (in press); C.N. Murray, D. Stanners and M. Jamet: "A deep ocean high pressure sediment corer"
2. Deep ocean operating system. Description given in Seminar on Operational Ocean Station Networks - COST 43 project; C.N. Murray, M. Weydert: "Design and construction of a deep ocean data operating system", 202-213, 1987
3. High speed retrievable instrument sledge. Description given in Journal of Ocean Energy; C.N. Murray, M. Jamet: "Development of a deep water high speed retrievable instrument sledge", Vol. 15, No. 1 (1988) 91-101
4. Vehicule sousmarin pour la measure de données au fond the la mer profonde. Description given in Oceanology International 88; C.N. Murray, M. Weydert, T.J. Freeman: "Real-time, long-term, communication system for deep ocean instrumentation", Brighton, March 1988
5. Independence probe antenna. Description in JRC report series on feasibility and safety of the disposal of heat generating wastes into deep oceanic geological formations; T.R. Fortescue: "The use of an impedence antenna for hole closure detection. Phase II. Detail design, electronics and software development", S.P./I.07.C2.86/II (1986) 98 pages
6. Control Programme for JRC Oceanographic Buoy (© M. Weydert, 1988)

JRC PUBLICATIONS

Published and/or presented in 1987

G. BIDOGLIO, P. OFFERMANN, A. SALTELLI
"Neptunium migration in oxidizing clayey sand", Appl. Geochemistry, Vol. 2 (1987) 275-284

A. SALTELLI
"PREP and SPOP utilities. Two Fortran programs for sample preparation, uncertainty analysis and sensitivity analysis in Monte Carlo simulation. Programs description and User's Guide", EUR report 11034 EN (1987)

F. ANTONIOLI, M. D'ALESSANDRO, F. MOUSTY and A. SALTELLI
"Elemental diffusion and oxidation phenomena along permeable fractures in clay formations from a quarry at Monterotondo (I)" AIPEA, Proc. Intern. Clay Conference, July 29 - August 5, 1985, Denver, Col. (USA), L.G. Schultz, H. van Olphen and F.A. Mumpton (Eds.), The Clay Minerals Soc., Bloomington, Indiana (1987)

A. SALTELLI, G. BERTOZZI
"Data uncertainty in long-term prediction. Present Trends in Risk Analysis with Monte Carlo Techniques", Proc. Workshop on Mathematical Modelling for Radioactive Waste Repositories, 10-12 December 1986, Madrid (Spain) ENRESA (1987)

A. SALTELLI, J. MARIVOET
"Performances of non parametric statistics in sensitivity analysis and parameter ranking", EUR report 11085 EN (1987)

J. MARIVOET, A. SALTELLI, N. CADELLI
"Uncertainty analysis techniques", EUR report 10934 EN (1987)

A. SALTELLI, E. SARTORI, T.M. ANDRES, B.W. GOODWIN, S.G. GARLYLE
"PSACOIN level 0 intercomparison". An international code intercomparison exercise on a hypothetical safety assessment case study for radioactive waste disposal systems, OECD/NEA publication, Paris (1987)

F. QUERCIA, M. D'ALESSANDRO, A. SALTELLI
"Performance assessment in an alpha waste deposit in a clay formation", ENEA report, RT/DISP/85/5, Roma (1987)

R. NANNICINI, H. DWORSCHAK, F. DANIELE
"The R&D activities carried out in Ispra, according to a cooperation between ENEA/COMB and JRC-Ispra in the field of Radioactive Waste Management", RT/COMB/87/7 (1987)

B.A. HUNT
"The PETRA hot cell facility", Technical Note NE.40.6140.001

Hj. MATZKE
"Radiation damage and defects in ceramics and glasses for safe long-time storage of radioactive waste", Proc. Intern. Conference on Lattice Defects in Ionic Crystals, Madrid (1986), Cryst. Latt. Defects and Amorph. Mat., Vol. 17 (1987) 21

Hj. MATZKE
"Nuclear waste materials", Chapter 12 in book: Ion Beam Modification of Insulators, G. Arnold and P. Mazzoli (Eds.), Elsevier, Amsterdam (1987) p. 501

Hj. MATZKE (Ed.)
"Indentation fracture and mechanical properties of ceramic fuels and of waste ceramics and glasses. Proc. Intern. Workshop, TU Karlsruhe, Nov. 1985, Europ. Appl. Res. Rep., Special Vol. 7 (1987) 995-1242

Hj. MATZKE
"Indentation techniques applied to nuclear materials. Introduction, basic needs", Europ. Appl. Res. Rep., Vol. 7 (1987) 1007

J.L. ROUTBORT, Hj. MATZKE
"A review on fracture properties of nuclear materials determined by hertzian indentation", Europ. Appl. Res. Rep., Vol. 7 (1987) 1063

Hj. MATZKE
"Definition of problems and of important parameters for indentation tests", Europ. Appl. Res. Rep., Vol. 7 (19877 1091

R. DAL MASCHIO, E. TOSCANO, Hj. MATZKE
"Fracture toughness of waste glasses at elevated temperatures", Europ. Appl. Res. Rep., Vol. 7 (1987) 1203

W.J. WEBER, Hj. MATZKE
"Fracture toughness in nuclear waste glasses and ceramics. Environmental and radiation effects", Europ. Appl. Res. Rep., Vol. 7 (1987) 1221

F. DYMENT, Hj. MATZKE, E. TOSCANO
"Diffusion of Rb-83 and Rb-84 tracers in waste glasses", J. non-Cryst. Solids, Vol. 93 (1987) 22

F. LANZA, A. MANARA, L. MAMMARELLA, P. BLASI, G. CECCONE
"Borosilicate HLW glass leaching in silica saturated solution", MRS Fall Meeting, December 1987, Boston, USA (in press)

E. ZAMORANI
"Water corrosion and release mechanism of cement matrix incorporating simulated MLW", Nuclear Technology, Vol. 77 (1987) 313

E. ZAMORANI, H. BLANCHARD
"Pore volume and pore size distribution of cement samples measured by a modified mercury intrusion porosimeter", EUR 11069 EN (1987)

G. BIDOGLIO, G. TANET, A. DE PLANO, G.P. LAZZARI
"Radionuclide chemical species determination in waste management studies", J. of Radioanal. & Nucl. Chemistry, Articles, Vol. 110, No. 1 (1987) 91-100

N. OMENETTO, P. CAVALLI, G. ROSSI, G. BIDOGLIO, G.C. TURK
"Thermal lensing spectrophotometry of uranium(VI) with pulsed laser excitation", J. Anal. Atomic Spectrometry, Vol. 2 (1987) 579-583

L. RIGHETTO, A. POLISSI, D. COMI, B. MARCANDALLI, I.R. BELLOBONO, G. BIDOGLIO
"A kinetic study of formation and growth of colloidal silica", Annali di Chimica, Vol. 77 (1987) 437-455

G. BIDOGLIO, G. TANET, P. CAVALLI, N. OMENETTO
"Uranium and lanthanide speciation by thermal lensing spectrophotometry", Inorganica Chimica Acta, Vol. 140 (1987) 293-296

G. BIDOGLIO, P. OFFERMANN, A. SALTELLI
"Neptunium migration in oxidizing clayey sand", Appl. Geochemistry, vol. 2 (1987) 275-284

L. RIGHETTO, G. BIDOGLIO, B. MARCANDALLI, I.R. BELLOBONO
"Adsorbimento di attinidi su silice colloidale", 22° Congresso Nazionale di Chimica Fisica, 1987, Como (I)

L. RIGHETTO, B. MARCANDALLI, G. BIDOGLIO, I.R. BELLOBONO
"Influenza di specie anioniche sulle caratteristiche dell'allumina colloidale", 22° Congresso Nazionale di Chimica Fisica, 1987, Como (I)

I.R. BELLOBONO
"Indagini su reazioni di interfaccia in aquiferi chimicamente non saturi", EDISPI 2677-85-04 (1987)

D.A. STANNERS, C. FLEBUS
"A stochastic radiological assessment of the seabed option for high-level radioactive waste disposal. The JRC contribution to the International Seabed Working Group", CEC, JRC-Ispra, Technical Note No. I.87.104 (1987)

C.N. MURRAY, M. WEYDERT
"Design and construction of a deep ocean data operating system", Intern. Symposium COST 43 on Operaational Ocean Station Networks, 20-21 February 1987, Brest

C.N. MURRAY, WEYDERT, M.
"Deep ocean/seabed relay for long-term quasi-real-time date transmission", J. Acoustical Soc. of America, Suppl. I, Vol. 81 (1987) S49

M. WEYDERT, C.N. MURRAY, H. PELLETIER
"Study and construction of a module to interface acoustically transmitted oceanic data to a Meteosat data collection platform transmitter". In: JRC Report Series "Study of the Feasibility of Safety of the Heat Generating Wastes into Deep Ocean Geological Formations. Part IV. Deep Ocean Instrumentation Development", C.N. Murray (Ed.), EUR 11302 EN (1987) 40 pp.

C. FLEBUS, D.A. STANNERS
"Coupling feasibility study of the MARK-A ocean box model and the probabilistic assessment code LISA for radioactive waste disposal". In: JRC Report Series "Study of the Feasibility and Safety of the Disposal of Heat Generating Wastes into Deep Oceanic Geological Formations. Part I. Radiological Safety Assessment", C.N. Murray (Ed.), SP.I.87.37 (1987) 42 pp.

F. LANZA, E. PARNISARI, R. PIETRA
"Evaluation of the leaching of a borosilicate glass and of the release of various elements in sea sediments". In: JRC Report Series "Study of the Feasibility and Safety of the Disposal of Heat Generating Wastes into Deep Ocean Geological Formations. Part II. Geochemical and Geotechnical Studies", C.N. Murray (Ed.), SP.I.87.30 (1987) 27 pp.

A.R. THOMAS, R. CHESTER — "The partitioning of trace elements in sediments and sequential methods of analysis". In: JRC Report Series "Study of the Feasibility of Heat Generating Wastes into Deep Oceanic Geological Formations. Part II. Geochemical and Geotechnical Studies, C.N. Murray (Ed.), SP.I.87.32 (1987) 31 pp.

Submitted for publication or in press

A. SALTELLI, J. MARIVOET
"Some observations about actual risk calculations"
J. Nucl. Waste Management & the Fuel Cycle

A. SALTELLI, J. MARIVOET
"Nonparametric statistics in sensitivity analysis for model output. A comparison of selected techniques", Nucl. Science and Engineering

B.A. HUNT, H. DWORSCHAK, S. BERTELLI, G. MAGNI R. NANNICINI
"A hot cell pre-industrial facility for waste management studies", Intern. Conference on Nuclear Fuel Reprocessing and Waste Management, August 1987, Paris (F), in press

Hj. MATZKE, A.G. SOLOMAH, E. TOSCANO, C.T. WALKER
"Neptunium doping of the crystalline ceramic waste form SYNROC B", J. Amer. Ceram. Soc.

M. THOMAS, Hj. MATZKE
"Sodium diffusion in the nuclear waste glass GP 98/12", J. Amer. Ceram. Soc.

Hj. MATZKE
"Radiation damage effects in nuclear materials"
Invited tutorial lecture for Intern. Conference on Radiation Effects in Insulators, July 1987, Lyon (F), Nucl. Instrum. Methods in Phys. Research B

Hj. MATZKE, E. TOSCANO, G. LINKER
"Alkali diffusion and radiation effects in the waste glass VG 98/12", Nucl. Instrum. Methods in Phys. Research B

Hj. MATZKE, G. DELLA MEA, R. DAL MASCHIO, J.C. DRAN, A.A. STEFANINI
"Effect of temperature during damage production on properties of nuclear waste glasses using ion implantation", Nucl. Instrum. Methods in Phsyics Research B

E. ZAMORANI, I. SHEIKH, G. SERRINI
"Measurement of physical properties and leaching behaviour of cement matrix for immobilization of chromium compounds", Environmental Pollution

E. ZAMORANI, I. SHEIKH, G. SERRINI
"Feasibility studies concerning immobilization of chromium compounds in cement matrix", T.N. I.88.32

E. ZAMORANI, I. SHEIKH, G. SERRINI
"A study of the influence of nickel chloride on the physical characteristics and leachibility of Portland cement", Cement and Concrete Research

I. GRENTHE, G. BIDOGLIO, N. OMENETTO
"On the use of thermal lensing spectrophotometry (TLS) for the study of mononuclear hydrolysis of uranium(IV)", J. of Phys. Chem.

G. DE MARSILY, V. BEHRENDT, D.A. ENSMINGER, C. FLEBUS, B.L. HUTCHINSON, P. KANE, A. KARPF, R.D. KLETT, S. MOBBS, M. PONTIN, D.A. STANNERS, D. WUSCHKE
"Radiological assessment of the consequences of disposal of high-level radioactive waste in subseabed sediments", Proc. ANS, 15-19 November 1987, Los Angeles, Calif. (USA)

G. DE MARSILY, V. BEHRENDT, D.A. ENSMINGER, C. FLEBUS, B.L. HUTCHINSON, P. KANE, A. KARPF, R.D. KLETT, S. MOBBS, M. POULIN, D.A. STANNERS
"Subseabed disposal of high-level radioactive waste. Vol. 2. Radiological assessment", OECD (NEA) Paris

D.A. STANNERS, R. CHESTER, A.R. THOMAS, R.E. CRANSTON
"Solid phase partitioning of elements in ESOPE core 48 from the South Nares Abyssal Plain in the North Atlantic". In Schüttenhelm et al. (eds.), Geoscience Investigations of two North Atlantic Abyssal plains - The ESOPE International Expedition OECD/NEA Seabed Working Group, Commission of European Communities, Joint Research Centre, Ispra

C.N. MURRAY, M. JAMET
"Development of a deep water high speed retrieval instrument sledge", J. of Ocean Engineering

C.N. MURRAY, M. WEYDERT
"Deep ocean/seabed-satellite relay for lont-term quasi-real-time date transmission", J. Acoustical Soc. of America, SUppl. I, Vol. 81 (1987) S49

T.J. FREEMAN, C.N. MURRAY, A.K.R. BROMLEY, C.G. FREWELLEN, P. PLATT, R. DUJARDIN
"BRE/JRC penetrator experiments: Shipboard measurements". In Schüttenhelm et al. (eds.), Geoscience Investigations of two North Atlantic Abyssal plains - The ESOPE International Expedition OECD/NEA Seabed Working Group, Commission of European Communities, Joint Research Centre, Ispra

T.J. FREEMAN, A.K.R. BROMLEY, N. COOPER,
C.N. MURRAY
"BRE/JRC penetrator esperiments: Analysis of results and comparison with predictions". In Schüttenhelm et al. (eds.), Geoscience Investigations of two North Atlantic Abyssal plains - The ESOPE International Expedition OECD/NEA Seabed Working Group, Commission of European Communities, Joint Research Centre Ispra

C.N. MURRAY, R. DUJARDIN, T. FREEMAN
"Technology for waste disposal into the seabed: Development of a real-time satellite data link for long-term investigations". In Schüttenhelm et al. (eds.), Geoscience Investigations of two North Atlantic Abyssal plains - The ESOPE International Expedition OECD/NEA Seabed Working Group, Commission of European Communities, Joint Research Centre, Ispra

T.J. FREEMAN, N. COOPER, A.K.R. BROMLEY,
C.G. FLEWELLEN, R.F. MATHAMS, C.N. MURRAY
"HOCUS cruise report : BRE and JRC penetrator experiments", ENEA Environmental Studies Series

C.N. MURRAY, M. WEYDERT, FREEMAN, T.J.
"Real-time, long-term communications system for deep ocean instrumentation". Advances in Underwater Technology, Ocean Science and Offshore Engineering

C.N. MURRAY
"The disposal of heat generating nuclear waste in deep ocean geological formations. A feasible option". Advances in Underwater Technology, Ocean Sciences and Offshore Engineering

T.J. FREEMAN, C.N. MURRAY, R.T.E. SCHUTTENHELM
"The TYRO 86 penetrator experiments at Great Meteor East", Advances in Underwater Technology, Ocean Sciences and Offshore Engineering

C. FLEBUS, D.A. STANNERS
"A stochastic assessment using LISA: models, data and results". In: JRC Report Series "Study of the Feasibility and Safety of the Disposal of Heat Generating Wastes into Deep Oceanic Geological Formations. Part I. Radiological Safety Assessment", C.N. MURRAY (Ed.), EUR 11754 EN, 159 pp

SCIENTIFIC STAFF OF THE PROGRAMME

Programme Manager : **F. Girardi**

Coorcination of activities at TUI Karlsruhe : **J. Fuger***

Research Area 1

S. Bertelli, H. Bokelund*, L. Bondar, M. Cockerelle*,
H. Dworschak, J.P. Glatz, W. Hage, B. Hunt
F. Mcusty

Research Area 2

A. Avogadro, G. Bidoglio, M. D'Alessandro, F. Lanza,
A. Manara, Hj. Matzke*, A. Saltelli, E. Toscano*,
T. Visani, E. Zamorani

Research Area 3

C.N. Murray, D. Stanners

*) Staff of the Transuranium Institute of the JRC-Karlsruhe

GLOSSARY

AD	Apparent density
ADECO	Atelier decontamination: the hot-cell system of JRC
AERE	Atomic energy research estabishment
BWR	Boiling water reactor
CEA	Comissariat energie atomique
CEC	Commission of European Communities
CEN/SCK	Centre d'etude de l'Energie nucléaire/ Studiecentrum vor Kernenergie
CGC	Comité Consultatif en Matière de Gestion et de Coordination
CIEMAT	Centre de Investigaciones Energeticas Medio Ambientales y Técnologicas
COCO	Colloids and complexes
CPDF	Cumulative probability distribution function
CS	Compressive strength
CSH	Calcium silicate hydrate
CV2	Cape verde-2
DNPDE	Dounreay nuclear power demonstration establishment
DOE(UK)	Department of environment
DOE(USA)	Department of energy
EC	European Community
EDAX	Energy dispersive X-ray analysis
ENEA	Ente nazionale energie alternative
ENEA-DISP	Ente nazionale energie alternative - Divisione sicurezza e protezione
ENRESA	Empresa Nacional de Residuos Radioactivos
ESCA	Electron spectroscopy for chemical analysis
ESOPE	Etude des Sédiments Océaniques par Pénétration
ESTER	Esperienze Trattamenti Effluenti Radioattivi
ET-AAS	Electro-thermal atomic absorption spectroscopy
FBR	Fast breeder reactor
GME	Great Meteor east
GSF	Gesellshaft fuer Strahlen Forschung
HAW	High activity waste
HLLW	High level liquid waste
HLW	High level waste
HMI	Hahn-Meitner Institut
IAEA	Interational Atomic Energy Agency
ICP-ES	Inductively coupled plasma - emission spectrograph
ICP-MS	Inductively coupled plasma mass spectroscopy
IPSN	Institut de Protection ed Sûreté Nucléaire
JRC	Joint Research Centre
KfK	Kernforschung Karlsruhe
LAW	Low activity waste
LISA	Long term Isolation Safety Assessment
LMA	Laboratoire moyenne activité
LWR	Light water reactor
MAW	Medium activity waste
MIRAGE	MIgration of RAdioisotopes in the GEosphere
MLLW	Medium level liquid waste
MLW	Medium level waste
NDA	Mon-destructive analysis
NEA	Nuclear Energy Agency
NED	Nuclear Experiments Division
NFCD	Nuclear Fuel Cycles Division
NRPB	National Radiation Protection Board
OXAL	Process for actinides separation by oxalate precip.
OXAL-MAW	Process for actinides separation by oxalate precip. - from medium active waste
PAGIS	Performance Assessment of Geological Isolation System
PD	Pycnometer density
PDF	Probability distribution function
PETRA	Plan for Evaluation and Testing of Rad-waste treatment Alternatives
PFA	Pulse fluctuation analysis
PREP	Pre Processor
PSAC	Probabilistic safety assessment codes
PTP	Pulse to pulse analysis
PUREX	Plutonium-Uranium-Reduction-Extraction-Process
PWR	Pressurized water reactors
RATG	Radiological assessment task group
SA	Sensitivity analysis
SE/C	Solid element/cement ratio
SNAP	South Nares Abyssal Plain
SPOP	Statistical Post Processor
SWG	Seabed Working Group
TCA	Time correlation analysis
TROUGH	(TROUGH: Computer Code)
TU	Transuranium (Institute)
TUI	Transuranium Institute
UKAEA	United Kingdom Atomic Energy Authority
VDC	Variable dead-time counter
WAK	Wieder aufasbeitungs Anlage Karlsruhe
W/C	Water/Cement ratio
XPS	X-ray induced Photoelectron Spectroscopy

European Communities - Commission

EUR 11914 — Radioactive Waste Management

F. Girardi

Luxembourg: Office for Official Publications of the European Communities

1988 - II, 74 pp. — 21.0 x 29.7 cm

Series: Nuclear Science and Technology

EN

The safe and cost-effective management of the radioactive waste produced in the exploitation of nuclear energy requires an important research and development effort in order to be fully implemented at an industrial level. The Joint Research Centre initiated its activities in the field of radioactive waste management in 1973. Four multiannual plans have been completed (1973-76, 1977-79, 1980-83 and 1984-87). The act vities of the JRC are carried out under the Plan of Action on Fission, which also includes programmes on Nuclear Materials Management and Control, Reactor Safety, Decommissioning of Nuclear Plants and Nuclear Fuels and Actinide Research. These programmes are carried out by the JRC and by shared-cost act ons. Coordination and Management Committees assure coordination among the various actions and with similar activities carried out in national laboratories. In addition to the research action programmes, the Council approved in February 1980 a Community Plan of Action in the field of Radioactive Waste (1980-1982) which assures the continuity of the R&D effort throughout the period and entrusts the Commission with a wider role in the implementation of waste management practices. The activities of the radioactive waste management programme of the JRC are largely executed by the Ispra Estbalishment, with a participation of the Karlsruhe Establishment. Strict relationships are maintained with the corresponding shared-cost action programme on radioactive waste management. Important Community projects such as PAGIS (Performance Assessment of Geological isolation Systems) and MIRAGE (Migration of Radioisotopes in the Geosphere) are jointly coordinated.

The JRC programme is structured in three research areas :

1. **Waste Management and the Fuel Cycle** aims at characterizing waste streams of the nuclear fuel cycle and minimizing them, particularly for what concerns the radionuclides which are responsible of long-term risks.
2. **Safety of Waste Disposal in Continental Geological Formations** aims at evaluating the long-term risks of waste disposal. It includes both theoretical evaluation act vities and experimental activities in view of providing the necessary models and data base for the evaluation.
3. **Feasibility and Safety of Waste Disposal in Deep Oceanic Sediments** aims at evaluating feasibility and long-term risks of this advanced disposal option. These activities are carried out in the framework of a NEA-coordinated programme and the JRC contributes both in experimental and theoretical activities and in the programme coordination.

CDNA 11914 ENC